UNIVERSITY OF CALIFORNIA,
IRVINE

Assistive Technologies for the Aging Population

DISSERTATION

submitted in partial satisfaction of the requirements
for the degree of

DOCTOR OF PHILOSOPHY

in Biomedical Engineering

by

Peyton Elizabeth Paulick

Dissertation Committee:
Assistant Professor Mark Bachman, Chair
Associate Professor Hamid R. Djalilian
Professor G.P. Li

2014

DEDICATION

To
My Parents: Kim and William
My Second Parents: Uncle Marty and Auntie Heather
My Siblings: Kelley, Avery, Jordan and Andrew

The great journey that was graduate school would not have been possible without your never-ending support, encouragement, positivity, and unconditional love. I am deeply grateful.

TABLE OF CONTENTS

LIST OF FIGURES

ACKNOWLEDGMENTS

The adventure of graduate school has been one of the most rewarding journeys of my life. From the first time I visited the University of California Irvine campus to the day I submit this dissertation, the research and all other experiences that came with it would not have been possible without the support of the many people I met along the way.

While the support of various faculty members was pivotal to the completion of this work, I would like to give a special thank you to the support staff of the Biomedical Engineering Department, namely Karen Stephens. Karen Stephens, aka BME Mom, was the first person I met when visiting UCI as a prospective graduate school. While cutting edge research and university rapport guide ones decision in selecting a program, the way a place makes you feel ends up being the deciding factor. Karen makes her students feel supported, informed, educated, confident, and prepared to embark on the expedition that is a Ph.D. Thank you Karen.

I would like to also thank my doctoral advancement committee: Dr. Abraham P. Lee, Dr. Laura Mosqueda, Dr. G.P. Li, and Dr. Susan Charles. Working with you to build a roadmap for my doctoral studies was invaluable. I was humbled to be in a room with individuals of such diverse expertise weighing in on how to make a meaningful and impactful contribution through my doctoral work in medical technology. Thank you for your time, enthusiasm, and support of my research.

Who knew I would be able to combine my love for travel and science with a year collaboration overseas in Germany? Thank you to all my colleagues at the Ludwig Maximilians Universität München Generation Research Program: Dr. Herbert Plischke, Dr. Ernst Pöppel, Dr. Niko Kohls, Renate Ertlmeier-Maeli, Philipp Novotny, Jennifer Oyaga-Padilla, Sebastian Glasl, and Fred Zimmermann. Thank you for an amazing year, both academically and culturally.

I am beyond grateful to have been given the opportunity to be advised by Dr. Mark Bachman. Mark, you are an idea powerhouse filled with so many creative technological solutions. I respect you not only as a colleague and mentor, but as a friend. Thank you for giving me so many opportunities, inside and outside the lab, to grow and develop both personally and professionally.

The opportunity to be co-advised by Dr. Hamid Djalilian, a physician with an innovative engineering core, was invaluable. Your expertise from the clinic brought a perspective to our project that was application-driven and motivated from a true need in the medical practice. This not only made our projects that much more clinically valuable, but created an excitement about our work in knowing that there was a well defined end user with a high need. Thank you Hamid for your dedication, enthusiasm, and never-ending support of our efforts.

To Hamid's right hand man, Dr. Hossein Mahboubi, this research would not have been possible without you. Thank you for always being willing to offer your help when it came to cadaver testing, clinical testing, and grant and manuscript writing. I think we made a great physician/engineer team and I thank you for your years of dedication.

A massive part of the graduate research experience is your lab mates. These are the ones who are with you during the late night data collection sessions, the search for the missing multimeter, and the support team for an impeding deadline. Thank you to all members of the Li-Bachman lab, especially to Nizan Friedman, Spencer Chang, Jason Luo, Sara Saedinia, Sarkis Babakian, Jordan Linford, Mike Klopfer, Ryan Smith, Lily Wu, Arthur Zhang, Melinda Malley, Jordan Ritkes, Maneka Bandriath, Stephanie Eng, and Nicholas Gunn for your support and teamwork the last 4.5 years.

I would like to especially thank Mark Merlo, a mentor and a friend, who helped introduce me to life in the lab. His impeccable work ethic, desire to understand a phenomena or concept entirely, and his nature to always do things properly and completely helped shape me as an engineer and researcher. I am thankful for the years with you during graduate school and I look forward to working with you in the future.

I wish to express my deep gratitude to my parents who instilled in me a profound sense of confidence throughout my life. This confidence allowed me to embark on a career in science and technology that I am passionate about and believe that my work can make a positive difference. Your unwavering support of my education, travel addiction, personal growth, and well-being has made me eternally grateful.

A grand thank you to all the funding agencies that made the research presented here possible: The Eugene-Cota Robles Fellowship, The UCI Center for Hearing Research, NIH National Institute on Deafness and Other Communication Disorders Predoctoral Training Grant (5 T32 DC010775), The Whitaker Foundation International Fellows Program, the ARCS Foundation-Orange County Chapter, and The Samueli Institute.

I also wish to thank individuals who donate their bodies and tissues for the advancement of education and research, and in particular the University of California Irvine School of Medicine Willed Body Program.

Lastly, I would like to thank the University of California for my Bachelors, Masters, and Doctoral career. The UC system is truly a place of opportunity, and I am thankful to have made a home here for the past 10 years.

CURRICULUM VITAE

Peyton Elizabeth Paulick

EDUCATION

2009	B.S. in Bioengineering with a minor in Spanish Studies, University of California, San Diego
2011	M.S. in Biomedical Engineering, University of California, Irvine
2014	Ph.D. in Biomedical Engineering, University of California, Irvine

HONORS AND AWARDS

2009	Eugene Cota-Robles Graduate Diversity Fellowship
2011	Paul Merage School of Business – Business Plan Competition – Prosperitas Ideas to Action Award
2011	Featured in California Institute for Telecommunication and Information Technology *Interface* Magazine
2011	Featured in the University of California Irvine's "I am an Anteater" Campaign
2011	National Institutes of Health – National Institute on Deafness and Other Communication Disorders Graduate Training Grant – University of California Center for Hearing Research
2012	Whitaker Foundation International Fellowship – Munich, Germany
2012	Featured in German Newspaper *Tölzer Kurier* "Diagnostik-Brille"
2013	Invited Speaker Munich University of Applied Sciences *Medical Technology Lecture*
2013	Featured in German Television Station ZDF (Zweites Deutsches Fernsehen) Research Special Episode "Abenteuer Forschung: Licht und Gesundheit" (Adventure Research: Light and Health)
2013	Research Featured in *Orange County Register* "Sounds of Research" Article
2013	ARCS Foundation Scholar – Orange County Chapter

FIELD OF STUDY

Medical Technology

PUBLICATIONS

Peyton Paulick, Hossein Mahboubi, Mark Merlo, Hamid R Djalilian, Mark Bachman. "A Micro-Drive Hearing Aid: A Novel Non-Invasive Hearing Prosthesis Actuator", *Biomedical Microdevices*. IN REVIEW

Peyton Paulick, Hossein Mahboubi, Hamid R Djalilian, Mark Bachman. "Short-Term Clinical Performance of the Direct-Drive Hearing Device" *Otology & Neurotology*. IN REVIEW

P. Justin Rossi, Philipp Novotny, Peyton Paulick, Herbert Plischke, Nikola Kohls, James Giordano "Decision Technologies in Medical Research and Practice: Practical Considerations, Ethical Implications, and the Need for Dialectic Evaluation" Ethics in Biology, Engineering & Medicine – An International Journal 4(1):25-36 (2013).

Amy Yao, Hossein Mahboubi, Melinda Malley, Christian Conderman, Peyton Paulick, Mark Bachman, Hamid Djalilian. "Direct-Drive Acoustic Amplification Using a Tympanostomy Tube" *Proceedings Otolaryngology – Head and Neck Surgery*, vol. 149 no.2 suppl P96, September 2013.

Hossein Mahboubi, Peyton Paulick, Mark Bachman, Hamid Djalilian. "Novel Completely-In-The-Canal Magnet-Drive Hearing Device – A Temporal Bone Study" *Otolaryngology – Head and Neck Surgery*, 2012.

Hossein Mahboubi, Peyton Paulick, Saman Kiumehr, Mark Merlo, Mark Bachman, Hamid Djalilian. "Investigation of a Novel Completely-In-The-Canal Direct-Drive Hearing Device: A Temporal Bone Study". *Otology & Neurology*. 34:115-120, 2012.

Paulick, Peyton. "StabilitySole: Embedded Sensor Insole for Balance and Gait Monitoring" *HCI International 2011*, Orlando, FL, USA, 2011.

Paulick, Peyton et al. "Novel Chromatic Pupillometer : Portable Pupillometry Diagnostic System." *HCI International* 2013, Las Vegas, NV, USA, July 21-26, 2013, Proceedings, Part I, Volume 8019, 2013, pp. 158–166.

PRESENTATIONS

American Otological Society Meeting at COSM, "Short-Term Clinical Performance of the Direct-Drive Hearing Device", Las Vegas, NV, 2014. (presented by collaborator).

Munich University of Applied Sciences "Medical Technologies" Lecture, Munich, Germany, 2013.

American Academy of Otolaryngology – Head and Neck Surgery Annual Meeting, "Direct Drive Acoustic Amplification Using a Tympanostomy Tube", Vancouver, BC, 2013 (presented by collaborator).

Human Computer Interaction International "Novel Chromatic Pupillometer : Portable Pupillometry Diagnostic System." Las Vegas, NV, 2013.

IEEE EMBS Micro and Nano Technology in Medicine, "A Novel Micro-Drive Hearing Prosthesis Actuator With Custom Tympanic Membrane Interface", Maui, HI, 2012.

Biomedical Engineering Society "A Novel Micro-Drive Hearing Prosthesis Actuator", Atlanta, GA, 2012.

American Academy of Otolaryngology – Head and Neck Surgery Annual Meeting, "Completely-In-The-Canal Magnet-Drive Hearing Device – A Temporal Bone Study", Washington, DC, 2012 (presented by collaborator).

American Otological Society Meeting at COSM, "Direct Drive Micro Hearing Aid: Investigation of a Novel Completely-in-the-Canal Hearing Aid", San Diego, CA, 2012 (presented by collaborator).

University of California Bioengineering Symposium, Berkeley, CA, 2012.

International Association for Dance Medicine & Science 22st Annual Meeting, "Design and Testing of a Sensor System to Measure Foot Pressures in Ballet Pointe Shoes", Singapore, 2012 (presented by collaborator).

University of California Irvine Center for Hearing Research Symposium, Irvine, CA, 2012.

Human Computer Interaction International "Novel Chromatic Pupillometer: Portable Pupillometry Diagnostic System", Orlando, FL, 2011.

International Association for Dance Medicine & Science 21st Annual Meeting, "Development of a Pressure and Accelerometry Insole System for Tap Shoes", Washington, DC, 2011 (presented by collaborator).

BaCaTec (Bavaria California Technology Center) Workshop, "Assistive Devices and Systems for Hearing and Balance", Munich, Germany, 2010.

PATENT APPLICATIONS

Peyton Paulick, Mark Bachman Hamid Djalilian, Mark Merlo. "Direct Drive Micro Hearing Device" U.S. Patent Application: US 13/487,597.

Peyton Paulick, Mark Bachman, Hamid Djalilian " Direct-Drive Acoustic Amplification Using a Tympanostomy Tube" U.S. Provisional Patent Application 61/8884821.

ABSTRACT OF THE DISSERTATION

Assistive Medical Technology for the Aging Population

By

Peyton Elizabeth Paulick

Doctor of Philosophy in Biomedical Engineering

University of California, Irvine, 2014

Assistant Professor Mark Bachman, Chair

The United States is experiencing an unprecedented growth of its older adult population from now until 2050. The current health paradigm, which is focused on the provider model of health, is not going to be able to handle this growth and demand on the system. A health model where patients and other stakeholders participate in healthcare may be sustainable. However, these people need to be empowered, and technology can play a big role. Thus, it will become of increasing importance to discover the most appropriate way to integrate technology into daily living to maintain proper quality of life for this adult cohort. The work contained in this doctoral dissertation is driven by the needs of older adults, and represents examples of the types of technologies and design methods that will be needed in keeping older adults healthy. These medical technologies aim to address some the prevalent healthcare issues facing older adults in an appropriate and dignity preserving way.

Three technologies will be discussed here, the first is a novel hearing technology that addresses many of the concerns older adults have with the presently available hearing devices. The device is located deep in the ear canal and recreates sounds with mechanical movements of

the tympanic membrane. The DHD successfully recreated ossicular chain movements across the frequencies of human hearing while demonstrating controllable magnitude. Moreover, the device was validated in a short-term human clinical performance study where the DHD successfully recreated sound in healthy subject.

The second is an exploratory non-invasive diagnostic system that analyzes a subject's pupil light reflex to gain insight into neurological health. This prototype was developed and validated on a small population to evaluate the ease-of-use of this portable system and to establish a viable testing protocol to evaluate a population of retinal cells that are believed to be involved in a variety of neurological disorders.

Lastly, a non-obtrusive insole was developed to measure a subject's balance and gait in many different environments. This technology has been designed and is currently undergoing testing in the Department of Orthopedic Surgery at the University of California Irvine Medical Center.

PREFACE

The motivation for this work began with the desire to develop technological solutions for problems that physicians were facing in the clinic. The Li-Bachman lab had a standing tradition to work closely with physicians to develop real world applications that could be deployed and validated in the clinic. My interest was to develop medical technology that could monitor, aid, and assist human function, and develop a technology from idea inception to tested prototype. I began this exploration working with Dr. Hamid Djalilian, an Otolaryngologist at the UCI Medical Center, specializing in hearing and balance to discuss some of the potential issues he was facing and how technology could provide solutions. One reoccurring theme that came up in our discussion was that many of the solutions he was seeking were for the older adult population. While this may not be surprising, the baby boomers are getting older, and advanced technology will be needed to properly deliver healthcare to this group, but it begged for deeper exploration of this group of individuals. This doctoral dissertation will explore the role that technology can play in improving independence and quality of life for older adults.

INTRODUCTION

The United States is currently experiencing an unprecedented growth of its older adult population from now until 2050, where the population of individuals aged 65 and older will more than double[1]. This number is projected to be 88.5 million people over the age of 65 in the United States alone (Fig. 1). This growth of the aging population will have a wide spectrum of implications for the country[1], and one area of particular interest that will be heavily affected, is healthcare. Older adults are the largest users of health care services in the United States with adults aged 65-75 spending approximately $9,000 annually and adults aged 85 and over spending approximately $23,000 annually[2] (Fig. 2). In 1960 the national health expenditures as a percentage of GDP was 5.2%, since then it has been steadily on the rise, and as of 2012 that percentage jumped to 17.9% in 2012[3].

Reflecting on this population change over the next four decades and the increased need for healthcare services, demands a modification in the way our nation delivers health care. This older adult population will be too large to be properly cared for using traditional government programs[4,5], and there is a strong belief that technology can play a role in this paradigm shift. The current health paradigm, which is focused on the provider model of health, is not going to be able to handle this unprecedented growth and demands on the system. A health model where patients and other stakeholders (e.g. family, community) participate in healthcare may be sustainable. However, these people need to be empowered. Technology can play a big role here. Thus, it will become of increasing importance to discover the most appropriate way to integrate technology into daily living to maintain proper quality of life for this adult cohort.

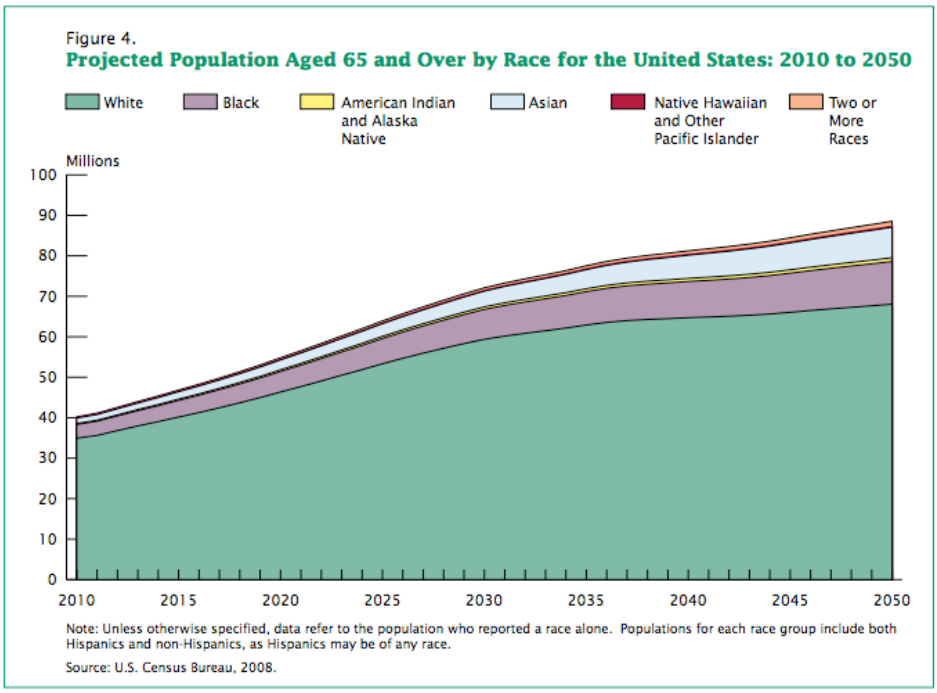

Fig. 1 Projected population aged 65 and over from 2010 – 2050 in the United States[1].

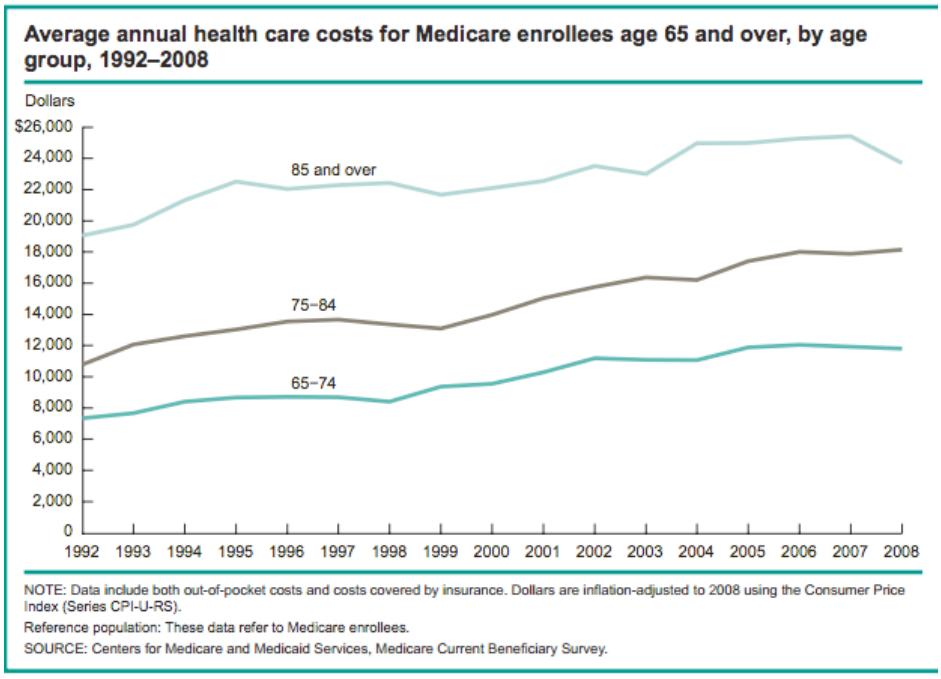

Fig. 2 Average Annual Health Care Cost for Medicare Enrollees Age 65 and Over[2]

To meet these changing demands, healthcare professionals must look for solutions to increase efficiency and decrease cost throughout the continuum of care – from the intensive care unit, to an outpatient facility, to the patients home[6]. This need for low cost and efficiency has created a demand for medical technologies that are versatile and portable to move through these different environments[6]. With the massive increase in population, the burden of healthcare will have to shift to individuals and stakeholders. People will need to become collaborators in their healthcare, not just recipients.

In order to truly bring about this paradigm shift in the way healthcare is delivered, a new approach to how our society views disability and aging must be adopted[4]. The old vision was described as one where older adults with disabilities were completely dependent and in constant need of professional guidance. This approach focuses on the individual and their deficits[4] and reduces their role in addressing their personal healthcare and daily needs. The new and improved model focuses on the *abilities* of older adults, and how those can be used to support independent living.

This older adult cohort is different than cohorts of the past and is sparking demand for a variety of products and interactive environments that will accommodate and adapt to their changing physical and sensory needs. With life expectancies increasing we will need to develop solutions to allow this group of adults to maintain active lifestyles both inside and out of the home. Moreover, according to the AARP, upon retirement 9 out of 10 seniors prefer to stay in their homes as they age, and thus this demands new dignity preserving technologies for maintaining an independent and healthy life. Of utmost concern to this adult cohort as well as care providers to this cohort is maintaining independence. Reserving the ability to perform basic self-care activities such as bathing, dressing, and eating without assistance, or activities of daily

living, are fundamental to maintain independence and quality of life. Loss of the ability to perform these activities of daily living has been associated with institutionalization, increased caregiver burden, higher resource use, and death[7]. With these needs in mind we can begin to develop, as Professor James Pirkl describes it, technologies for older adults that "sympathize instead of stigmatize"[8].

While technology is rapidly changing and developing creative solutions to solve problems in health care, without adoption and proper use of these technologies, their value is diminished. The ability and desire to adopt technology in general is becoming increasingly important for individuals to be functionally independent[9]. In general, older adults are less likely than younger adults to use technology[9]. Many research groups are investigating this phenomenon to better understand the reasons for this and develop tools to make technology more accessible. Some factors attributed to low adoption rates of technology are: computer anxiety, performance anxiety, high-perceived cost, and low perceived need[9], interest in a particular technology, cognitive abilities, and privacy concerns[10]. Overall the adoption of technology is extremely complex, influenced by many factors, highly individual specific, and not only explained by education and socieoeconomics[9].

It has also been found that attitudes and abilities are among the most powerful predictors of technology use, and for adoption of technology to occur designers must take in to account age-related changes in ability[10]. Consideration of age-related changes in perception, cognition, and motor systems are essential when designing technology for older adults[11]. Designers need to be aware that older adults *literally* perceive technology differently – visual acuity, color perception, background noise interference, difficulty with high-pitched sounds, all play a role in this interaction[10]. As one author put it "Imagine you are handicapped with a brain injury that

renders you twice as slow at acquiring information as you were before. How would that affect your willingness to learn a new technology[10]?" For the benefit of technology in healthcare to be fully realized, the needs and abilities of older adults must be considered in the system design[12]. It is critical for the end users to be involved in the research and development as well as training of professionals that will help deliver these technological supports. The engineering community must complement their innovation with contextual factors of the user population[4]. Technology development for this field will have many common requirements: portability, small size, integratable, ease of use, low-cost, good aesthesis, high function/effectiveness, and a natural feel.

Having a better understanding of the end user and increased awareness for technology design, it is important to recognize what are the prevalent heath care issues facing older adults[1,2].

1. *Balance disorders and falls:* Nearly 5 million older adults are annually institutionalized due to a balance related fall. These balance related falls are the leading cause of elderly institutionalization each year.
2. *Osteoarthritis:* Osteoarthritis is the most common form of arthritis and causes pain swelling, and reduced motion in the joints[13]. Osteoarthritis is the single most common cause of disability in older adults, with 51% of the population over 65 reporting a form of arthritis[1,2].
3. *Hearing Loss:* 37.5% of the population over 65 has some level of hearing loss, while only 14% are using hearing aids. Hearing loss is associated with isolation, depression, low self-esteem, and changes in function status[14].
4. *Dementia:* Dementia is a collective term for describing a variety of conditions that develop when nerve cells in the brain no longer function normally. This leads to a change in one's memory, behavior, and ability to think clearly. Alzheimer's is the most common

type of dementia. 1 in 8 older Americans has Alzheimer's and it is the 6th leading cause of death in the US. In 2012 approximately $200 billion in payments for care of those with Alzheimer's disease[15].

5. *Obesity*: In 2010 72.8% of the U.S. population over 65 was overweight[2]. Obesity is a major cause of preventable diseases and early death. Obesity is associated with increased risk of coronary heart disease, Type 2 diabetes, cancer, and respiratory problems, to name a few[2].
6. *Pain*: Pain is a common complaint among the elderly, which often goes untreated and negatively affects quality of life. It is estimated that between 25-50% of community dwelling older adults and 45-80% of nursing home-dwelling older adults, have important pain problems that interfere with everyday life[16,17].

Many of these heath issues that older adults are facing do not need to be addressed solely in the clinic with a physician at their side. This is an opportunity for physicians, psychologists, and technologists to develop solutions that will empower older adults with the opportunities to take an active role in their healthcare. The work contained in this doctoral dissertation is driven by the needs of older adults, and represent examples of the types of technologies and design methods that will be needed for keeping older adults healthy. These medical technologies aim to address some the prevalent healthcare issues facing older adults in an appropriate and dignity preserving way.

Three technologies will be discussed, the first is a novel hearing technology that aims to address many of the concerns older adults have with the presently available invasive and non-invasive hearing devices. The second is an exploratory non-invasive diagnostic system that

analyzes a subject's pupil light reflex to gain insight to neurological health. And lastly, a non-obtrusive insole to measure a subject's balance and gait in many different environments.

CHAPTER 1

Hearing Loss and Current Hearing Technology

1. Introduction

Hearing loss is one of the most prevalent chronic conditions in the U.S., affecting over 10% of the population, totaling 34.25 million in 2008[18]. This figure jumps to 360 million individuals worldwide suffering from hearing loss[19]. Hearing loss can result from a variety of pathological conditions of the sound transduction pathway[20,21].

The hearing pathway begins where sound pressure waves are funneled by the external ear (pinna) and pass down the auditory canal to the tympanic membrane (eardrum). Attached to the TM is the ossicular chain, composed of the malleus, incus, and stapes, which convert sound vibrations from the air into mechanical into mechanical movements processed by the inner ear[21]. The footplate of the stapes couples to and transfers these mechanical movements to the oval window of the fluid filled cochlea. The organ of Corti is a part of the cochlea that is composed of small sensor transducers called hair cells[21]. These hair cells sense the movement of the fluid in the cochlea and translate sound information and characteristics into an electrical potential. These electrical signals are then passed down the auditory or cochlear nerve for higher brain processing and interpretation[21]. A disruption in any component of this pathway may result in hearing loss[21]. However, the pathologic conditions of the brainstem or auditory nerve don't often result in hearing loss[20]. The cochlea is most commonly involved, and to a lesser extent the middle and external ear are involved in development of hearing loss[20].

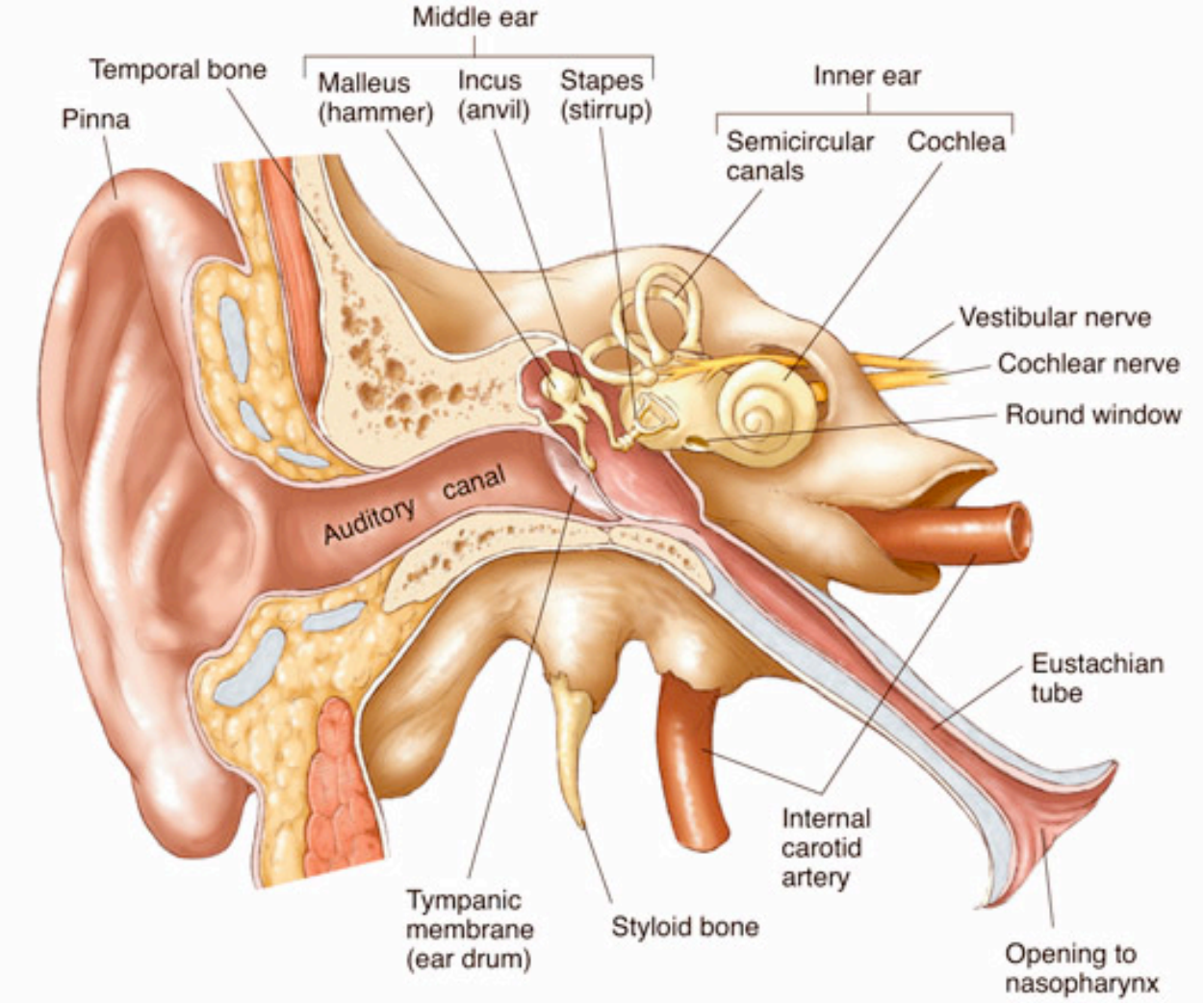

Fig. 3 Anatomy of the Human Ear[22]

Hearing loss is typically described as conductive, sensorineural, or mixed. Conductive hearing loss is when a change in the external or middle ear prevents sound waves from reaching the cochlea. Sensorineural, on the other hand, results from changes in the inner ear structures that result in the inability for nerve impulse to be successfully transmitted to the auditory cortex of the brain[21]. Mixed hearing loss is characterized as having elements of both sensorineural and conductive hearing loss.

Hearing aids remain the most common method for treating hearing loss, yet fewer than 24% of people who need a hearing aid actually own one [23]. Reasons for this low adoption rate include cost (51%), stigma and appearance (43%), and sound quality (24%). Stigma and appearance issues are attributed to the visibility of the hearing aid and sound quality dissatisfaction is in part due to feedback and the occlusion effect [23].

Hearing aid designs must compromise between visibility, feedback, and the occlusion effect. Two common methods for preventing feedback are to: (1) separate the microphone from the speaker; or (2) occlude the ear canal. The former makes the hearing aid more visible and the latter increases the occlusion effect. The occlusion effect can be reduced by adding vents to allow sounds trapped in the ear canal to escape [24]. However, these vents reduce the attenuation between the microphone and the speaker and therefore feedback is more likely to occur, reducing the level of amplification that can be applied. For those with severe hearing loss, a visible behind-the-ear hearing aid is the only option.

Groups have developed middle ear implants (MEI) to address the problems with hearing aids [25,26]. In general, these implants work by moving the ossicles, oval window, or round window with direct mechanical movements. This is in contrast to hearing aids, which uses amplified sound pressure to move the tympanic membrane. By driving the ossicles directly, the MEI operates silently and the occlusion effect and feedback are eliminated. This translates to better sound quality compared to conventional hearing aids [27,28]. Examples of these devices include the Vibrant Soundbridge (MED-EL; Innsbruck, Austria) and the Carina (Otologics; Boulder, CO). Despite the promise of middle ear implants, they suffer from several disadvantages, including prohibitive cost, invasive surgery, irreversible surgery, surgery for removal, and unknown

performance until after implantation.

Given the shortcomings of hearing aids and MEIs, there is a need for a hearing prosthesis for moderate to severe hearing loss that is invisible, produces no occlusion, and does not require invasive surgery.

2. Hearing Technology Background

The introduction provided a brief glimpse of the current hearing technologies available to those suffering from hearing loss, but this section will provide more detailed information about each group of devices. There are four main categories of hearing technologies commercially available today: traditional hearing aids, cochlear implants (CI), middle ear implants (MEI), and bone anchored hearing aids (BAHA).

Traditional Air Conduction Hearing Aids

Hearing aids are small electronic devices that are worn in and/or around the ear that function by taking environmental sound and amplifying it closer to the ear drum or tympanic membrane. These devices are composed of five general parts: a microphone, an analog to digital converter, digital processing unit that includes an amplifier stage, a digital to analog converter, and a speaker (also known as a receiver or loudspeaker)[29]. The greater a patients hearing loss the greater amplification needed to perceive sound. Approximately 1 in 4 individuals with a form of hearing loss are using a traditional hearing aid[18]. Adults and children, as early as 6 months of age, can be fit with hearing aids, and amplification level will be based on the patients hearing evaluation and reported difficulties[29].

These devices come in 5 main styles as depicted in Fig. 4: Behind-the-ear (BTE), “mini” BTE, In-the-ear (ITE), In-the-canal (ITC), and Completely-in-canal (CIC)[30]. The BTE hearing aid is generally used for mild to severe earing loss, while the CIC hearing aid is used for moderate to severe hearing loss. While the BTE has the disadvantage of being more visible, these devices are generally more powerful, produce less feedback, and provide better sound localization[14,30,31]. The CIC has advantages of being less visible, while suffers from more profound occlusion effect, higher cost, and less comfortable[14]. The cost of hearing aids range from a few hundred dollars to thousands of dollars per unit[14,32]. Additionally, hearing aids are generally not covered by most health insurance plans or Medicare; in some cases insurance may cover a portion of the cost[14,32]. Some of the leading companies that develop and manufacture hearing aids are: Oticon, Phonak, ReSound, Rexton, and Bernafon.

Fig. 4 Hearing Aid Styles[30]

Fig. 5 Mini behind-the-ear (BTE) hearing aid, the 'Milo' by Phonak[33].

The Lyric hearing aid (InSound Medical, Inc., Newark, CA) has recently been developed to address some of the concerns with traditional air conduction hearing aids, namely the aesthetic component. This device operates by the traditional sound amplification principle that other hearing aids use, but is placed deep within the ear canal and is not visible externally. The device is placed by a physician and remains constantly in place for approximately 3-4 months[29], then the user comes back in to have the device replaced. Users can shower with the device but it is not recommended for swimming or diving. However, due to potential feedback problems associated with a short distance between microphone and speaker, the device is only indicated for people with mild to moderately severe hearing loss who do not require significant amplification. The cost is based on a annual subscription model and is greater than the cost of replacing a standard hearing aid every 5 years[29].

A study conducted by to evaluate safety and comfort, and in this study 23% of the participants gave up using Lyric[34]. Some users report pain in the ear, irritation of the ear canal, and occlusion or moisture build up[35]. It was reported that a main issue for users removing the Lyric was the pain in the ear canal due to ear canal geometry being unsuitable for the Lyric device. However, of those who did keep the device in, 90% preferred the Lyric compared to their previously worn hearing aids[34].

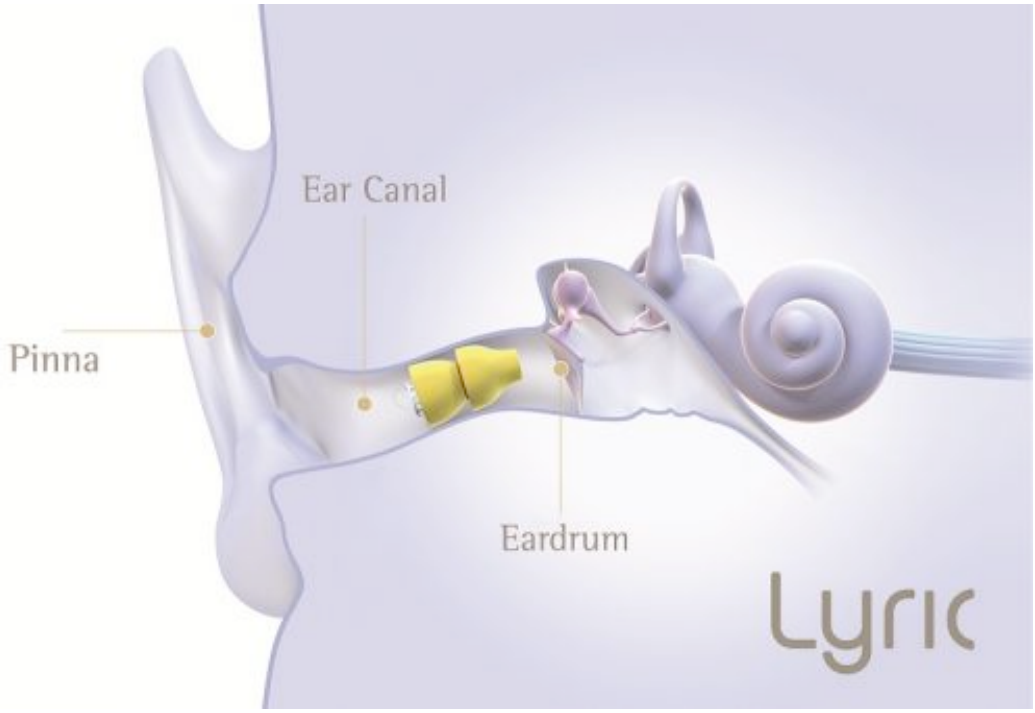

Fig. 6 The Lyric hearing aid by Phonak[36]. (Image courtesy of Phonak and reused with permission).

While hearing aids remain the most common technology used by those suffering from hearing loss, cost, stigma and appearance, and poor sound quality lead to low adoption rates and poor satisfaction reviews by users.

Bone Anchored Hearing Aid

The bone-anchored hearing aid (BAHA) is a technology that uses the principle of bone conduction to treat hearing loss. This device works by taking environmental sound and transmitting it to the inner ear through the bone, bypassing the ear canal and middle ear[37]. These devices are generally used in the treatment of hearing loss for those individuals with conductive and combined hearing loss[37,38]. Specifically, these devices are used where traditional air conduction devices are not appropriate; such as in patients with chronic otitis externa (also known as swimmer's ear), congenital ear canal atresia (non-developed ear canal), narrow ear canal, patients with anatomical abnormalities following mastoid surgery, or one-sided deafness [38–40].

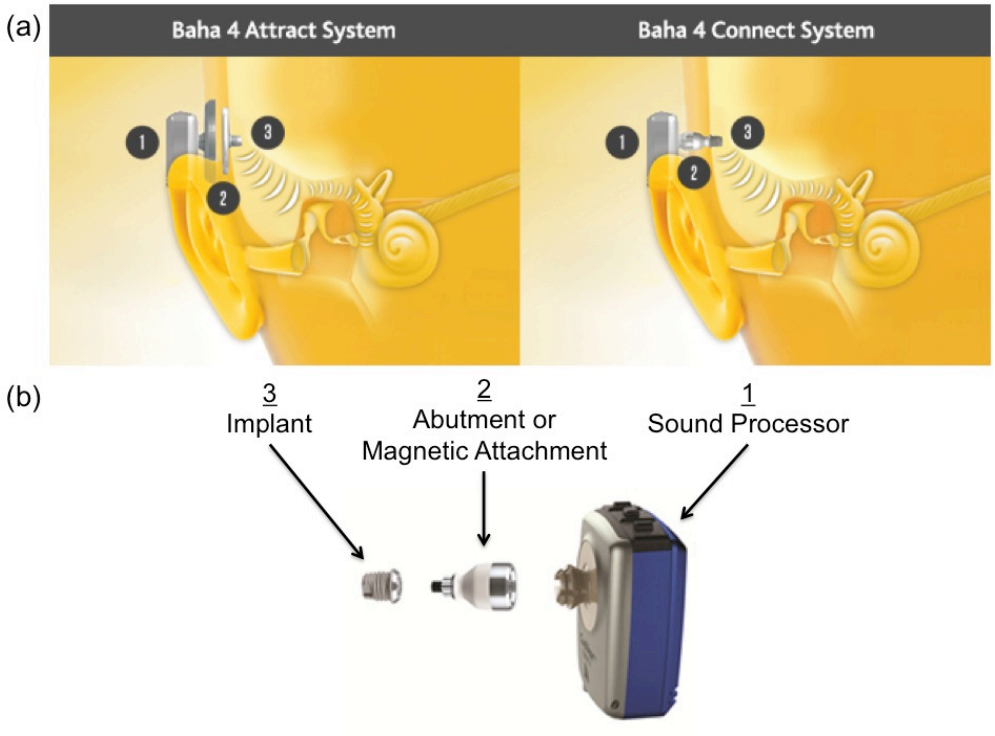

Fig. 7 Bone-Anchored Hearing Aid or BAHA (image in part taken from Cochlear™ (Sydney, Australia)[41]) (a) the BAHA consists of three main components: 1) sound processor 2) abutment or magnetic attachment 3) implant (titanium screw). This figure demonstrates two different BAHA systems, the one on the left has a magnetic attachment while the figure on the right has a trantional abutment where the titanium implant comes through the skin. (b) Exploded view of the three components of the BAHA device.

The BAHA device consists of three main components: the implant (titanium screw), the abutment, and the sound processor/bone conductor that attaches to the abutment [39,42,43]. The two primary companies who make the BAHA are Cochlear™ (Sydney, Australia) and Oticon Medical AB (Askim, Sweden). The procedure can be done under local anesthetic, but for children is generally under general anesthesia, and the entire procedure takes less than an hour[38]. The surgery consists of inserting the titanium implant into the bone, and is left to heal for approximately three months to allow for proper integration of the implant into the bone. Then the abutment and sound processor are placed. The 'BAHA Attract' system by Cochlear™, uses a slightly different attaching system where a magnet is placed under the skin with the implant and the sound processor is then attached magnetically as opposed to having the implant come through the skin[38].

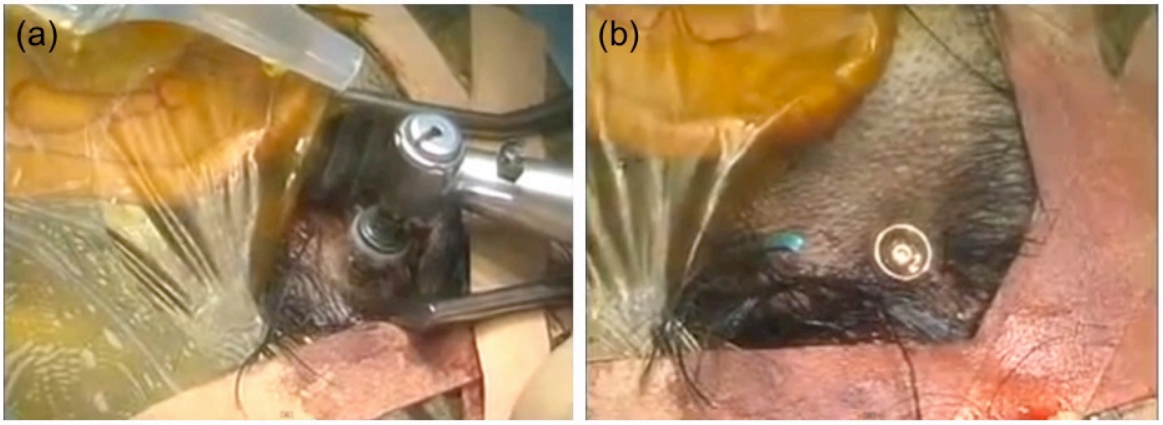

Fig. 8 Bone-anchored hearing aid surgical procedure (a) drilling of the titanium implant into the skull of the patient (b) completion of implant insertion. Next the patient will wait 3-6 months to allow for complete healing before the sound processor is placed. Images courtesy of Dr. Hamid Djaliilan at the University of California Irvine Medical Center[38].

One major advantage of this technology is the surgery is completely reversible if sound quality is not satisfactory for patients or if they change their mind. Some disadvantages of this

technology include, surgery, implant failures, adverse skin reactions, and a larger external prosthesis (less aesthetically pleasing)[44]. However, this technology is still considered to be a reliable and effective treatment for selected patients[44] and provides a good alternative if a patient can no longer use an air-conduction hearing aid[43,45].

Cochlear Implants

Cochlear implants work by using electrical stimulation to activate the auditory nerve[46]. In normal hearing sound pressure waves mechanically drive the TM, attached ossicular chain, oval window, and thus induce pressure oscillations within the cochlea[47]. These movements induce pressure oscillations in the cochlear fluids which create a traveling wave of displacement along the basilar membrane of the cochlea[47]. The basilar membrane is a specialized structure that divides the cochlea along its length, and is narrow and stiff at the base and wide and flexible at the apex. Lower frequencies create a maximum displacement near the apex of the cochlea, while higher frequencies produce maxima near the base of the cochlea, thus leading the cochlea to be organized tonotopically[47,48].

Hair cells are attached to the top of the basilar membrane in a matrix called the organ of Corti and sense the movement of the membrane. These hair cells are mechanotransducers and thus when they are deflected, create an electrical spike or action potential[48]. The combined activation of hair cells sends information along the auditory nerve to higher brain centers for complete processing of auditory information. In the case of hearing loss, and primary cause can be the malfunction of the sensory hair cells. The cochlear implant works by bypassing the missing or malfunctioning hair cells and directly stimulates the surviving neurons of the auditory nerve, and thus facilitating sound transmission.

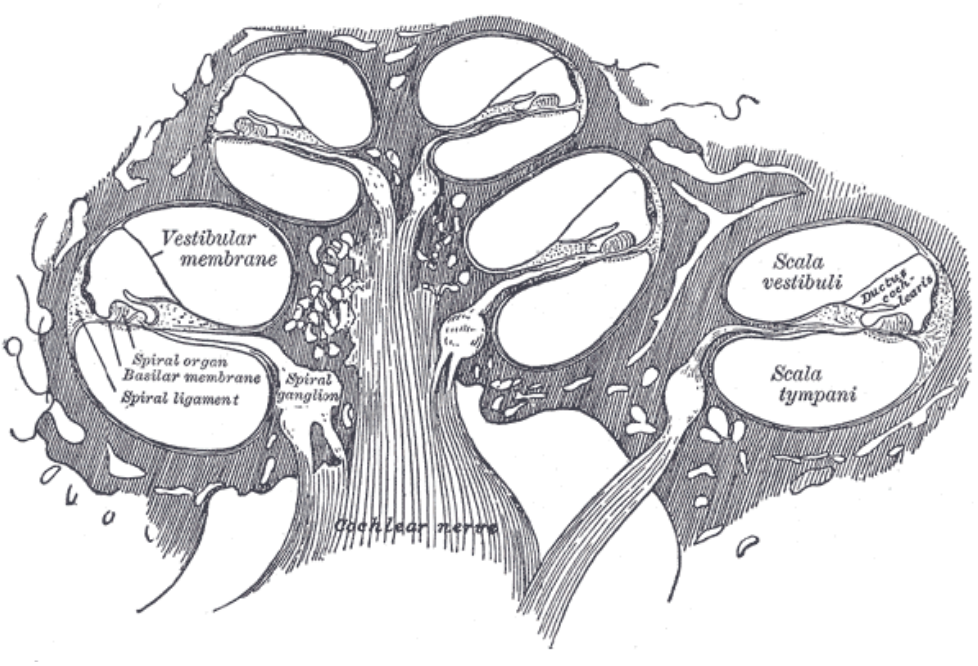

Fig. 9 Longitudinal cross section of the cochlea (image courtesy of Grays Anatomy)[49]

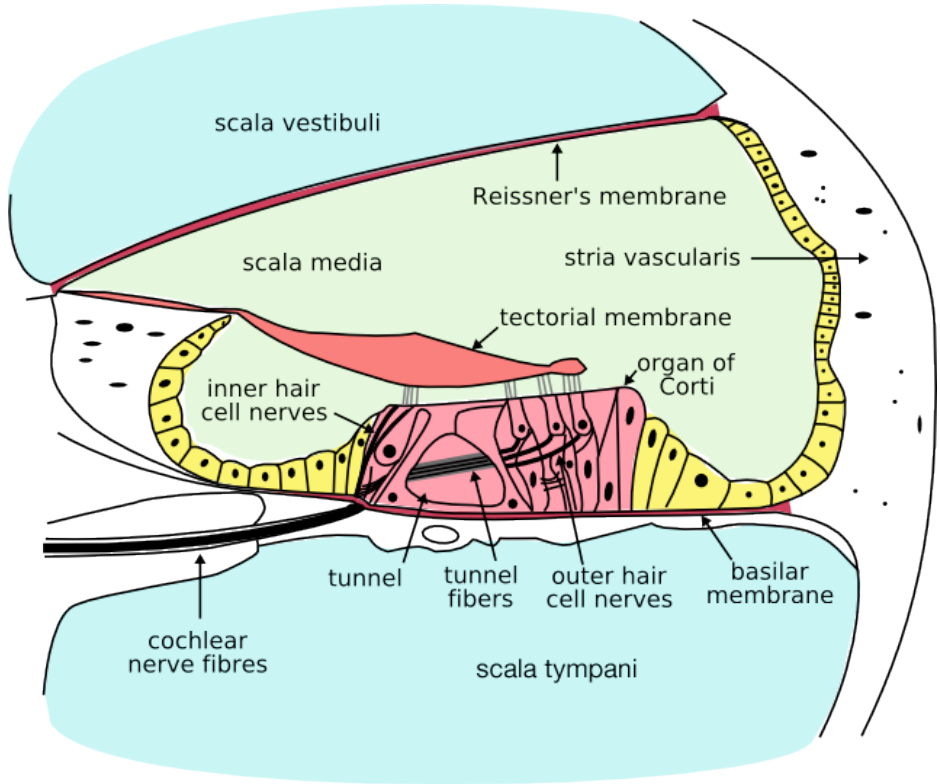

Fig. 10 Cross section of the human cochlea (image courtesy of Oarih Ropshkow)[50].

The primary companies that develop and manufacture cochlear implants are Cochlear ™ (Sydney, Australia), MED-EL GmbH (Innsbruck, Austria), and Advanced Bionics (Stäfa, Switzerland). Recently, Oticon Medical acquired the French Neurelec SA (a division on William Demant), which is also a cochlear implant manufacturer bringing a fourth major company into the cochlear implant space[51].

The Food and Drug Administration (FDA) reports that as of December 2012 approximately 324,200 individuals worldwide have been implanted with a cochlear implant[52]. The United States has roughly 58,000 adult recipients and 38,000 child recipients.

A typical cochlear implant system has five key components: a microphone, speech processor, transmitter, receiver/stimulator, and an electrode array[46]. The system works by the microphone picking up environmental sound and sending the sound information via a wire to the speech processor worn behind the ear. Then the speech processor converts the sound into a digital signal that is tailored specifically to the patients' type and level of hearing loss. That signal then travels to the transmitter that contains a coil transmitting coded radio frequencies across the skin to the receiver. The transmitter is magnetically held in place and coupled to the receiver that is implanted under the skin[46]. The receiver contains a coil and hermetically sealed electronic circuits that receives the radio frequency signal, decodes it, and converts it into an electric current. This signal is sent down a wire to the electrode array that has been implanted in the cochlea. These electrode sites will then stimulate the auditory nerve, which is then perceived by the user as sound.

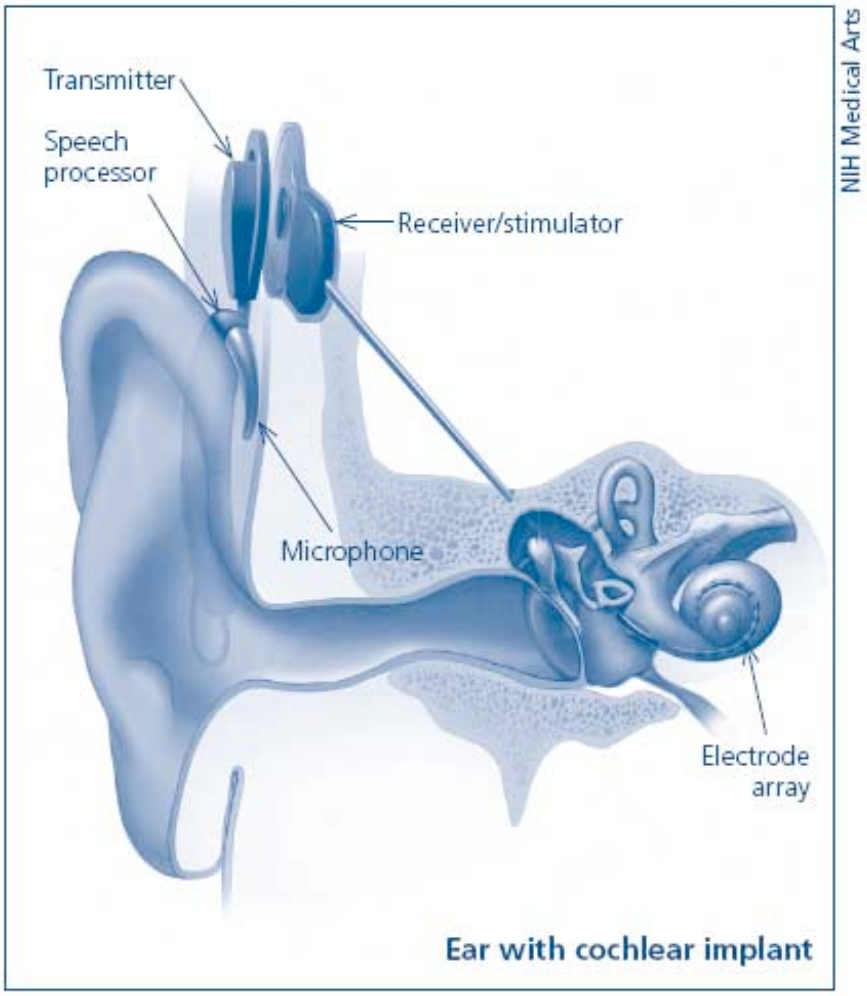

Fig. 11 Cochlear implant (courtesy of NIH Medical Arts[53])

A cochlear implant, which includes surgery, adjustments, and training, costs approximately $60,000 (in 2010)[54]. In recent years health care coverage for cochlear implants has improved, and now many providers give some level of benefits for the device and services associated with the implant. The American Speech-Language-Hearing Association believes this increase in coverage is due to increased education and awareness of the outcomes of cochlear implants. Additionally, they believe that that recent federal and state laws, such as the Americans with Disabilities Act, prohibit exclusionary practices by insurance companies that prevent candidates from alleviating their hearing loss[55].

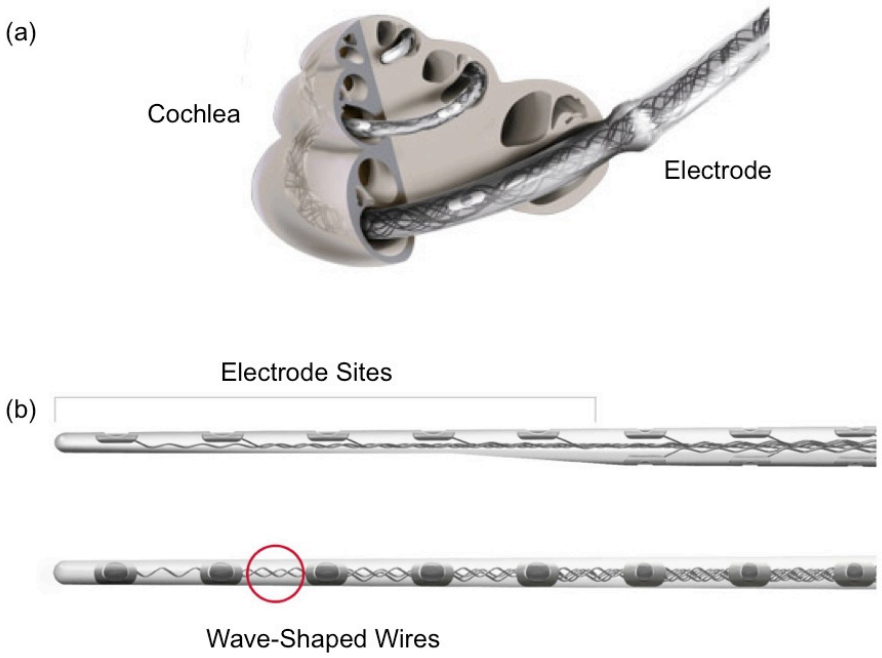

Fig. 12 Cochlear implant electrode (image in part courtesy of MED-EL Corp. (Innsbruck, Austria)[56] (a) electrode implanted in the cochlea of the inner ear (b) stretched out electrode with electrode sites and wires visible.

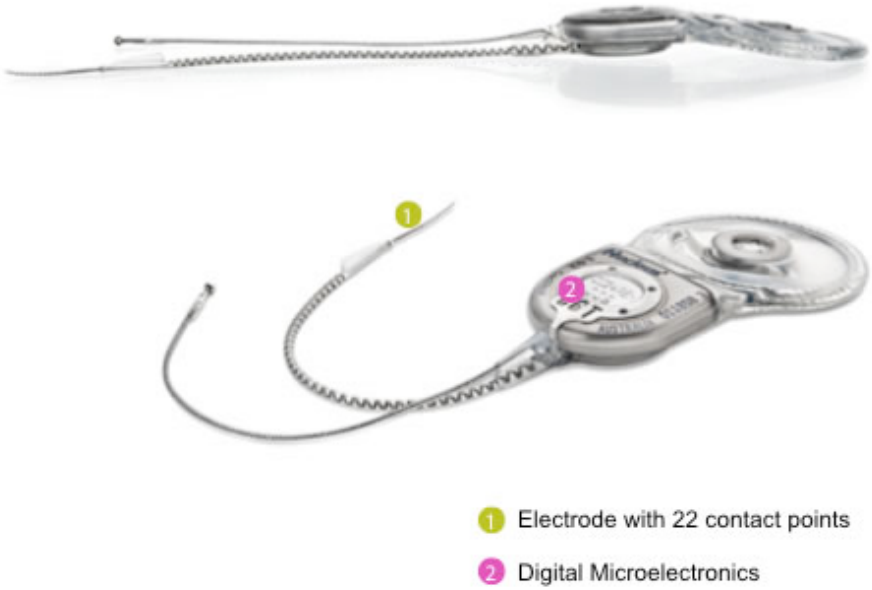

Fig. 13 Cochlear™ Hybrid implant (image courtesy of Cochlear (Sydney, Australia)[57]. This is the receiver/stimulator that is implanted under the skin and the electrode (1) is placed within the cochlea. The second electrode that is not marked is the ground electrode. This specific implant is for a hybrid implant technology, and treats mostly high frequency hearing loss and thus has a shorter stimulating electrode.

Middle Ear Implants (MEIs)

Some of the first instances of implantable hearing devices that mechanically drive the middle ear system came in 1935, when Wilska and colleagues placed magnets on the tympanic membrane and drove them using a coil in the outer auditory canal[37,58,59]. This discovery then paved the way for other embodiments that could mechanically drive the middle ear system to facilitate sound transmission and serve as a solution for both conductive and sensorineural hearing loss. Direct drive stimulation of the middle ear drastically reduces the main problems associated with the traditional air conduction hearing aids such as poor acoustic quality, feedback, occlusion, and ear canal hygiene issues[60]. This section will review a series of the technologies and methods that have been used to drive the middle ear system.

Rion Device

The "Rion Device Type-E" is a piezoelectric device that is used for both conductive and sensorineural hearing loss. This device was the first piezoelectric semi-implantable device, which was originally developed in 1983 by Yanagihira, Gyo, Honda, Sato, and Hinohira[37]. It has since been implanted in about 100 patients in Japan[61]. This device has an internal unit that consists of a ossicular vibrator and a magnetic coil connected by a wire, and the external unit has a microphone, amplifier, external coil, and battery. The ossicular vibrator can be attached to multiple places on the ossicular chain, preferably the incus, but if portions of the chain are missing it can also be connected to a columella on the footplate. While this device continued to work in some patients for up to 15 years, many of the devices were removed due to termination of function[62]. Therefore the device has decreased efficacy over time[59]. It has also been stated the device is no longer in production due to manufacturing issues[63,64].

Vibrant Soundbridge

The Vibrant SoundBridge (VSB) device is produced by MED-EL GmbH (Innsbruck, Austria) and is a FDA approved middle ear implant used to treat sensorineural hearing loss[60,65]. This device was originally manufactured by Symphonix (San Jose, CA, USA), but was then taken over by MED-EL[63]. It is the most commonly used MEI and is composed of both internal (surgically implanted) and external components.

Fig. 14 Vibrant Soundbridge middle ear implant components[66] (a) actual image of the internal components of the VSB that is implanted under the skin with the FMT attached to the long process of the incus (b) actual image of both external and internal components of the VSB middle ear implant system. (Image courtesy of MED-EL GmbH, reused with permission)

The internal is composed of the vibrating ossicular prosthesis (VORP) that consists of a receiver with a coil and processing element (implanted under the skin), which then connects to the floating mass transducer (FMT). The FMT is an electromagnetic transducer that clips to the incus of the intact ossicular chain. The external component of the VSB contains the audio processor, the microphone, the battery, transmitting coil, and magnet to couple the external and internally component. Sound is received by the external component, processed, passed transcutaneously to the internal component, and lastly that signal is used to mechanically drive the FMT[37]. It has been shown the Vibrant SoundBridge device remains a highly reliable implant system and the performance does not deteriorate over time (studies in patients implanted for 5-8 years)[67,68]. More recently the device has been explored as a solution in mixed hearing loss by positioning the FMT adjacent to the round window[64,69].

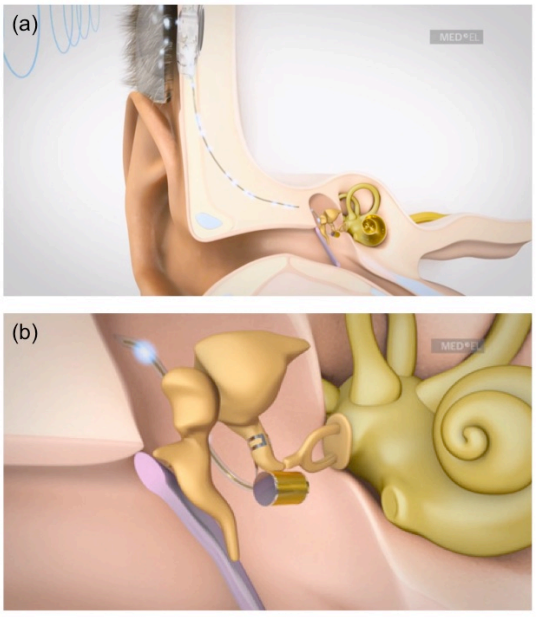

Fig. 15 Vibrant Soundbridge System animation[66] (a) entire system of internal and external components (b) close up of the FMT attached to the incus mechanically driving the ossicular chain and facilitating sound transmission. (Image courtesy of MED-EL GmbH, reused with permission)

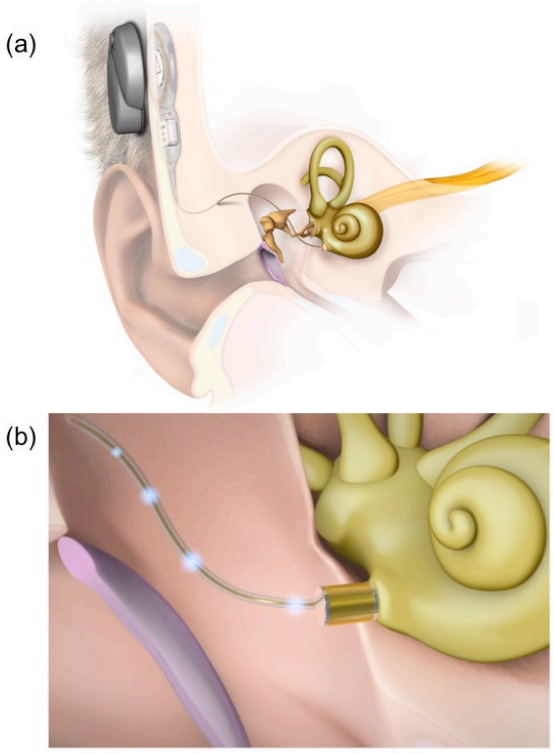

Fig. 16 Vibrant SoundBridge animated device placement for mixed or conductive hearing loss applications[66]. (a) entire system with FMT coupled to the round window (b) magnified view of the FMT coupled to the round window. (Image courtesy of MED-EL GmbH, reused with permission)

Fig. 17 MED- EL Sports Headband[66]. This can be used for patients with the implant during any physical activity to hold the external process in place correctly. It can also be used to have the device less visible and more aesthetically pleasing. (Image courtesy of MED-EL GmbH, reused with permission)

Soundtec Direct / Ototronix Maxum Device

The MAXUM Hearing Device was originally developed an manufactured by SOUNDTEC, Inc. (Oklahoma City, Oklahoma) but was then acquired by Ototronix (Houston, Texas) in 2009. This system works by using a Neodymium-Iron-Boron (NdFeB) magnet that is surgically implanted on the incudostapedial joint on the ossicular chain[70,71]. The surgical placement of the magnet is a tympanoplasty under local anesthetic in an office setting; this is a much less involved surgical procedure when compared to other MEI type devices[64]. Therefore this device is totaled a 'minimally invasive' hearing technology. The earmold/coil assemble is placed in the ear canal and has an embedded electromagnetic coil. The sound processor that is also encased in this unit take environmental sound, converts it to an electrical signal, amplifies the signal, sends that to the coil to introduce an electromagnetic field that will in turn drive the implanted magnet[70].

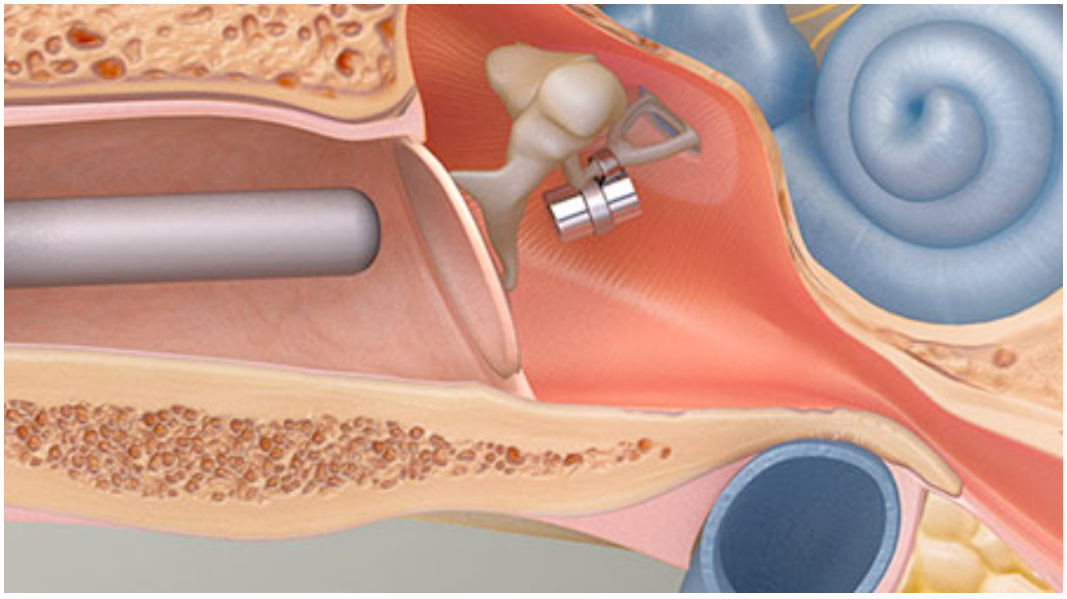

Fig. 18 Magnified view of the MAXUM device implant attached to the ossicular chain.

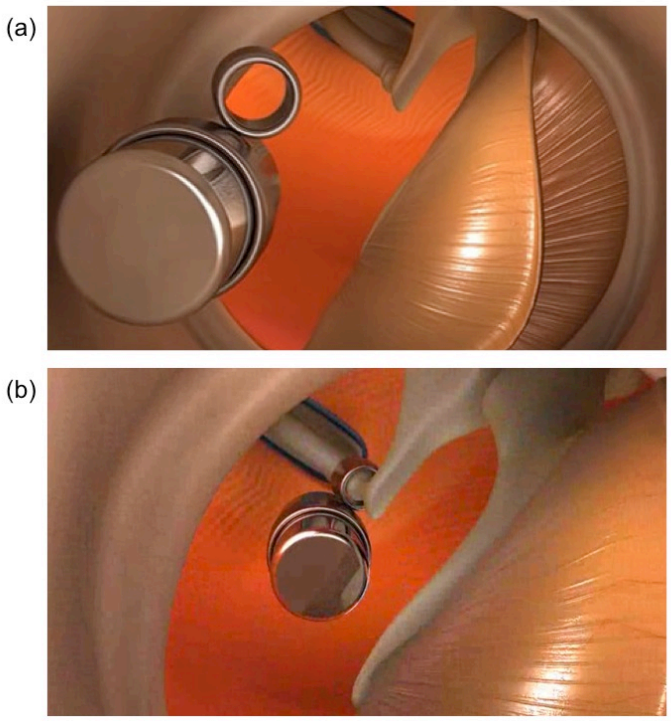

Fig. 19 MAXUM hearing device implant during the minimally invasive surgical placement (a) animation of tympanoplasty and placement of the MAXUM magnet implant (b) final placement of the MAXUM implant on the ossicular chain.

Since this device does not have a speaker feedback is reduced or eliminated. In addition, the component that is placed within the ear canal does not completely block the ear canal occlusion can be minimized[72]. This device is currently FDA approved.

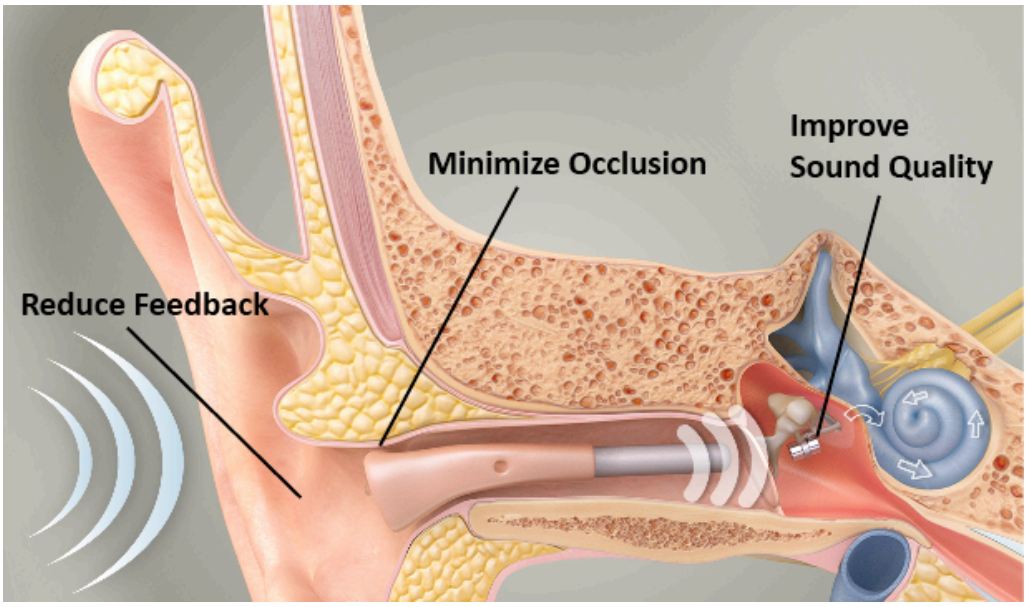

Fig. 20 MAXUM Hearing Device System

Otologics Middle Ear Transducer (MET) Carina® Device

This device is produced by Otologics LLC (Boulder, Colorado, USA). This device obtained approval to treat both sensorineural and conductive/mixed hearing loss[73]. This is a different than other MEI technologies as it is a completely implantable device, and thus can be used while swimming or showering[64]. This device consists of a subcutaneous microphone, an internal amplifier, and a piezoelectric actuator that drives the incus[64]. This device has been shown to be a viable treatment for moderate to severe hearing loss[73,74].

The device is intended to connect to the incus body, but can also be attached to the stapes super structure, stapes footplate, and the round window as depicted in the figure[37]. The reactive power of the transducer is absorbed by the fixation of the implant to the mastoid bone, and thus has more efficient energy expended as compared to other MEIs[37]. One major disadvantage of this technology is since the device is fully implantable, a surgery is required for battery

replacement, which is guaranteed by the manufacturer for 5 years[37]. The devices are currently underdoing FDA approved clinical studies. However, in 2012 Otologics LLC filed for Chapter 11 bankruptcy and are currently negotiating with possible buyers[75]. The device is still available upon request[37].

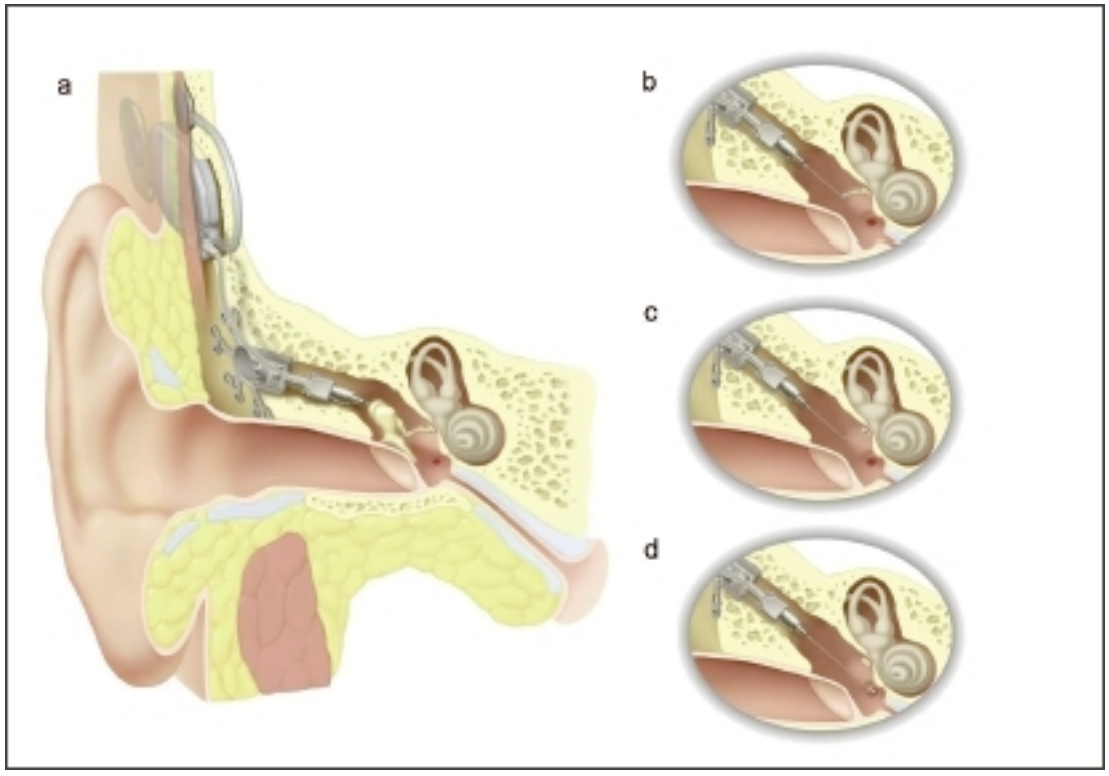

Fig. 21 The fully implantable Carina® hearing device (Otologics LLC, Boulder, CO, USA)[37,76]. (a) Intended connection to the incus body (b) different connection embodiments to the: stapes superstructure (c) stapes footplate (d) round window membrane. (Image courtesy of Otologics LLC and the National Library of Medicine)

Envoy Esteem

Esteem® The Hearing Implant™ is a FDA-approved (March 2010) fully implantable middle ear hearing device used to treat moderate to severe sensorineural hearing loss in adults. The device is developed and manufactured by Envoy Medical (St. Paul, MN, USA). This device

functions by using a piezoelectric sensory and actuating element connected to the processor and battery element that is implanted in the parietal bone bed. The surgical procedure is reversible[77].

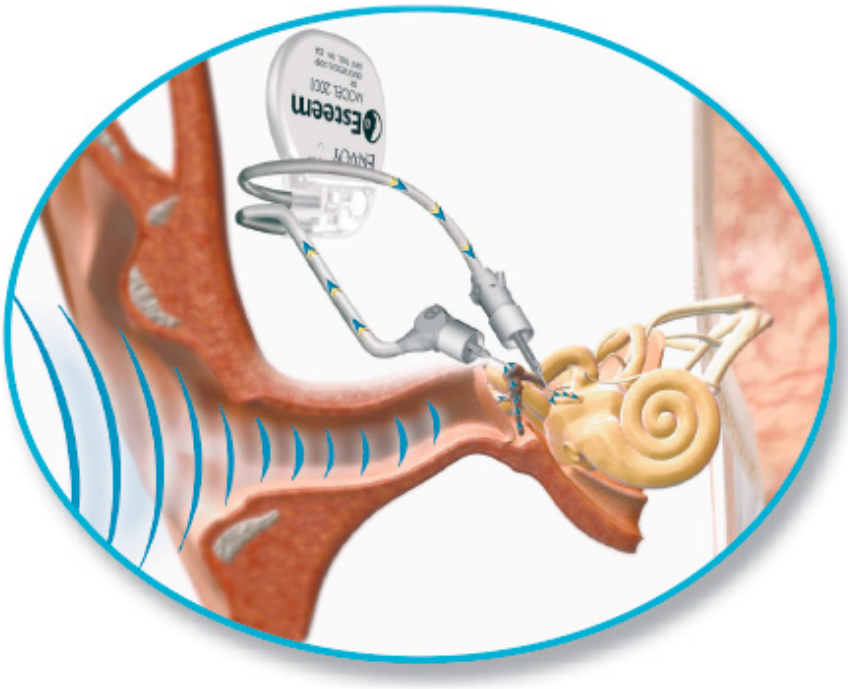

Fig. 22 Totally implantable Esteem® Hearing Implant by Envoy Medical.[78] (Image courtesy of Envoy Medical; St Paul, MN)

The sensing element is coupled to the incus body and functions as a microphone by sensing the vibrations of the incus due to sound. The piezoelectric driver is cemented to the stapes head. This embodiment requires a severing of the ossicular chain at the long process of the incus. Vibrations are picked up by the incus sensor, filtered and amplified by the processor, and transferred to the stapes driver. As with the Carina® device, this system is fully implantable, and this requires the battery to be surgically replaced. The manufactures quote the battery to last from 4.5 to 9 years depending on usage, but can be as short as 2.8 years when the highest gain settings are used[78]. In Phase I trials patients perceived the Envoy System to have increased benefit over their traditional hearing aid including communication in high background noise situations[79].

Overall clinical trials describe the Esteem System to be a safe and reliable system for hearing restoration for moderate to severe sensorineural hearing loss[80].

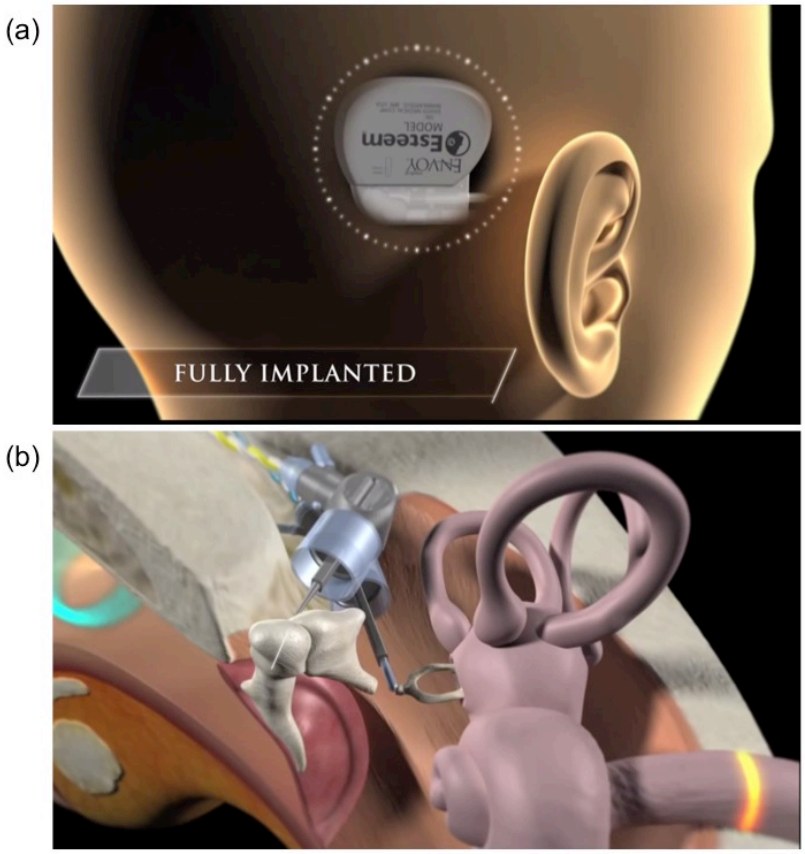

Fig. 23 Esteem Hearing Implant[78] (Envoy Medical, St, Paul, MN, USA) (a) Implanted battery and processing unit (b) magnified view of the sensing and driving system. (Image courtesy of Envoy Medical; St Paul, MN)

EarLens

This EarLens® technology had its beginning in 1996 with Rodney Perkins and colleagues who formed ReSound Corporation (Then: Redwood City, CA USA Now: Bloomington, MN, USA). The technology then moved to EarLens® Corporation (Redwood City, CA, USA) where it currently resides. The original device was composed of two elements: the transducer and a magnetic field generating device to drive the transducer[81]. The transducer was composed of a magnet mounted on a thin conical silicone platform similar to a contact

lens[81]. The lens was held in place with a droplet of mineral oil. The magnetic field device came in two forms, one that sat behind the ear and another that was worn around the neck. The device was successful in amplifying sound using the two embodiments without causing irritation to the TM. However, it was determined that this method was highly inefficient and proved to be impractical for a commercial product[82].

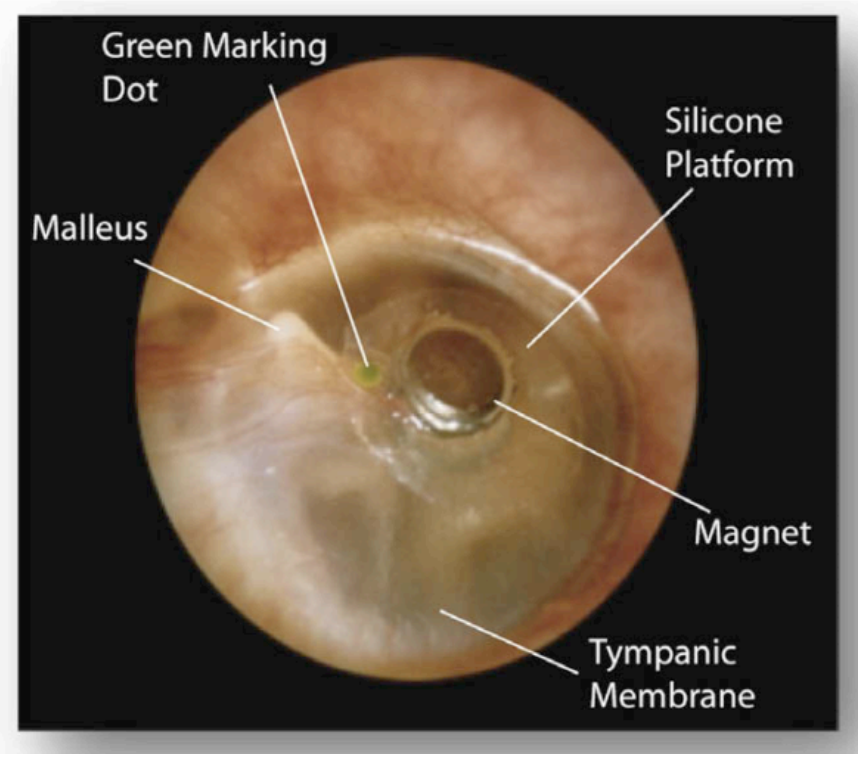

Fig. 24 Close-up view of the EarLens transducer system. This device is placed on the tympanic membrane and utilizes a green marking system to align the device with the malleus. (Image courtesy of Perkins et al,[82] reused with permission)

The next iteration of the device used the same concept for the tympanic membrane lens with an embedded magnetic, but this time used a new open-canal hearing device as the driving mechanism. Sound is picked up by the microphone, processed and amplified, and then used to drive a coil that is located near the TM transducer lens. The results of this study showed that TM lens was well tolerated and stayed in place for the 10-month period trial. It also showed this

system can produce output to ready threshold for this with as much as 60 dB HL of hearing impairment[82].

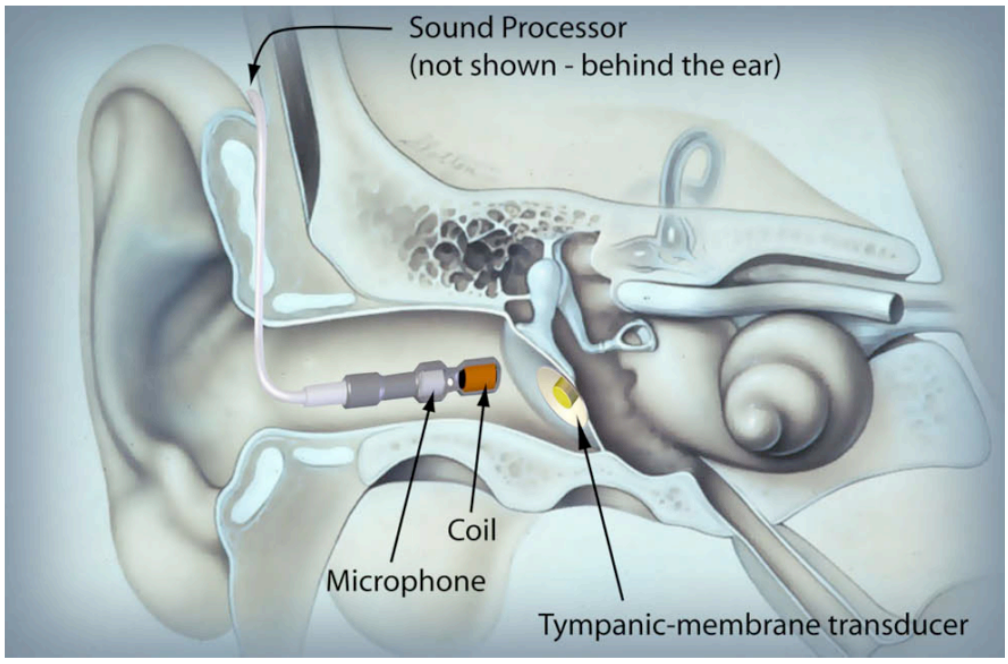

The most recent advancement of this technology is to use an alternative system that uses photonic energy to transmit both the signal and power to a photodiode and microactuator that is located on an EarLens platform[82,83]. They company is currently conducting a feasibility study with this new technology that is scheduled to be completed in 2014[84].

CHAPTER 2

The Direct Hearing Device (DHD)

1. Direct Hearing Device (DHD)

Our group is developing a direct hearing device (DHD), a novel auditory prosthesis for moderate to severe hearing loss that is invisible and can be placed without surgery. The device is placed deep in the ear canal and recreates sounds by driving the tympanic membrane or the umbo directly.

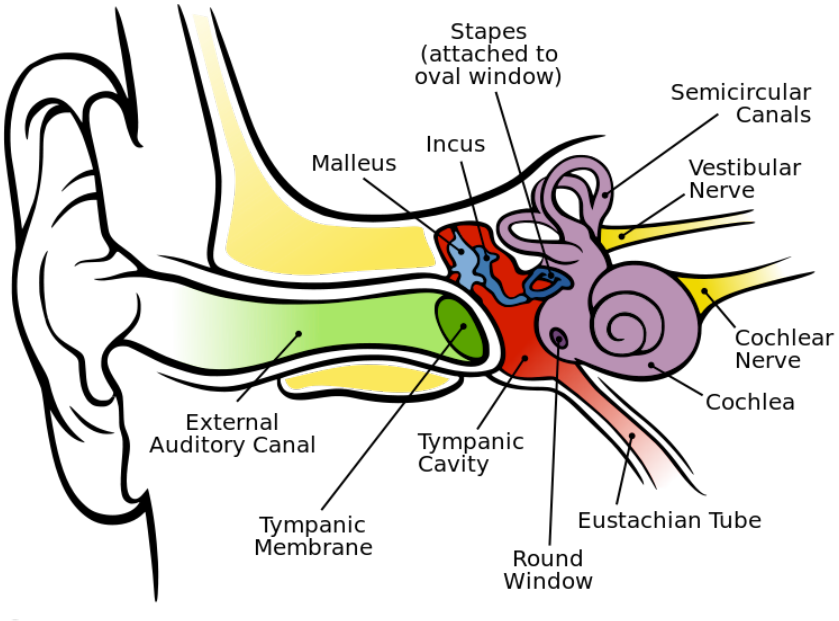

Fig. 25 Anatomy of the Human Ear[85]

Similar to a hearing aid, the device is placed in the ear canal and therefore no surgery is required for placement or removal. But, since it recreates sound by mechanically moving the tympanic membrane and ossicular chain, sound quality limitations, such as feedback and the occlusion effect, can be reduced. In addition to our work, other groups have also explored direct

actuation of the tympanic membrane and ossicular chain, for example, by using an electromagnet to drive a small magnet attached to the tympanic membrane [82].

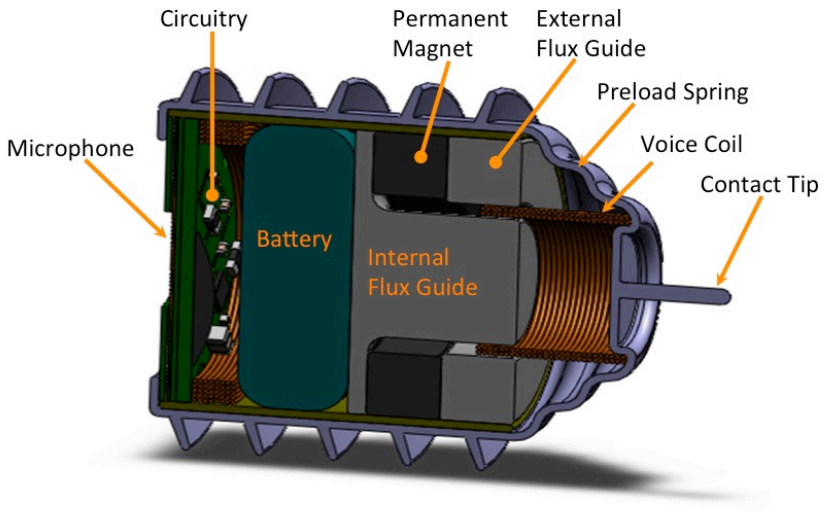

Fig. 26 Direct Hearing Device (DHD) conceptual design composed of the DHD actuator as well as battery, microphone and signal processing circuitry.

A direct hearing device would consist of a microphone, amplifying electronics, and a driver or actuator to drive the TM and the ossicular chain. A critical component of our direct hearing device is the direct hearing device actuator (DHDA), which must meet several criteria to be suitable as a tympanic membrane driver. This includes appropriate, smoothly varying frequency response, low-distortion movements, and silent operation. In this paper we give an overview of the DHDA and present initial characterization data demonstrating its suitability as a tympanic membrane and ossicular chain driver.

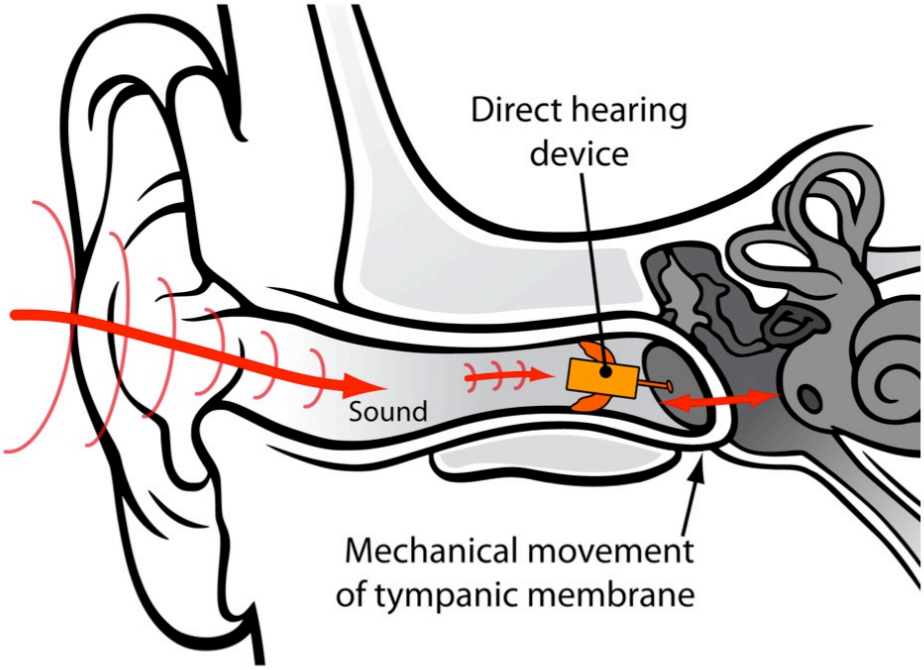

Fig. 27 Schematic drawing of a DHD in the ear canal. A microphone on the DHD detects sound entering the ear. The DHD actuator recreates the sounds with movements of the tympanic membrane (image in part from [85]).

2. Design

The DHDA must meet several performance criteria to faithfully reproduce sounds with mechanical movements. It has to satisfy several practical requirements to be feasible for prosthesis use. From a performance perspective, the DHDA must have the appropriate dynamic range in both frequency (20 Hz to 20 kHz) and displacement (10 µm to less than 1 nm) [8687]. The distortion across this range must be minimal since the sensitivity of the ear will translate these distortions into perceived noise to the user. Additionally, actuation must produce little or no sound. Audible noise from the actuator is a potential source of feedback and could be directly perceived by the user.

From a practical perspective, the DHDA must be small enough to fit within the bony portion of the ear canal. To ease placement requirements, it must accommodate relatively large

variations in distance from the tympanic membrane without influencing device performance. Performance should also not be influenced by the natural static movements of the tympanic membrane (e.g., from changes in air pressure).

A specialized voice coil actuator was designed for the driving mechanism. This design had several desirable features: (1) a lightweight moving component to minimize loading effects; (2) a flat response; (3) constant performance across large displacements since there was a constant number of coils in the active region and; (4) nearly frictionless motion.

The magnetic flux circuit of the DHDA was formed by a permanent magnet, outer flux guide, and inner flux guide. This flux circuit directed the magnetic flux through the small air gap between the inner and outer flux guides. The voice coil was located in this air gap and an axial force was produced when current passed through the coil. The density of voice coil turns within this air gap remained constant and therefore the force produced for a given current is constant over a large range of displacements. The spring held the voice coil in place and was used to provide a preload force between the interface tip and the tympanic membrane. This arrangement provided low friction, since the spring was the only source of friction. Frictionless motion was critical in achieving the large dynamic range in displacement and frequency without undue distortion.

3. Manufacture

The permanent magnet was a grade N45, nickel-plated, neodymium (NdFeB) magnet. The inner and outer flux guides were made of iron and were chosen due to iron's high magnetic permeability. The inner and outer flux guides are made on a computer numerical control lathe and mill (Haas Automation Inc.; Oxnard, CA). The voice coil was a two-layer, air core coil formed with 0.031 mm diameter (48 AWG), polyurethane-coated, copper magnet wire. The DC

resistance of the voice coil was 22 Ω and it had a maximum DC current threshold of ~95 mA (4.75 V) before failure.

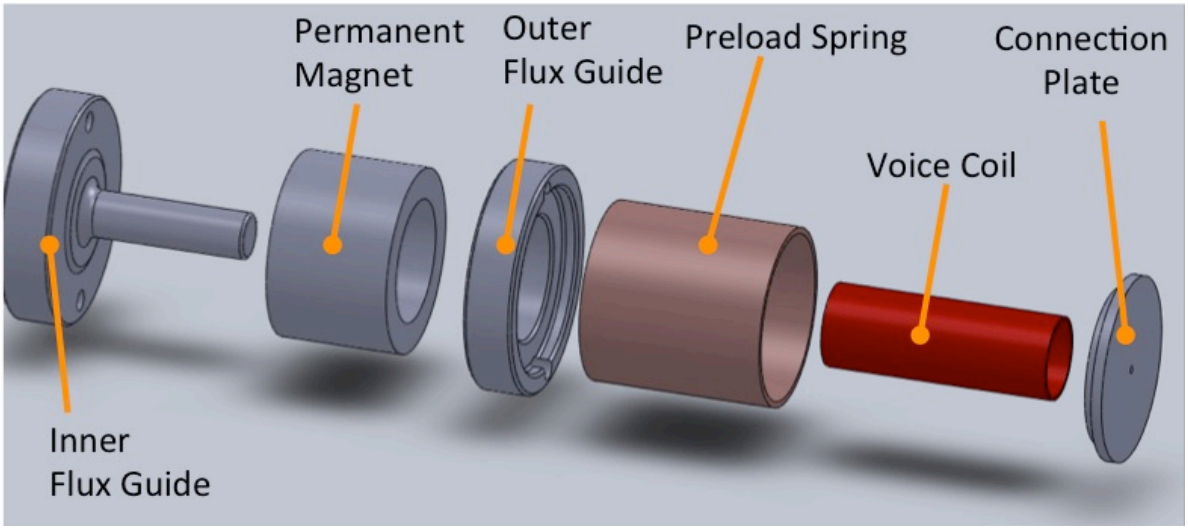

Fig. 28 Computer aided design (SolidWorks; Dassault Systems SolidWorks Corp.) 'exploded view' of DHDA component assembly

The spring had approximately 4 active turns, was formed from 0.089 mm diameter, silver-coated, beryllium copper wire, and has a spring rate of 0.0044 N/mm (Economy Spring and Stamping Co.; Southington, CT). This spring design was a balance between achieving a low spring constant and practical fabrication methods. It was also critical to have a completely nonmagnetic spring. Since the spring had a very small spring constant and was in contact with the magnetic flux circuit, springs with even the smallest magnetic properties (e.g., stainless steel) would collapse due to magnetic forces.

The DHDA displacement had an operating range of 3 mm. Pressure differences can exist between the middle ear cavity with ambient pressures reaching over 1 kPa. This static pressure change deforms the tympanic membrane and can result in tympanic membrane static displacements over 0.4 mm at 1.6kPa [88,89]. During natural hearing the tympanic membrane has a maximum displacement of 6 μm [90]. This gives the DHDA placement tolerance of ~2.6 mm, a

range large enough to allow the device to be placed by hand. The average human external auditory ear canal is composed of two segments; the lateral cartilaginous portion and the medial osseous portion [91]. The dimensions of the external auditory canal is approximately 7 mm in diameter and 26 mm in length; [92]. The osseous portion of the ear canal averages approximately 8.5 mm in length [91]. Therefore, with a diameter of 3.7 mm and a length of 6.2 mm, the DHDA was designed to fit completely within the bony portion of the ear canal.

This actuator design enabled nearly friction-free motion, which lowered movement distortion, allowed fine movements, and reduced any sound generated by the device. It also allowed large static displacements of the actuator without affecting its dynamic performance since the density of wire turns within the air gap was constant.

4. Assembly

The DHDA is assembled by hand and uses quick drying epoxy to adhere each individual component. To assure the leads of the voice coil are protected two holes are drilled in the outer and inner flux guide to provide protective slots for the leads. This way during assembly and operation the fragile wires are protected and not exposed. Once the actuator is completely assembled a protective sheath is slid over the entire actuator. This is a plastic sheath with a thin wall diameter as to not substantially add to the overall device diameter.

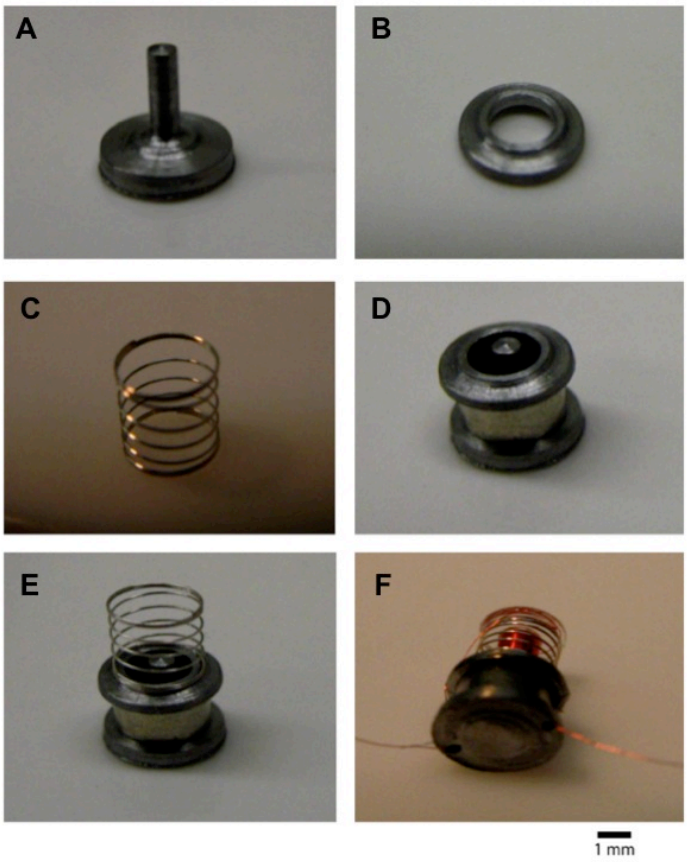

Fig. 29 DHD actuator components a) inner flux guide b) outer flux guide c) spring d) inner flux guide, permanent magnet, and outer flux guide assembly e) assembly in part d with spring added f) fully assembled actuator with micro holes drilled in the outer and inner flux guides to allow for the voice coil leads to be protected during operation

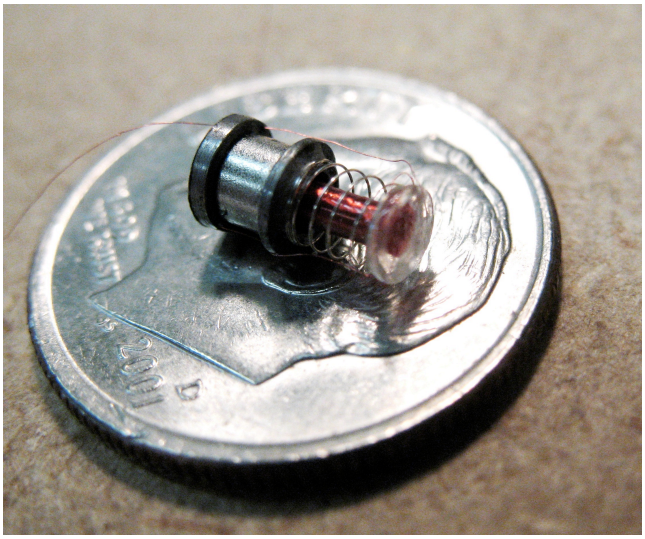

Fig. 30 Assembled DHDA on a dime.

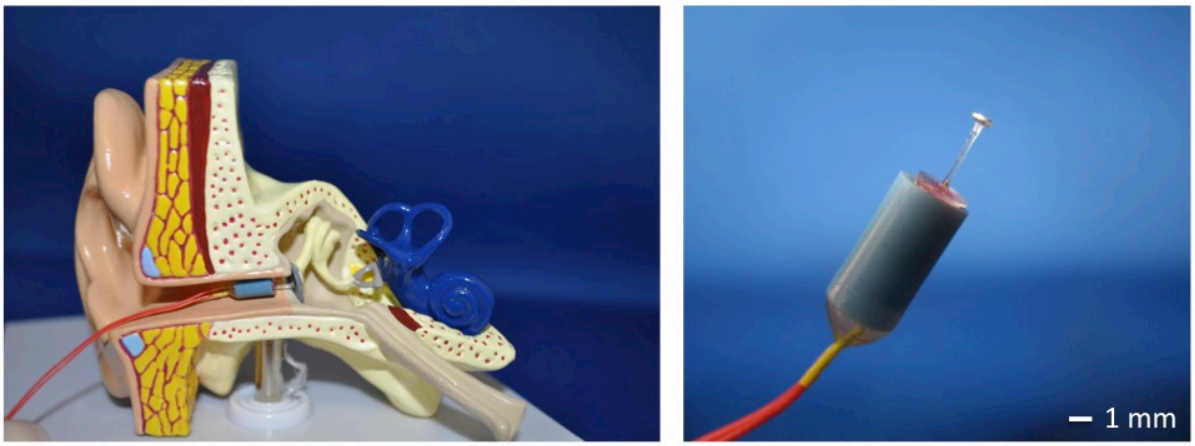

Fig. 31 (Left) DHDA placed within the ear canal of an artificial middle ear (right) DHDA assembled and placed within a protective sheath. An additional interface tip was added to the contact plate demonstrating one example of a possible tympanic membrane interface embodiment.

5. DHDA Characterization - Frequency Response

The DHDA was characterized at the California Institute of Telecommunications and Information Technology (CalIT2) Microscopy Center at the University of California Irvine. The frequency response, total harmonic distortion, and sound generation were determined by driving the device with a frequency sweep while recording its displacement. Displacements were measured with a laser Doppler vibrometer (LDV) system, which consisted of an MSA-500 Micro System Analyzer, an OFV-5000 Modular Vibrometer Controller, a DD-900 displacement decoder, and a VD-09 velocity decoder (Polytec; Irvine, CA).

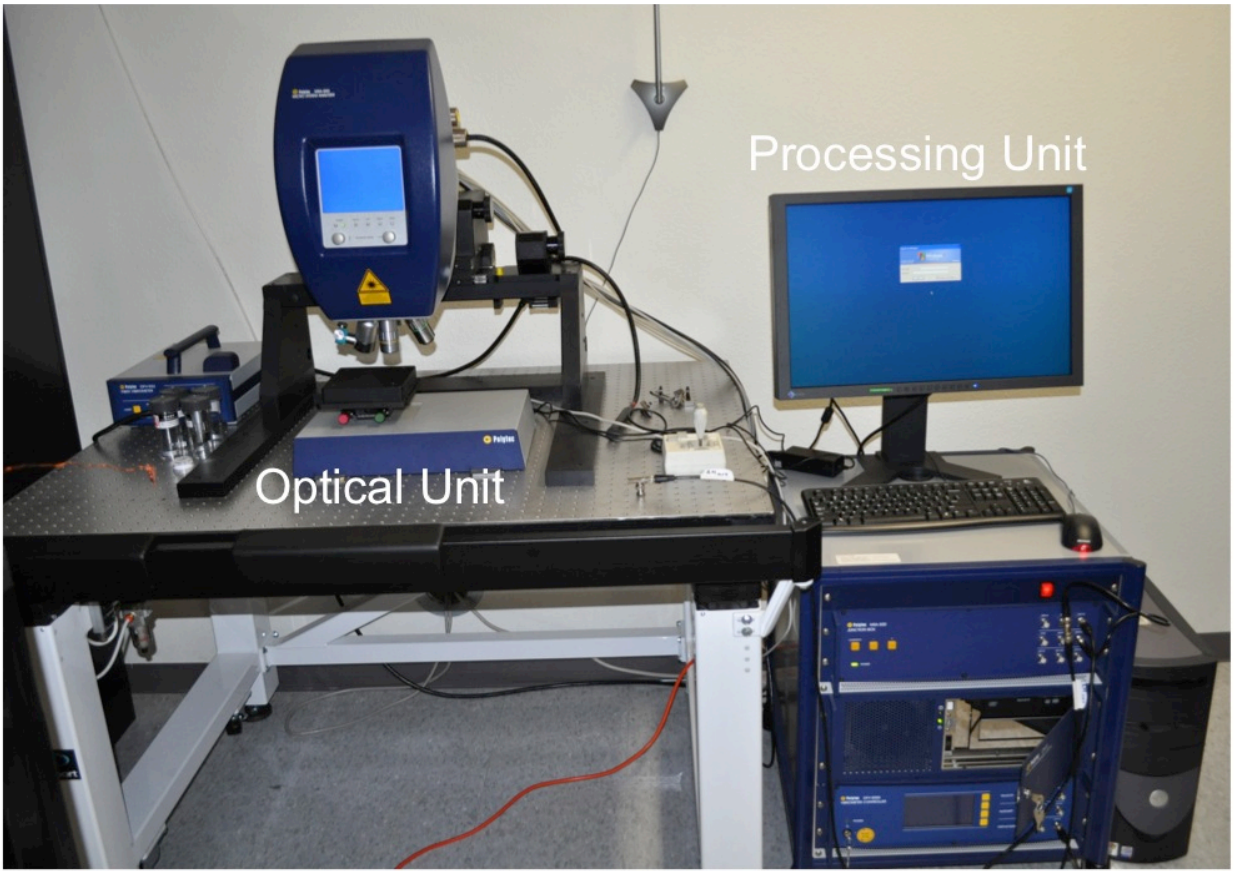

Fig. 32 Laser Doppler Vibrometer testing setup. The DHDA will be placed under the optical unit (left) and all displacement data will be sent to the processing unit (right) for analysis.

A small piece of retroreflective tape (Polytec) was placed on the connection plate to improve the reflectivity, increase laser signal strength, and reduce the influence of out-of-plane motions on laser signal strength. Displacements were measured with respect to a single point on the reflective tape, which was selected on the basis of maximizing laser signal strength.

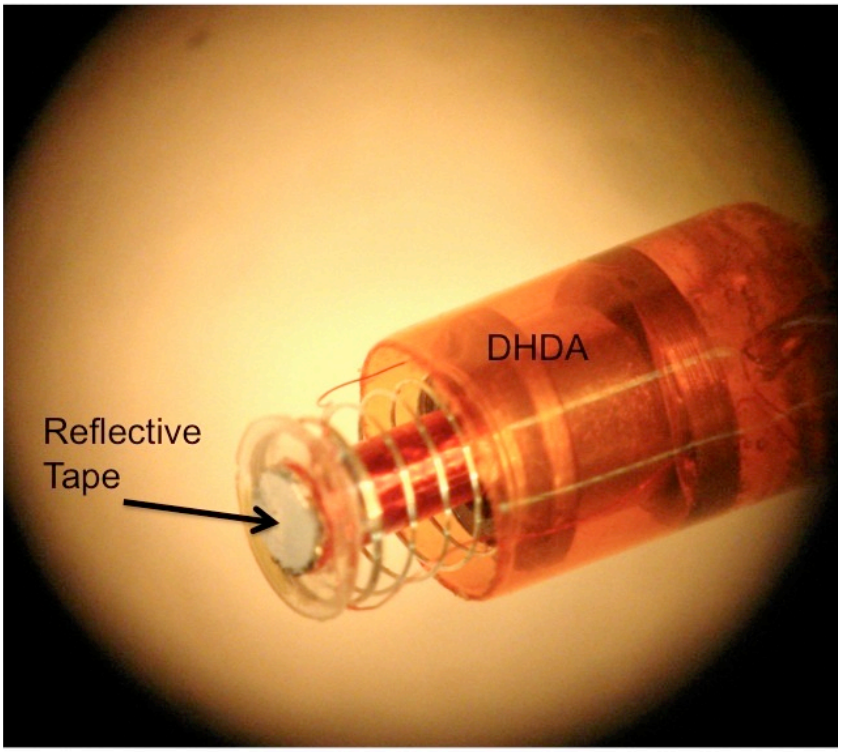

Fig. 33 DHDA with small circular piece of retro reflective tape placed on the contact tip. This tape allows for high reflectivity and thus betters tracking using the Laser Doppler Vibrometer system. The contact plate alone was not of desirable reflectivity for appropriate tracking. The small piece of tape is of negligible mass.

SoundCheck 8.0 (Listen, Inc.; Boston, MA) was used to acquire and analyze all data collected by a CDX-01 CardDeluxe sound card (Digital Audio Labs; Chanhassen, MN). Device displacement was acquired from the LDV's displacement card voltage, which was directly proportional to the measured displacement by a software-selectable range factor (i.e., 5 μm/V). The DHDA was driven by the headphone output of a calibrated amplifier (Crown Audio, Inc.; Elkhart, IN.; D-75A) with near unity gain (~1 V/V).

Sound near the DHDA was monitored with a calibrated ER-7C probe microphone (Etymotic Research, Inc.; Elk Grove Village, IL). The probe inlet faced the actuating portion of the device and was positioned approximately 1 mm radially from the device's outer diameter. The stimulus waveform was a stepped sine wave from 300 Hz to 20 kHz in 1/6 octave steps at a constant root-mean-square (RMS) voltage. Each frequency was played either 50 cycles or 100

ms, whichever was longer.

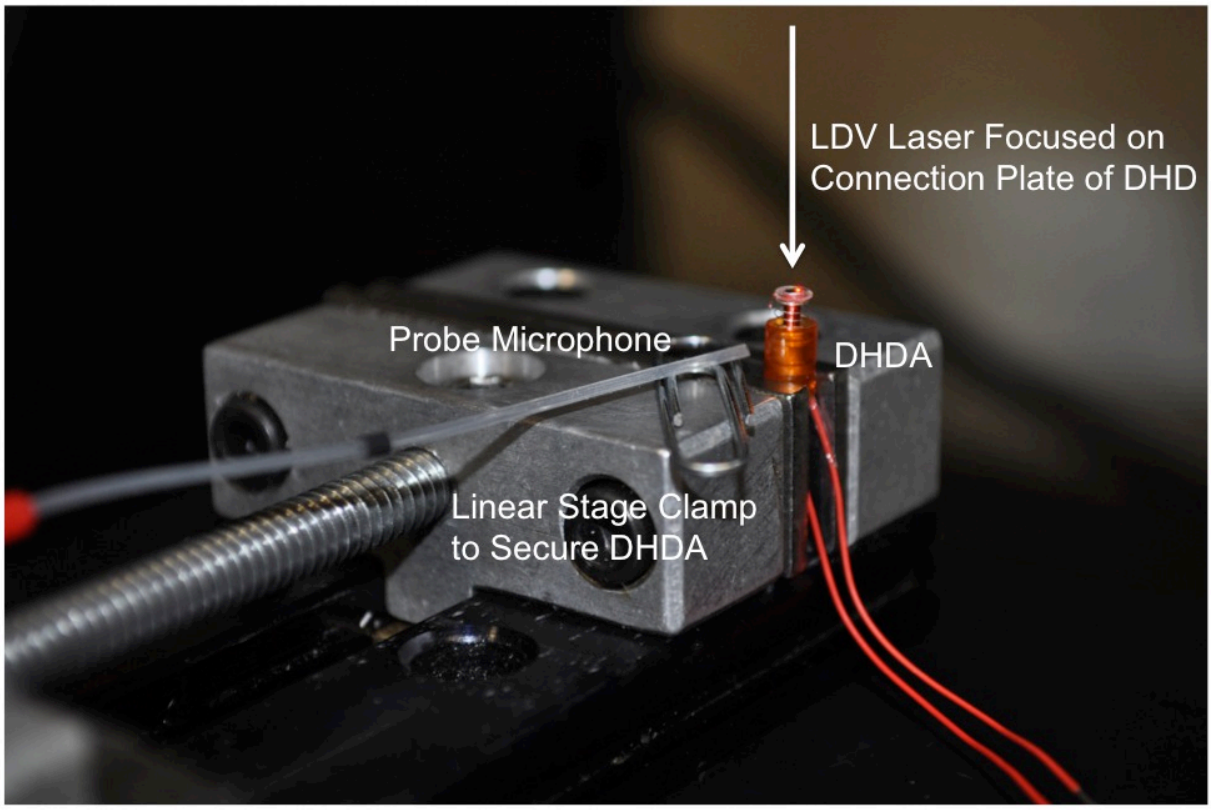

Fig. 34 DHDA frequency response setup using the LDV system.

The frequency response of the displacement waveform was calculated using the heterodyne algorithm in SoundCheck. This algorithm measured the fundamental response with good background noise rejection. The frequency response analysis discarded the first cycle of each frequency to remove any transient responses contributed to changing frequencies. Noise floor measurements were recorded in the same manner, except the actuator was disconnected from the driving signal.

The frequency response magnitude of an uncoupled direct hearing device is shown in Fig. 35. The device exhibited a smoothly varying response with no apparent distortions or resonances in the area of interest. Noise floor measurements from the LDV data acquisition system are

shown in red.

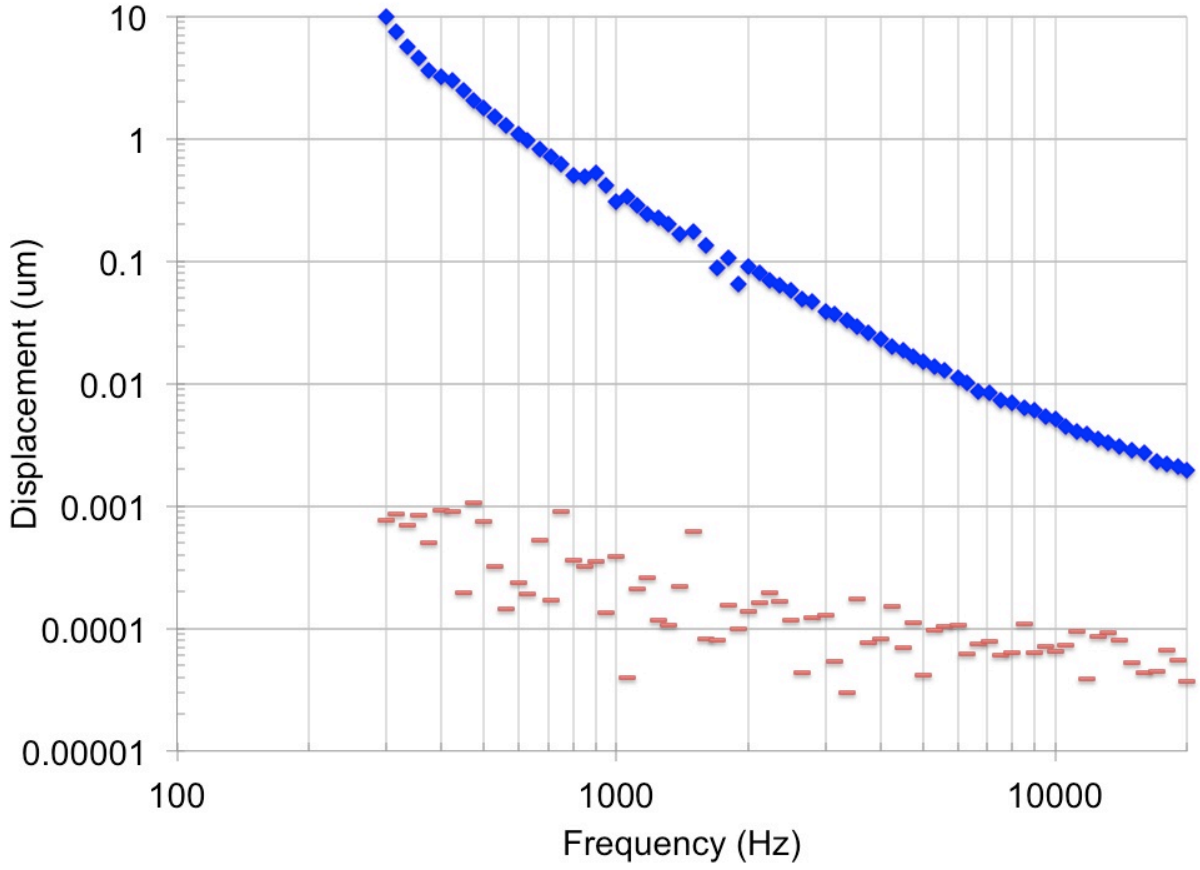

Fig. 35 Frequency response magnitude of an uncoupled DHDA. DHDA voltage was held constant at 50 mV RMS throughout the entire frequency sweep and a noise floor measurement was taken by disconnecting the device and repeating the measurement in an identical fashion. The DHDA displays a linear frequency response with a primary resonance occurring around 300 Hz.

6. DHDA Characterization - Total Harmonic Distortion and Noise Generation

Total harmonic distortion (THD) of the displacement was calculated using the THD analysis algorithm in SoundCheck, which utilized both the displacement and stimulus waveform. This algorithm calculated the noise contributed to the harmonics of the device. The first, second, and third harmonics were used in the THD analysis. Again, the first cycle of each driving frequency was discarded to remove any transient responses from changing frequencies. The acoustic broadband noise generation of the DHDA was calculated from the recorded waveform

of the probe microphone using the broadband RMS algorithm in SoundCheck. Background noise was measured in the same manner; except the device was disconnected from the driving signal and therefore the background noise measurements also includes electrical noise and other noise sources.

Below 0.5% THD is considered a reasonable level for an implantable hearing aid [93]. The THD is well below 0.5% above 400 Hz. The increase in THD in the lower frequency region appears to be correlated with the natural frequency of the device. This distortion could be from the DHDA, but drift in the displacement measurements of the LDV at frequencies near resonance could also be a contributing factor. The uncoupled DHDA did not generate any detectable noise above background levels. These measurements were not taken in a sound booth and the sound level of ~34 dB SPL was considered to be the actual acoustic noise of the room and not electrical noise in the experimental system.

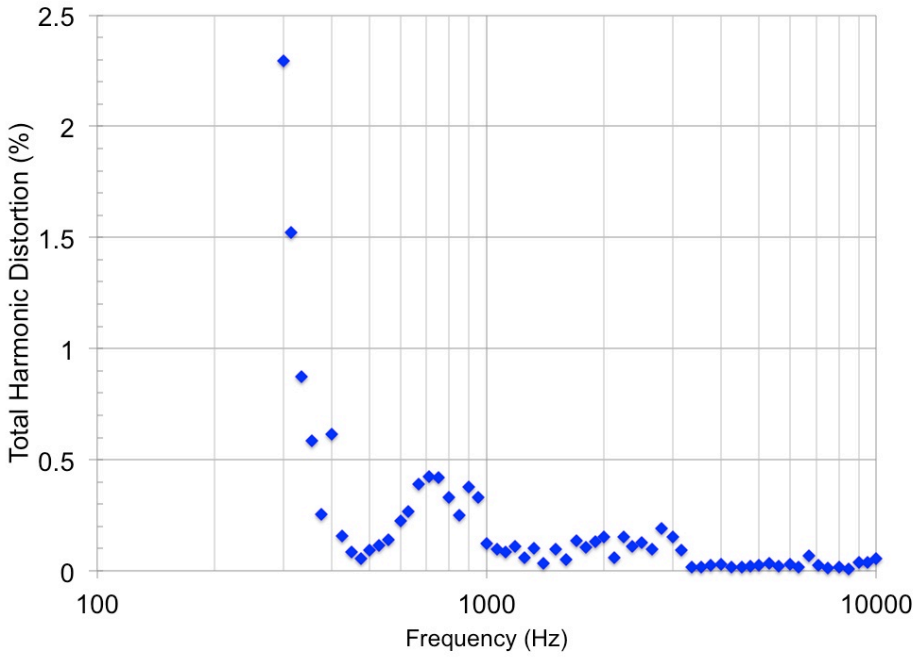

Fig. 36 Total harmonic distortion of an uncoupled DHD. Driving voltage was held constant at 50 mV RMS throughout the entire frequency sweep. The LDV range was adjusted at 3 kHz. Below 0.5% THD is considered suitable for an implantable hearing aid[93].

7. DHDA Characterization - Static Magnetic Field Strength

The assembled actuator has a static magnetic field strength of approximately 250 Gauss. This is well below the International Commission on Non-Ionizing Radiation Protection guidelines of 400 mT (4,000 Gauss)[94] as a limit of exposure to static magnetic fields by the general public. The static magnetic field was measured using a DC magnetometer with a flexible probe (Alpha Labs Inc. Serial #3025).

8. DHDA Characterization - Actuator Force Generation

The force generated by the DHDA was calculated by applying a current to the coils and measurement the displacement using the LDV system. The resulting force was calculated using the spring constant of the DHDA spring and the measured displacement.

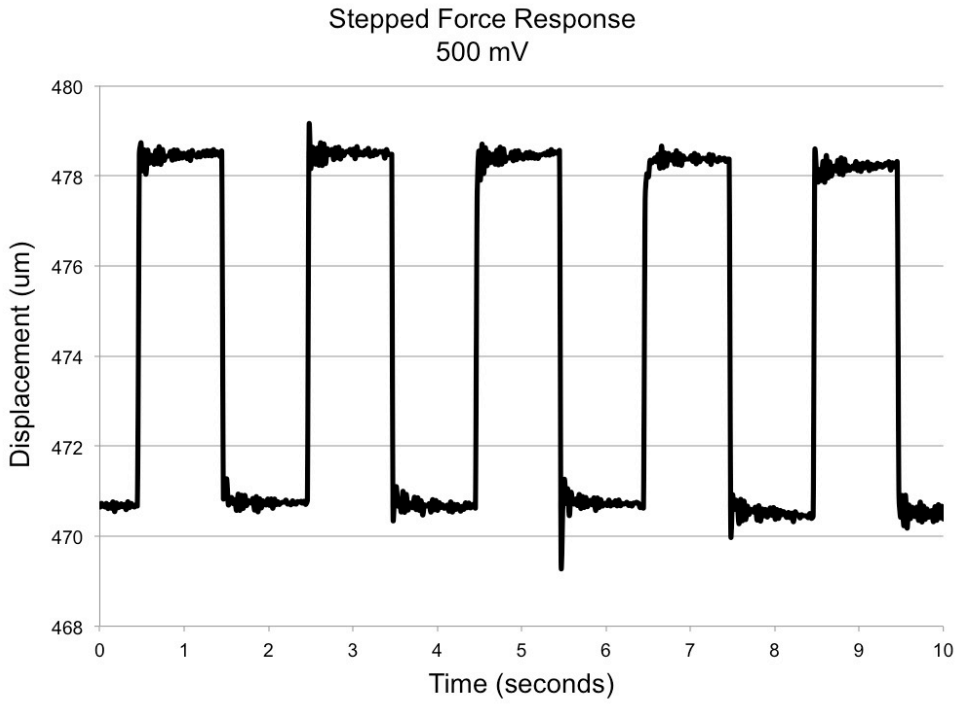

Fig. 37 Five different input step signals to the DHDA were measured: 90 mV, 100 mV, 250 mV, 500 mV, and 750 mV. The average of the five step trials was taken and used to calculate the corresponding force output of the DHDA.

The results of the force produced by the DHDA in response to current input are displayed in Fig 38. The DHDA produced a very controlled and reproducible force that was proportional to current that can be delivered to the TM and attached ossicular chain. A driving voltage of 800 mV (36 mA) results in a pressure delivered to the TM from the 3 mm DHDA contact plate of approximately 58 Pa. A 1% probability of TM rupture occurs at 16.5 kPa and a 90% probability of rupture occurs at 84.5 kPa [95].The pressure the DHDA delivers to the TM is well below any potentially harmful values.

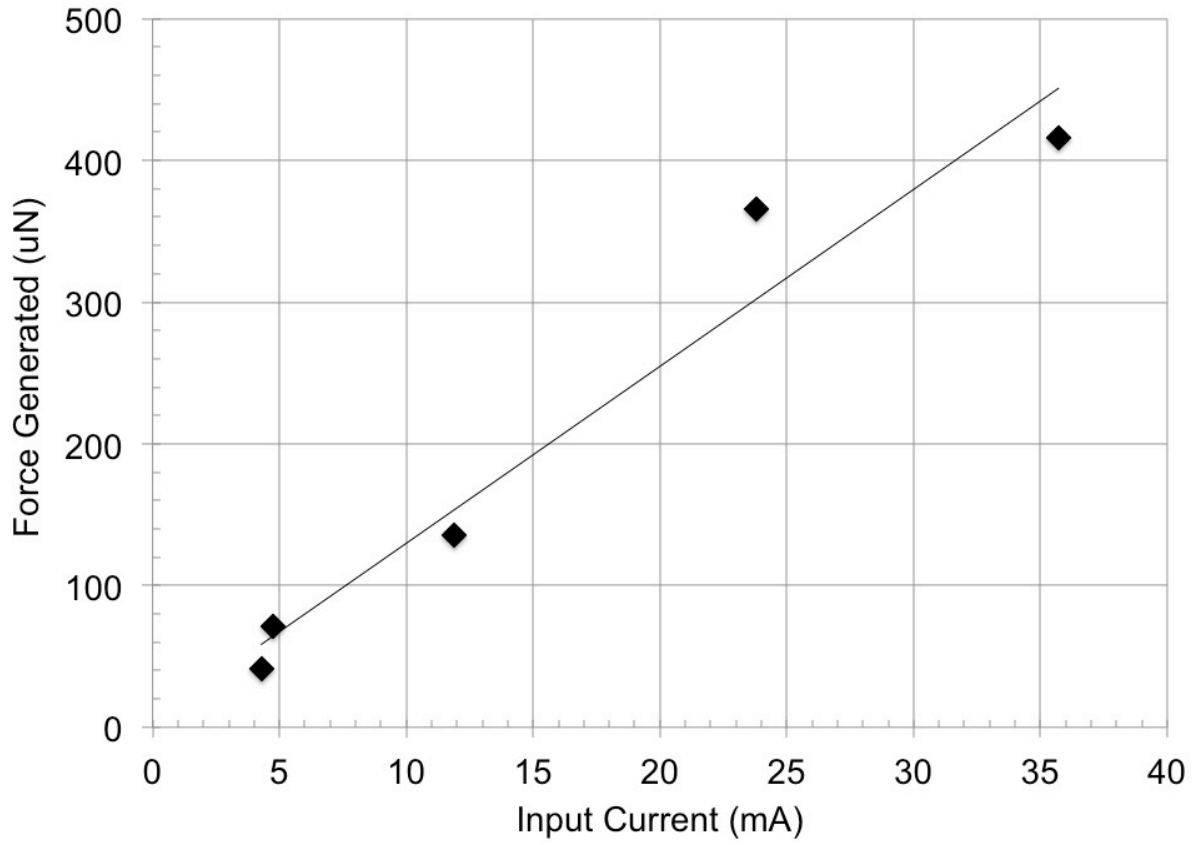

Fig. 38 Force generation of the uncoupled DHDA using a stepped input signal. The static displacements were measured using the LDV system and the corresponding force was calculated using the spring constant of the DHD.

CHAPTER 3

Direct Hearing Device Temporal Bone Studies

1. Cadaveric Temporal Bone Studies

Ossicular chain movements of a human temporal bone were measured to demonstrate the DHDA's ability to generate adequate ossicular chain displacements for sound reproduction. Baseline displacements from acoustic stimulation of the tympanic membrane were also measured for comparison purposes.

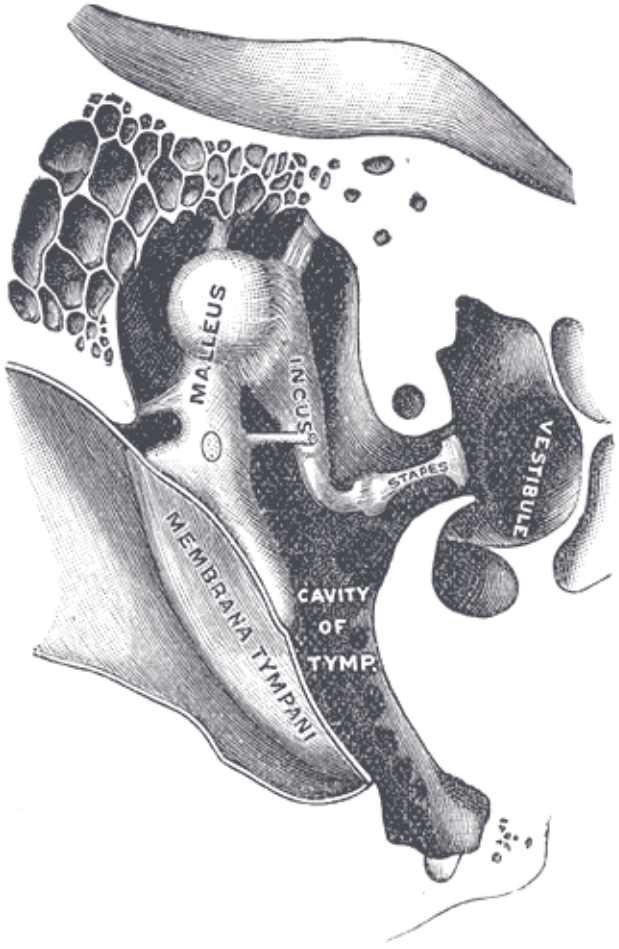

Fig. 39 Human middle ear anatomy[49]. This research project focuses on the movements of the cadaveric middle ear, specifically the stapes bone, when driven by sound pressure and the DHDA.

2. Temporal Bone Preparation

A left cadaveric temporal bone of a 59-year-old male with no history of middle ear diseases was obtained from the Willed Body Program at the University of California, Irvine. During the time of testing, the temporal bone was eight years post mortem. The bone had been fixed in a 10% solution of neutral buffered formalin and was kept at a temperature of 4 ºC. After securing the temporal bone in a bone holder, a simple mastoidectomy with facial recess approach was performed.

The bone was prepared using a mastoidectomy and posterior tympanotomy approach to provide a good view of the stapes footplate and posterior crus. Previous studies have shown both the umbo and the stapes footplate are effective locations for studying middle ear mechanics and ossicular chain displacement as a means of quantifying hearing [86,90,96]. Since the facial nerve and stapedius tendon were preserved, drilling only provided a view of the middle ear cavity. Therefore, the stapes footplate was not fully visible and the posterior crus was selected to measure displacement.

A small piece of retroreflective tape (~0.5mm x 0.5mm) (Polytec Inc.) was placed on the posterior crus of the stapes to assure strong signal strength of the reflected laser. Additionally, the placement of the tape on the posterior crus assures that displacement measurements were taken from the exact same location during each trial.

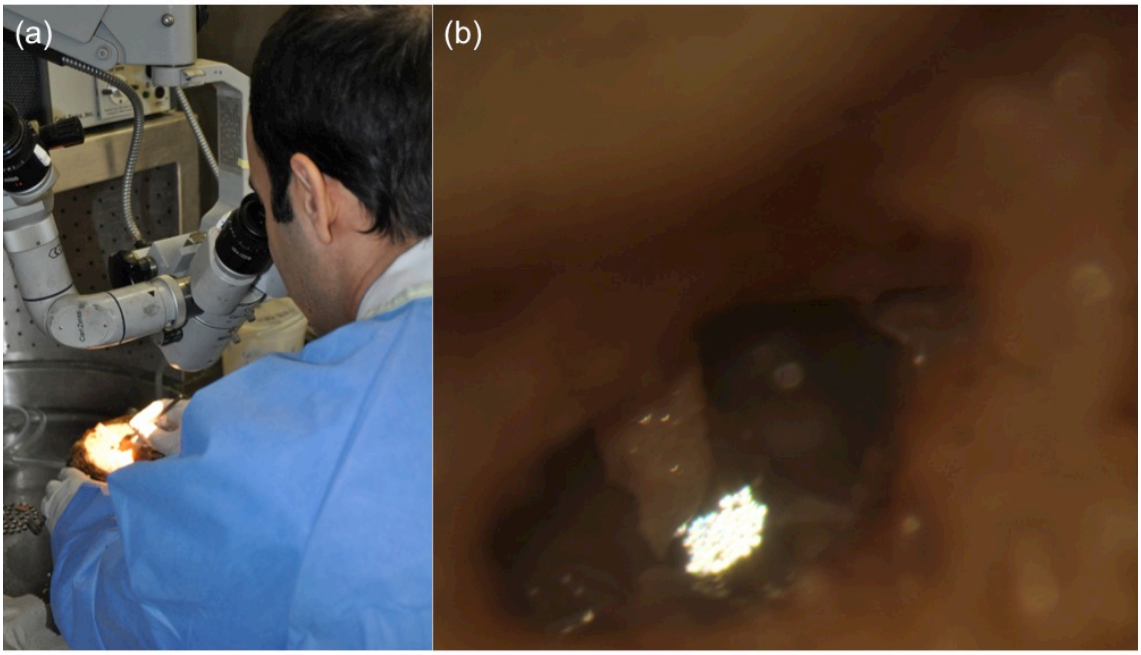

Fig. 40 Placement of retro reflective tape of the posterior crus of the cadaveric temporal bone (a) Dr. Hamid Djalilian placing the reflective tape in the temporal bone lab (b) image through mastoidectomy of the stapes with tape attached.

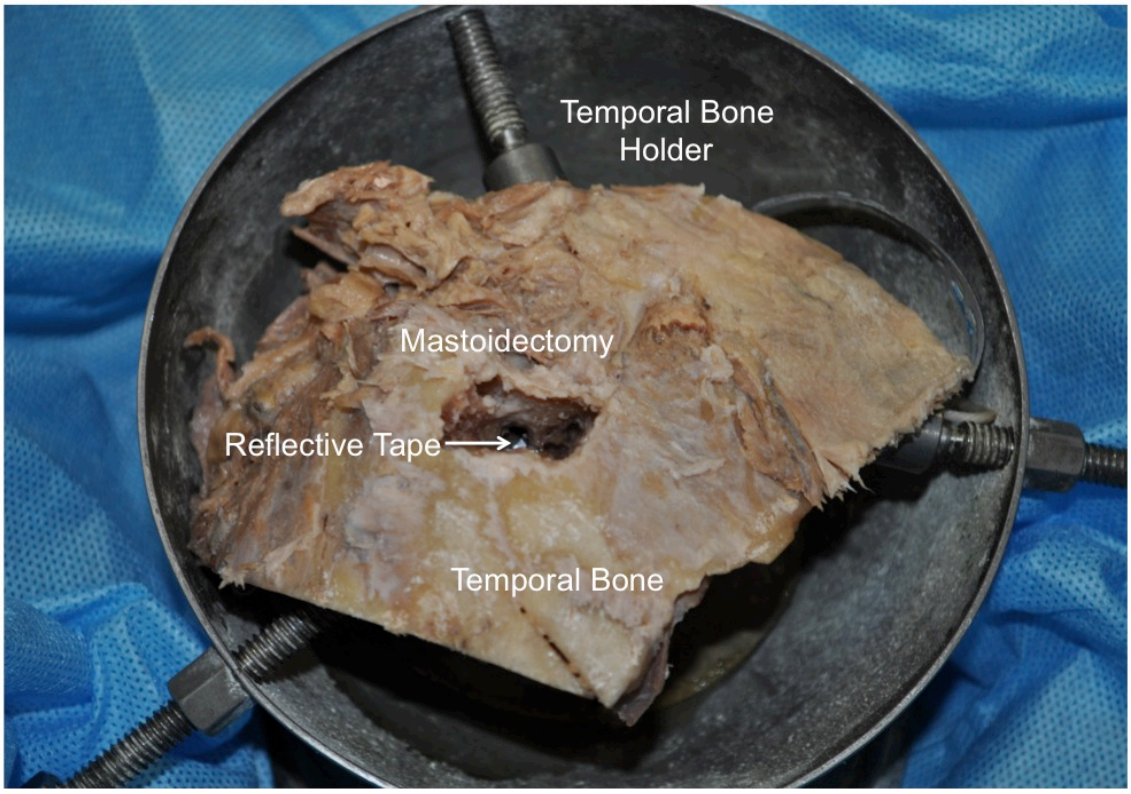

Fig. 41 Cadaveric Temporal Bone Setup. The temporal bone is secured within a bone holder and the mastoidectomy and piece of retroreflective tape is visible through the opening.

3. Temporal Bone Speaker Baseline Measurements

To demonstrate the DHDA as a tympanic membrane driver, a cadaveric temporal bone was used [90,96] and the corresponding posterior crus displacement was measured. Baseline measurements of the middle ear response were taken to account for size, age, and other physiological variability. The pure tone sound stimuli were delivered through a ER-5A insert earphone (Entymotic Research, Inc.; Elk Grove Village, IL) placed 2 mm from the tympanic membrane. Simultaneously, the sound pressure levels at the tympanic membrane were monitored with an ER-7C probe microphone (Etymotic Research, Inc.; Elk Grove Village, IL). The stimulus waveform was a stepped sine wave from 300 Hz to 10 kHz in 1/6 octave steps at 104 and 120 dB SPL. Each frequency was played either 50 cycles or 100 ms, whichever was longer.

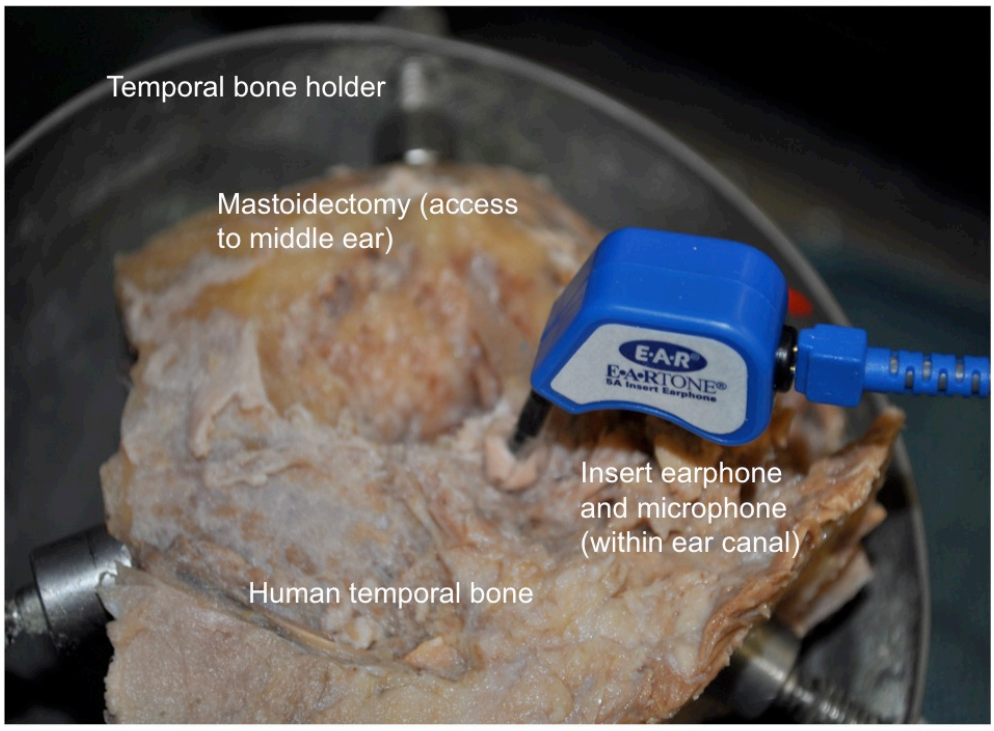

Fig. 42 Cadaveric temporal bone secured within bone holder. A mastoidectomy was performed that provides access to the middle ear for stapes footplate displacement monitoring with the LDV. This figure depicts the temporal bone stapes baseline displacement measurement setup. Insert earphones and probe microphone (for SPL monitoring) are placed within the ear canal and a frequency sweep at a designed SPL was played through the insert earphones while the correspoding stapes footplate displacement is measured using the LDV.

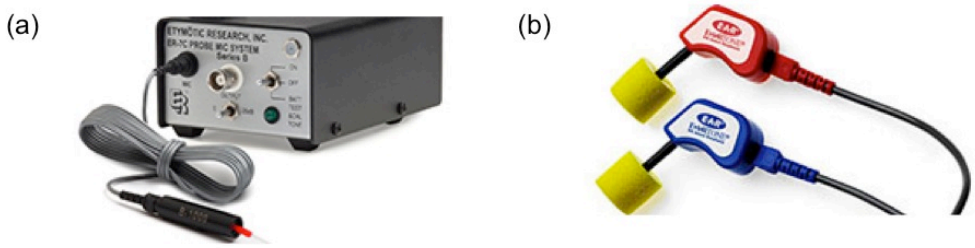

Fig. 43 Probe microphone and probe speaker used in cadaveric and device testing (a) Etymotic ER-7C Probe microphone (b) Etymotic insert earphone 5A. (Images courtesy of Entymotic)

The movement of the stapes bone was piston-like, however due to the geometry of the cadaveric middle ear and experimental setup this movement was measured at a small experimental angle. A cosine correction of the measured displacement was applied to account for the measurement angle offset [96]. An offset angle of 45° was determined by two independent observers and used to calculate the correct displacement.

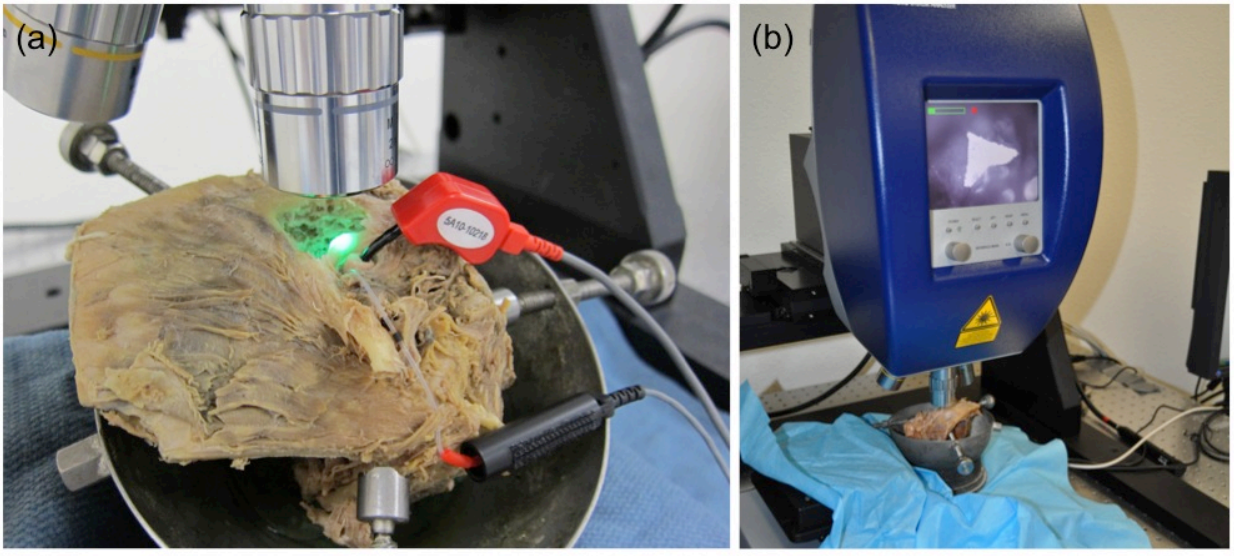

Fig. 44 (a) Temporal bone secured in holder and placed under optical system. This setup includes the probe microphone and probe speaker. (b) Zoomed out view of the optical system and temporal bone. The screen of the optical system shows the small piece of retro reflective tape placed on the stapes bone.

4. DHDA as a Tympanic Membrane and Ossicular Chain Driver

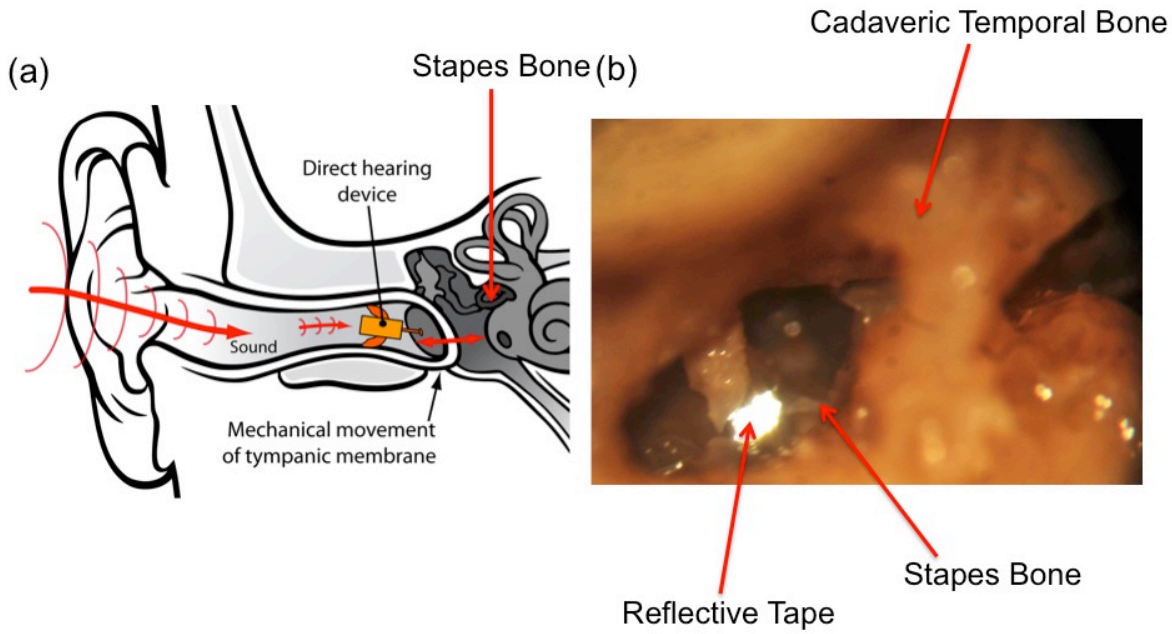

Fig. 45 Stapes movement when driven by the DHDA (a) computer aided design graphic to show how the DHDA will drive the TM and attached ossicular chain, and where the displacements recordings will be made. (b) cadaveric temporal bone visualization of the posterior crus after reflective tape has been placed.

Next, the DHD was carefully inserted inside the osseous external auditory canal, the contact tip was placed on the posterior-superior quadrant of the TM under direct microscope, and the device was secured using bone wax. The contact tip in this present embodiment was a flat acrylic plate 3 mm in diameter. The DHD was stimulated with a stepped sine wave from 300 Hz to 12 kHz in 1/6 octave steps and stimulating input at 200, 400, 600, 800 mV voltage levels. Fourth, the same procedure was repeated except that the DHD contact tip was placed on the umbo.

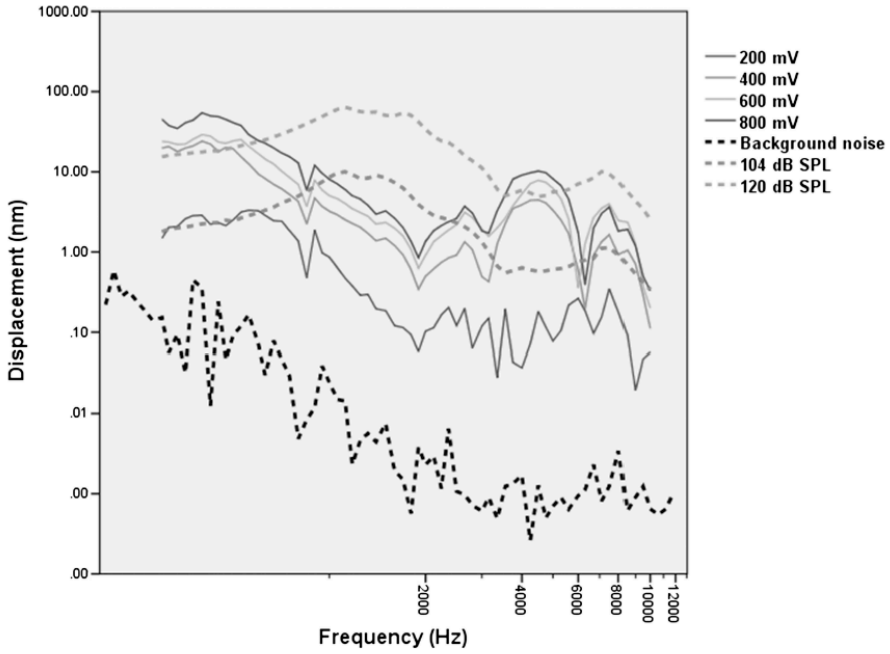

Fig. 46 Frequency response of the direct-drive hearing device at different voltage inputs when the device was coupled to the posterior-superior quadrant of the TM, compared to the background noise and the baseline measurements at 104 and 120 dB SPL[97].

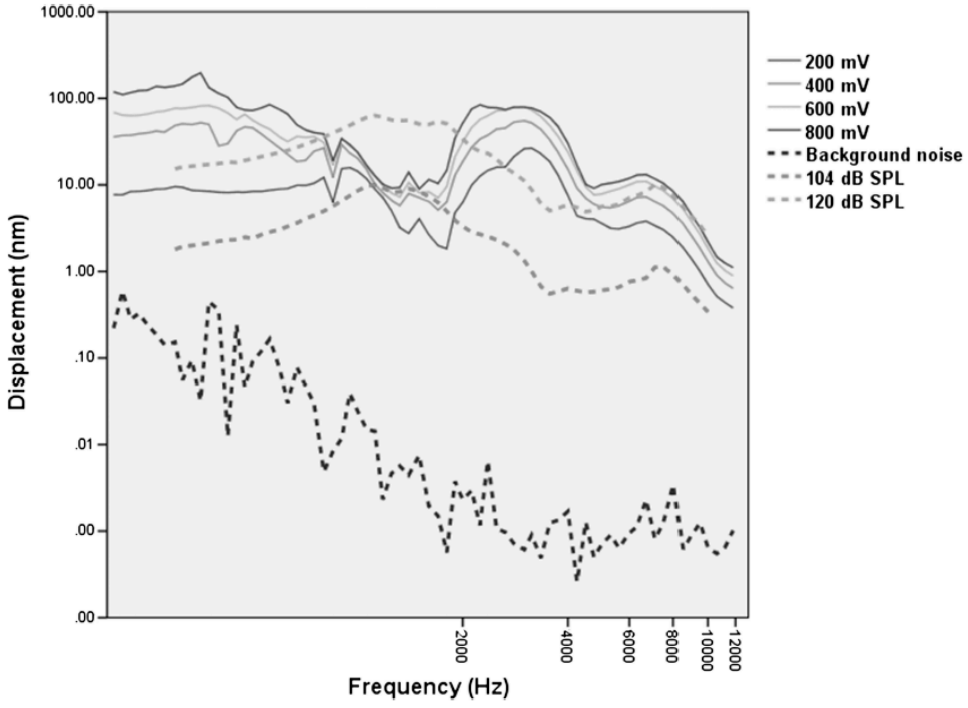

Fig. 47 Frequency response of the direct-drive hearing device at different voltage inputs when the device was coupled to the umbo, compared to the background noise and the baseline measurements at 104 and 120 dB SPL[97].

5. DHDA Interface – Custom Molded Tip

The complex structure of the tympanic membrane led our research group to explore alterative ways to couple the device to the tympanic membrane. While the flat acrylic contact plate was successful in driving the tympanic membrane and attached ossicular chain, we believe a more custom fit would allow for more efficient transfer of energy from the device to the TM and ossicular chain.

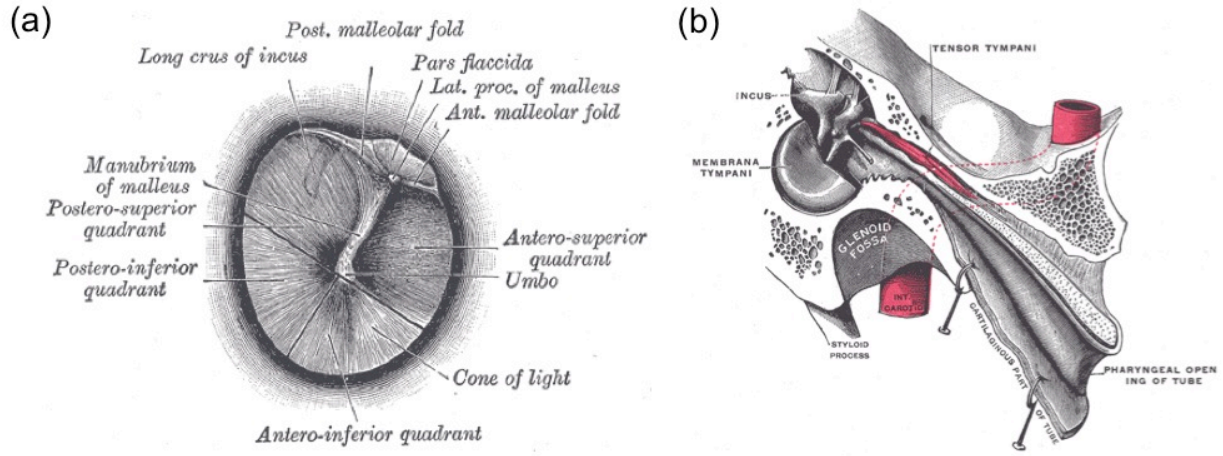

Fig. 48 Tympanic membrane structure[49] (a) right tympanic membrane as seen through the speculum (b) auditory tube, laid open by a cute in its long axis.

A custom interface tip was made by taking an impression from the TM of the cadaveric temporal bone using silicone impression material (Siemens Silhouette^{TM}), and then placed on the connection plate of the DHD facilitating a custom fit interface between the device and the TM.

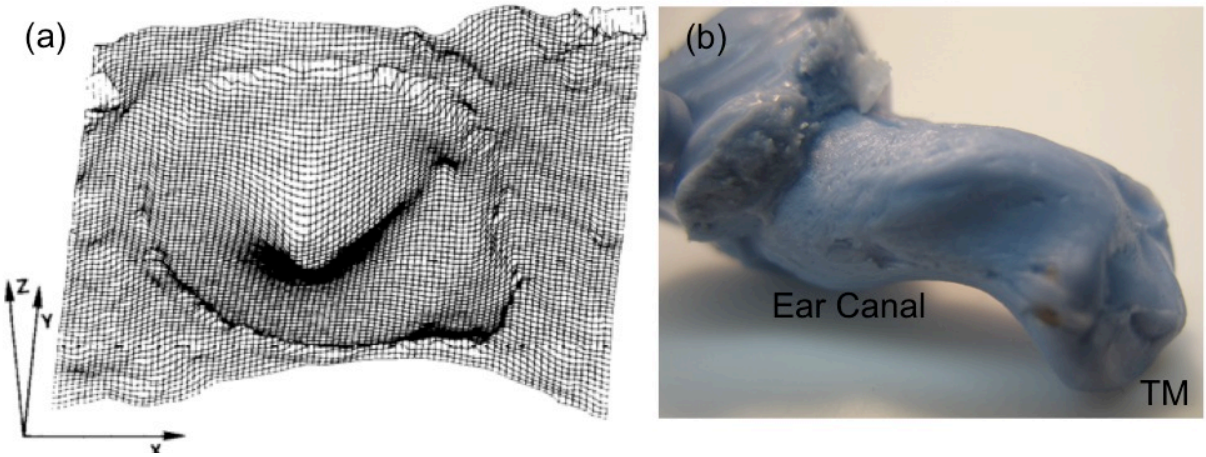

Fig. 49 Tympanic membrane geometry (a) 3D perspective of the TM[89] demonstrating the concavity at the umbo of the TM (b) silicone polymer mold taken from a cadaveric temporal bone used in the studies presented here demonstrating ear canal geometry and TM morphology.

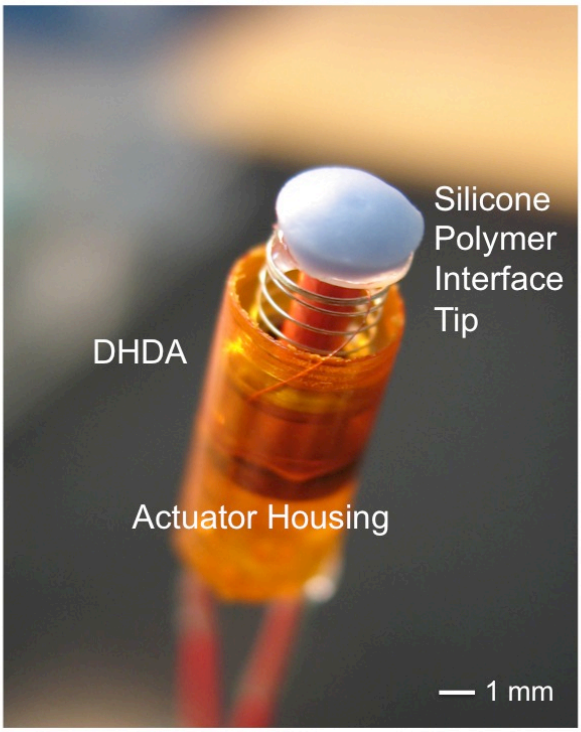

Fig. 50 DHDA with a custom TM interface. The custom contact tip is made from a silicone polymer mold taken of the cadaveric TM. A 3mm cutout of the umbo impression was then mounted on the DHD connection plate to provide a custom interface between the TM and device.

The DHDA was placed under a microscope at the umbo of the tympanic membrane and secured to the ear canal with surgical bone wax. The stapes displacement measurements and correction factor adjustments were performed in the same manner as the baseline measurements.

The stimulus waveform was a stepped sine wave from 300 Hz to 12 kHz in 1/6 octave steps. Each frequency was played either 50 cycles or 100 ms, whichever was longer. The RMS voltage of the waveform was selected and held constant during the entire frequency sweep. Selected input voltage levels were 50mV, 200 mV, 400 mV, 600 mV, 1V.

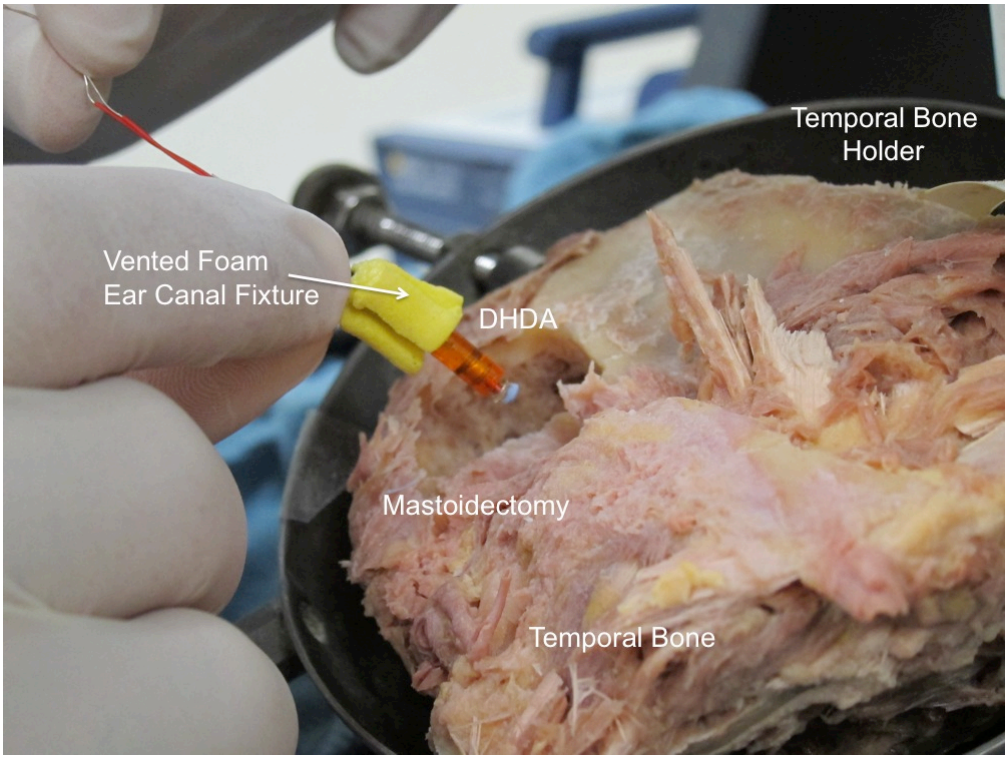

Fig. 51 Temporal bone testing setup for DHDA with custom TM tip. This setup utilizes a foam ear canal fixture to hold the device in place during operation. Different strategies were used to fix the device in place with the two most promising being the foam fixture and bone wax. Both embodiments allowed for full aeration of the ear canal.

The baseline frequency response of the stapes displacement is shown in Fig 52. At 40 dB SPL acoustic simulation, the posterior crus of the cadaveric stapes bone had a minimum displacement of ~0.01 nm at 10 kHz and a maximum displacement of ~0.65 nm at 2.1 kHz. At 90 dB SPL acoustic simulation, the stapes bone had a minimum displacement of ~1.1 nm at 10 kHz and a maximum displacement of ~140 nm at 2.1 kHz.

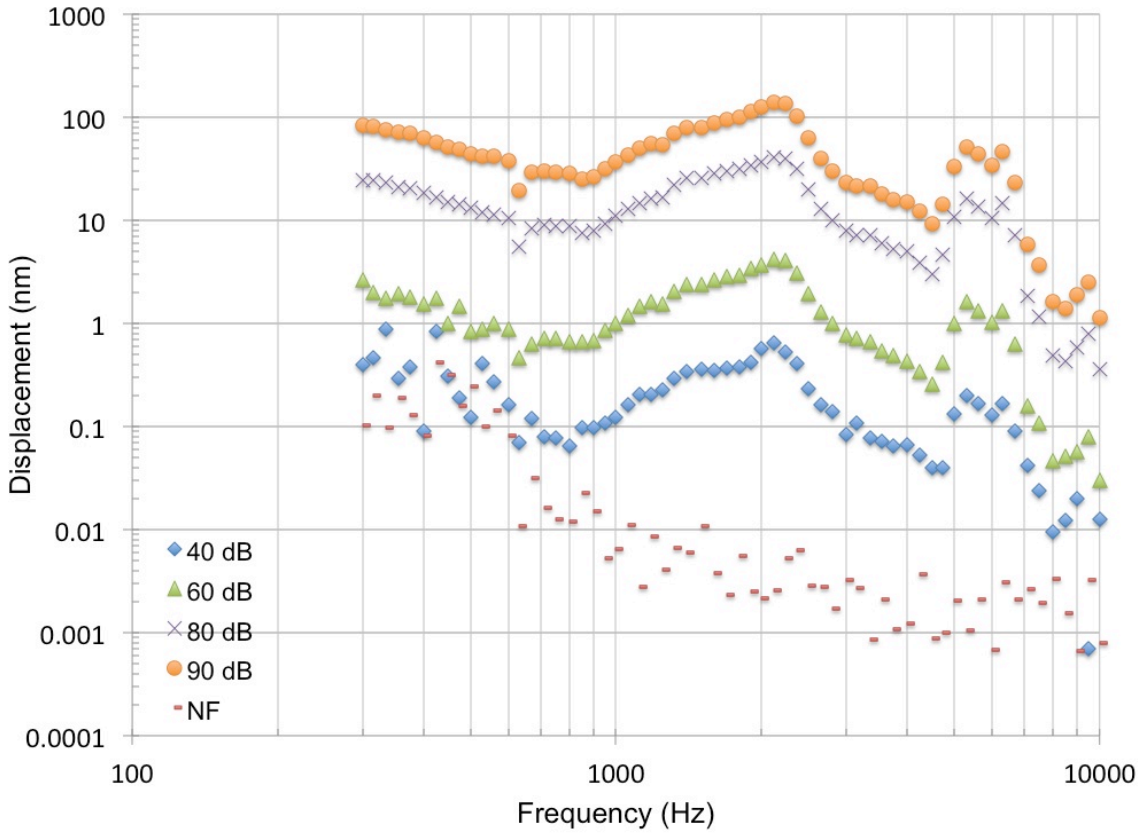

Fig. 52. Cadaveric middle ear frequency response. Each line depicts the LDV measured value of posterior crus displacement (nm) during each frequency sweep at the designed SPL. A cosine correction has been applied to the displacement values corresponding to the experimental angle, 45°, at which the measurements were taken. This experimental angle is due to the cadaveric temporal bone setup.The red data set depicts the noise floor, where measurements were taken when the earphone was disconnected from the driving system.

Additionally, the frequency response of this cadaveric temporal bone demonstrated the resonance of the middle ear system occurring at ~2120 Hz. This value is slightly higher than the reported middle ear resonance frequency at 1200 Hz [98]. This may be due to the natural ossification process of the cadaveric middle ear or the result of the preservation process.

The amplitude of the stapes displacement from the DHDA is shown in Fig. 53. The frequency response of the tympanic membrane and DHDA coupled system displayed a resonance mode at ~ 2.1 kHz. When energizing the DHD using a 200 mV driving signal, the posterior crus of the stapes bone had a minimum displacement of ~0.2 nm and a maximum displacement of ~5.4 nm. When energizing the DHDA using a 1V driving signal, the posterior

crus of the stapes bone had a minimum displacement of ~0.57 nm and a maximum displacement of ~34.5 nm. 200 mV actuation resulting in displacements comparable 60 dB. This corresponded to a power consumption of approximately 2 mW.

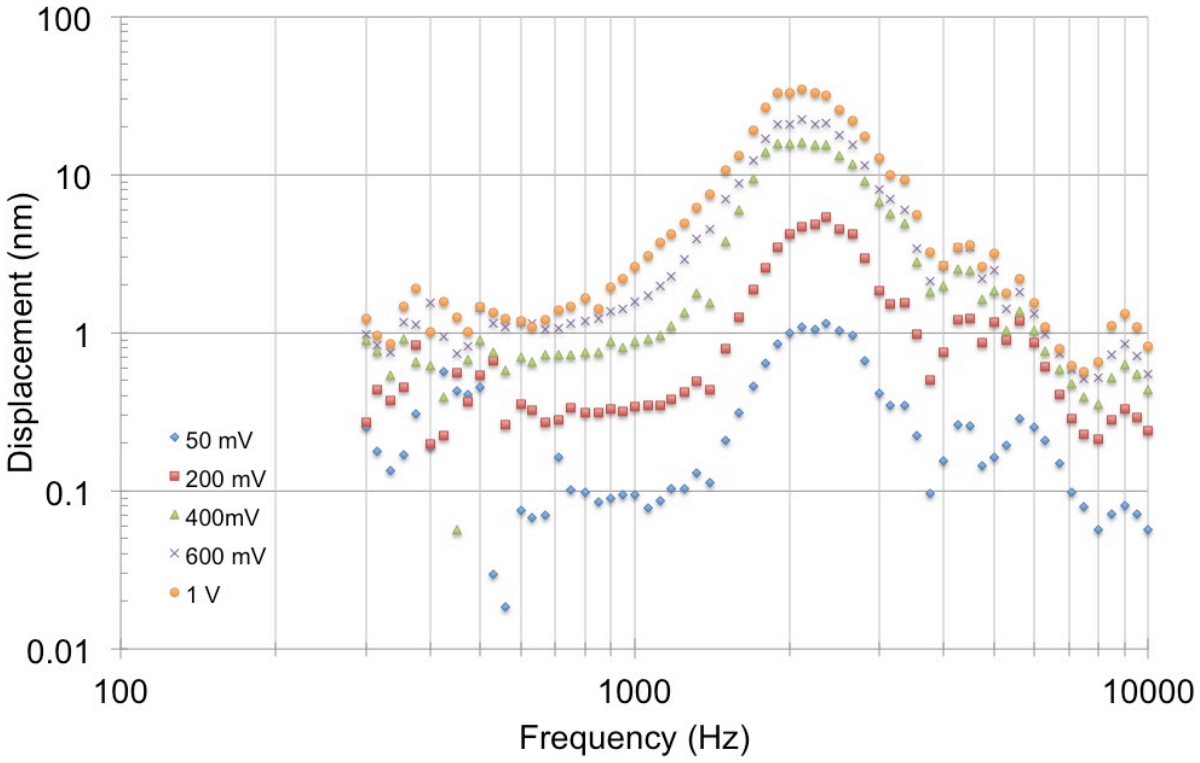

Fig. 53 Frequency response when the DHDA (with custom TM tip) was coupled directly to the tympanic membrane. Five different input voltage levels were tested and the increase in input voltage corresponds directly to an increase in displacement of the posterior crus. The voltage was held constant throughout the entire frequency sweep. A cosine correction has been applied to the displacement values corresponding to the experimental angle, 45°, at which the measurements were taken. This experimental angle is due to the cadaveric temporal bone setup.

6. DHDA Interface - Magnetic Drive Embodiment

The custom interface tip for the DHDA was a step in the right direction for creating a strong interface between the DHDA and the TM. However, our research group was interested in exploring different ways to connect the DHDA to the TM to assure a constant and strong contact between these two surfaces to maximize energy transfer and minimize unwanted noise. While it did not appear the DHDA was 'bouncing' on the TM as opposed to constantly being in contact, exploring a more secure 'latching' mechanism was a direction we were interested in testing. The

use of magnetic interface between the DHDA connection plate and the umbo sounded most promising and guided the next directions of this DHDA interface research[99].

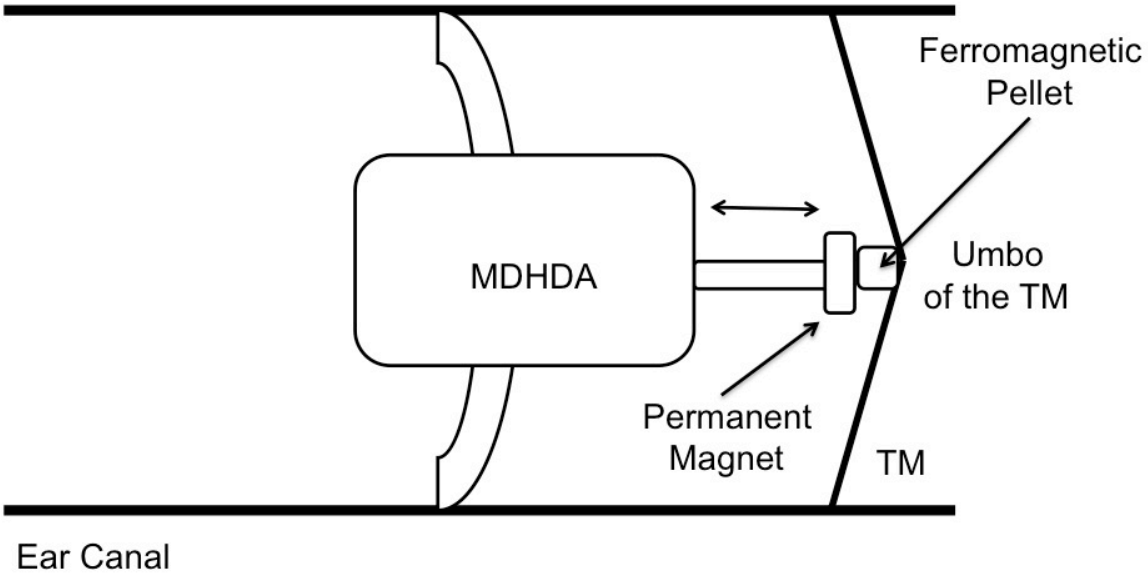

Fig. 54 CAD Conceptual design of the DHDA Magnetic Drive Embodiment. This embodiment includes the placing of a ferromagnetic nickel epoxy pellet to the umbo of the TM and coupling the DHDA with a small permanent magnet (now called the MDHDA) to it.

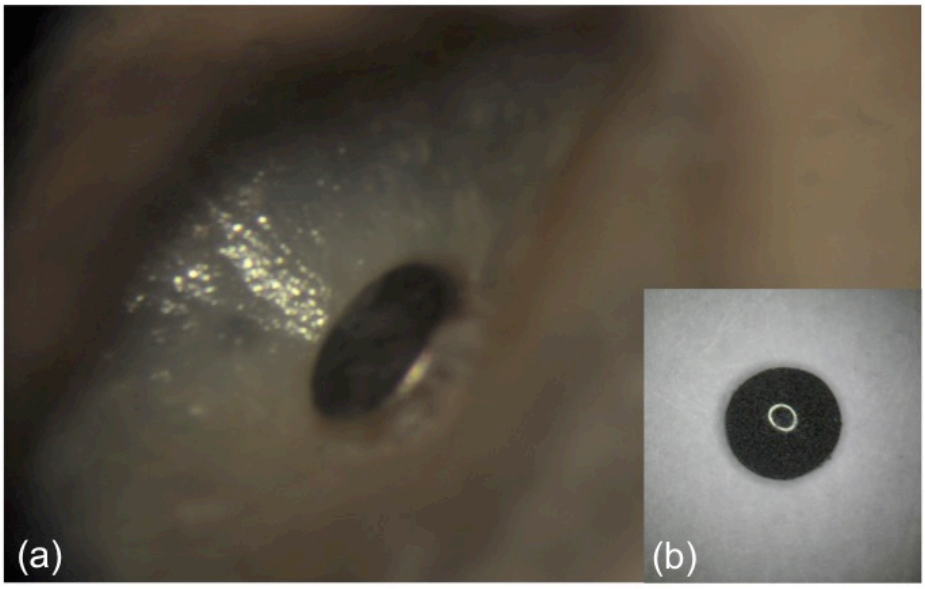

Fig. 55 Tympanic membrane - magnetic drive embodiment (a) a microscope image of the cadaveric tympanic membrane with a small neodymium magnet attached. While using a magnet directly on the umbo was out initial intention, our group decided instead to use a ferromagnetic pellet instead (b) ferromagnetic nickel epoxy pellet 1 mm in diameter replaced the magnet as seen in part a. The final embodiment was using this nickel epoxy pellet secured on the cadaveric umbo using a cyanoacrylate adhesive.

The magnetic direct hearing device actuator (MDHDA) is a small completely-in-the-canal hearing aid prototype that drives the tympanic membrane (TM) through a magnetic interface. A cadaveric temporal bone was prepared, and a 3 mg ferromagnetic pellet was made with nickel powder and epoxy glue was then attached with cyanoacrylate to the umbo. The MDHDA is the identical device that was presented in Chapter 1 (DHDA) with a novel magnetic interface. This interface consists of an 8 mg silicone polymer tip with a 1 mm neodymium magnet placed on top. From the previous studies using the DHD and custom interfaces it was discovered that the linear DHDA does not fully accommodate for the fact the tympanic membrane is angled ~ 30° relative to the ear canal. Although the previous devices had custom tips to fit within the umbo, it was possible the device was operating at an angle as opposed to be sitting horizontally within the ear canal. While the shape of each human ear canal and TM varies, it seemed appropriate to incorporate a tip that accounted for the general observation that the TM sits at a 30°. Therefore a silicone polymer tip that creates a 30° angled surface should allow for the device to more appropriately couple to the TM.

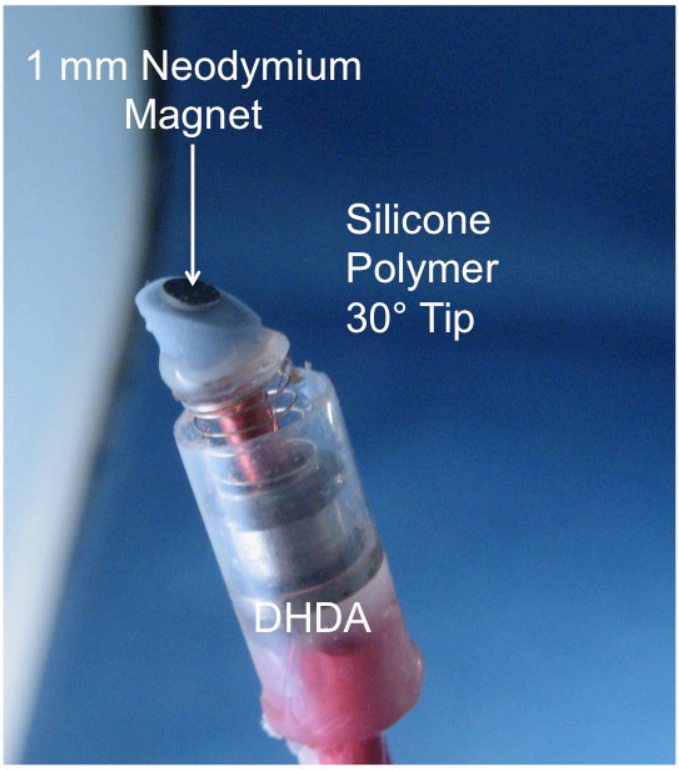

Fig. 56 Magnetic drive direct hearing device actuator (MDHDA). This figure demonstrates the DHDA with a silicone polymer tip and a 1 mm (5 mg) neodymium permanent magnet mounted on the tip. This device then couples to the ferromagnetic pellet that is attached to the umbo of the cadaveric temporal bone allowing for a secure contact interface.

Baseline measurements were performed prior to and after attaching the pellet to record the displacements of the stapes in response to natural sound delivered by insert earphones of 70 and 80 dB SPL from 300 Hz to 10 kHz. The displacements of the posterior crus of the cadaveric temporal bone were made using the LDV system.

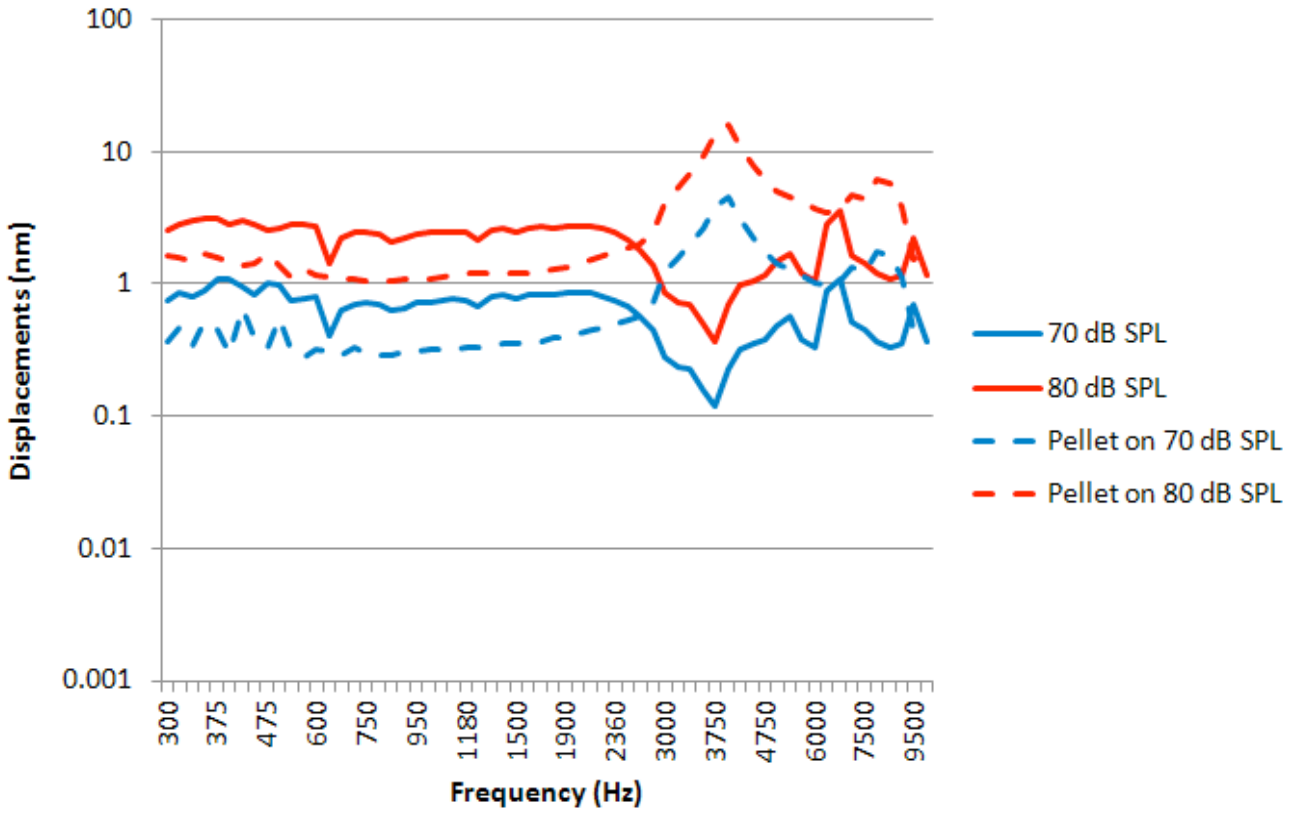

Fig. 57 Magnetic drive speaker baseline results[99]. This figure depicts the response of the middle ear of a cadaveric temporal bone in response to sound. The solid lines represent the system without the addition of the ferromagnetic pellet and the dotted lines represent the response when the ferromagnetic pellet was added.

Both testing scenarios of this experiment (with and without ferromagnetic pellet) demonstrating an interesting feature in the response of the cadaveric middle ear around 3.7 kHz. The addition of the pellet seemed to cause an inverse in the resonance feature at that specific frequency due to some mass loading effects.

After the baseline measurements were taken the MDHDA was inserted into the osseous portion of the ear canal and coupled to the ferromagnetic pellet glued to the umbo. Frequency sweeps between 0.3 to 10 kHz were performed and the MDHDA was driven with various levels of current. Displacements of the posterior crus of the stapes were measured using the LDV system as described previously and compared to sound-induced displacements. Inputs of 100 and

300 mV produced displacements equivalent to those of the natural sound at 70 and 80 dB SPL, respectively.

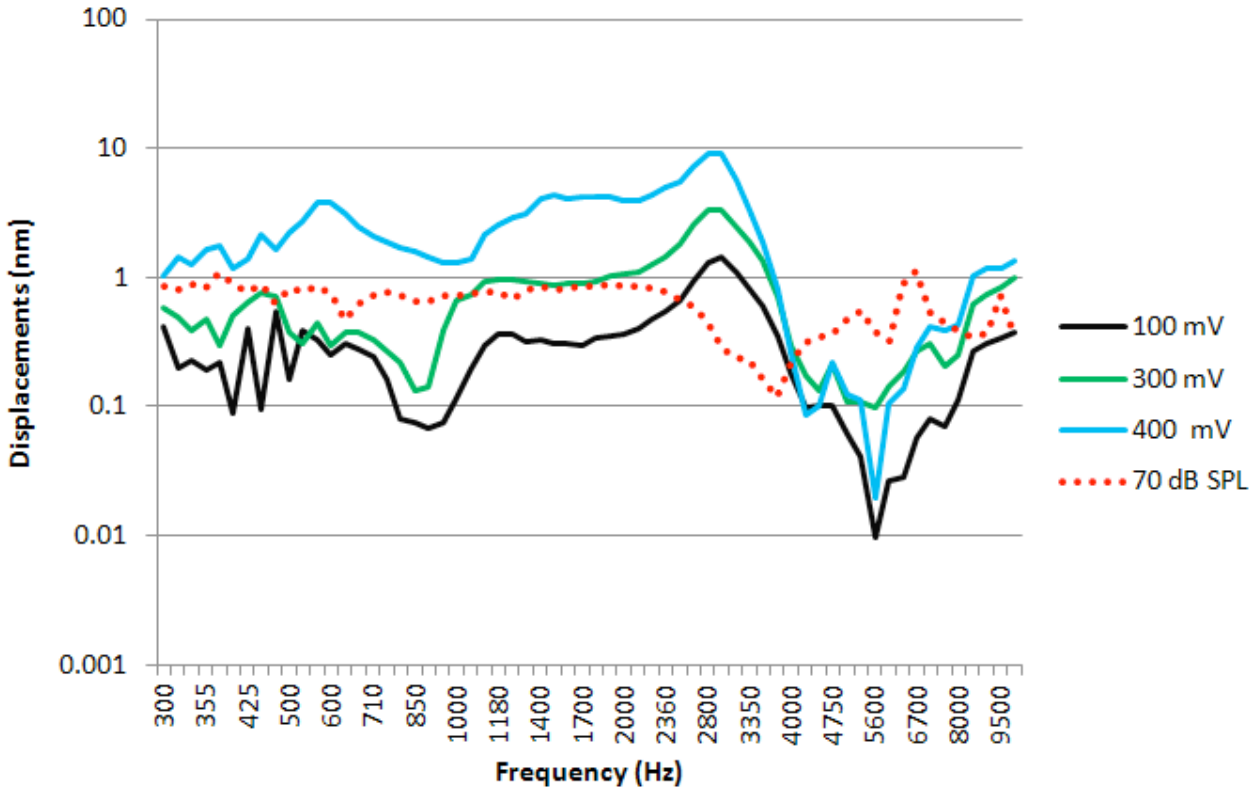

Fig. 58 Magnetic DHDA results[99]. This graph demonstrates the frequency response of the MDHDA when coupled magnetically to the umbo of the cadaveric temporal bone. Three different driving voltages are displayed here and speaker baseline results from the 70 dB frequency sweep is overlaid for reference.

7. DHDA Interface - Tympanostomy Tube Embodiment

To continue the exploration of appropriate methods to couple the DHDA to the TM our group sought a way to continue to use the magnetic attachment approach, however to utilize already existing technologies. While placing a ferromagnetic cap on the umbo is relatively simple, it may run the risk of becoming displaced due to natural processes occurring on the TM – moisture and wax buildup, epithelium migration, etc. Our group sought to use the already commercially available and commonly used tympanostomy tube (grommet), as a vehicle to

house our ferromagnetic cap. The insertion of a tympanostomy tube or ventilation tube is a common procedure where a small tube is placed within the tympanic membrane to allow for middle ear aeration. These tubes are often used in children and adults who have reoccurring otitis media (ear infections)[100] and are placed under general anesthesia in an office visit.

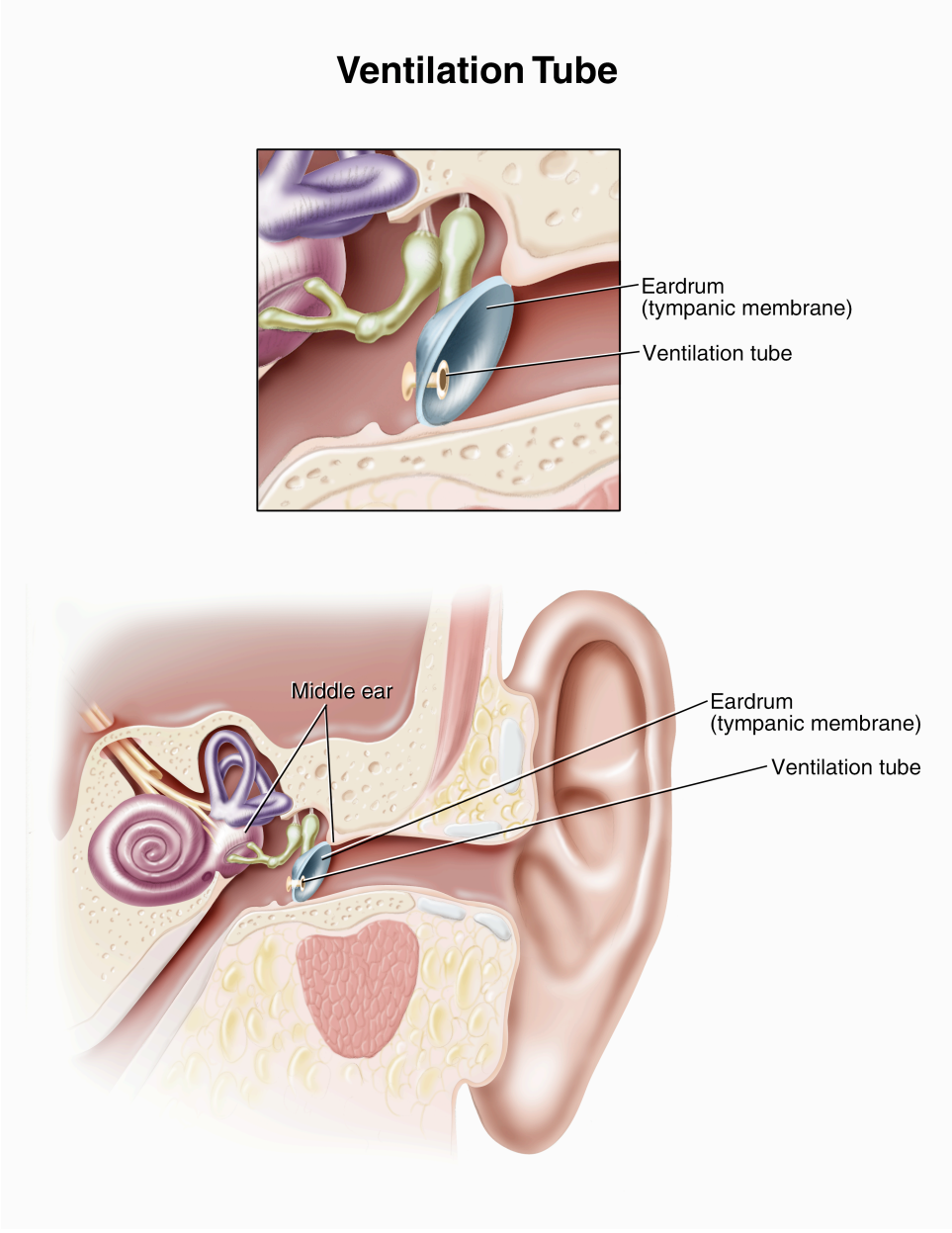

Fig. 59 Tympanostomy or ventilation tube[101] used for aeration of draining of the middle ear. Our group is interested in using this device as a vehicle to couple the DHDA to magnetically.

Our research group sought to determine whether a tympanostomy tube with a ferromagnetic cap could be actuated to displace stapes[102]. A ferromagnetic pellet was glued to the outer flange of an Armstrong V Grommet. The tube was then placed into the tympanic membrane of a cadaveric temporal bone. The MDHDA presented in the magnetic drive embodiment section was the device used in this new tympanostomy tube embodiment. The MDHDA is coupled directly to the ferromagnetic tympanostomy tube to actuate the TM and attached ossicular chain.

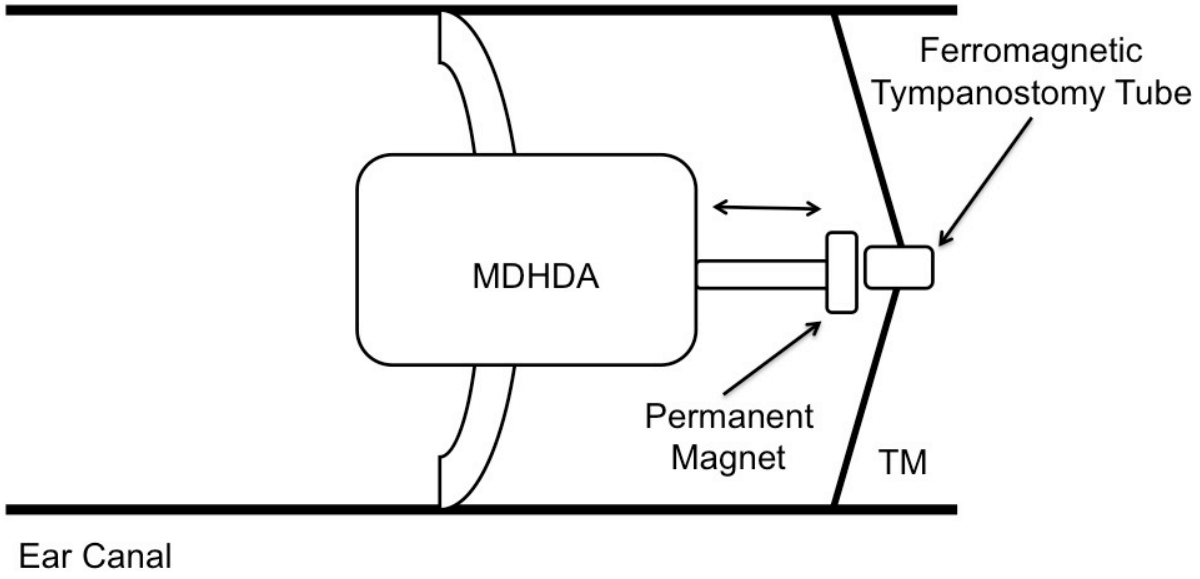

Fig. 60 CAD conceptual design of the DHDA tympanostomy tube embodiment. This figure describes how the MDHDA will magnetically couple to a ferromagnetic tympanostomy tube that has been inserted into the TM.

The tympanostomy tube used for this study was an Armstrong V Grommet, H/C-Flex® with 1.14 inner diameter and 2.1 mm inner flange diameter (Medtronic Xomed, Jacksonville, FL). A mixture of epoxy and nickel powder (3:1) was made (2 mg weight) and glued to the outer flange of the tube. After making an incision in the pars tensa portion of the TM, the ferromagnetic tube was placed and sealed.

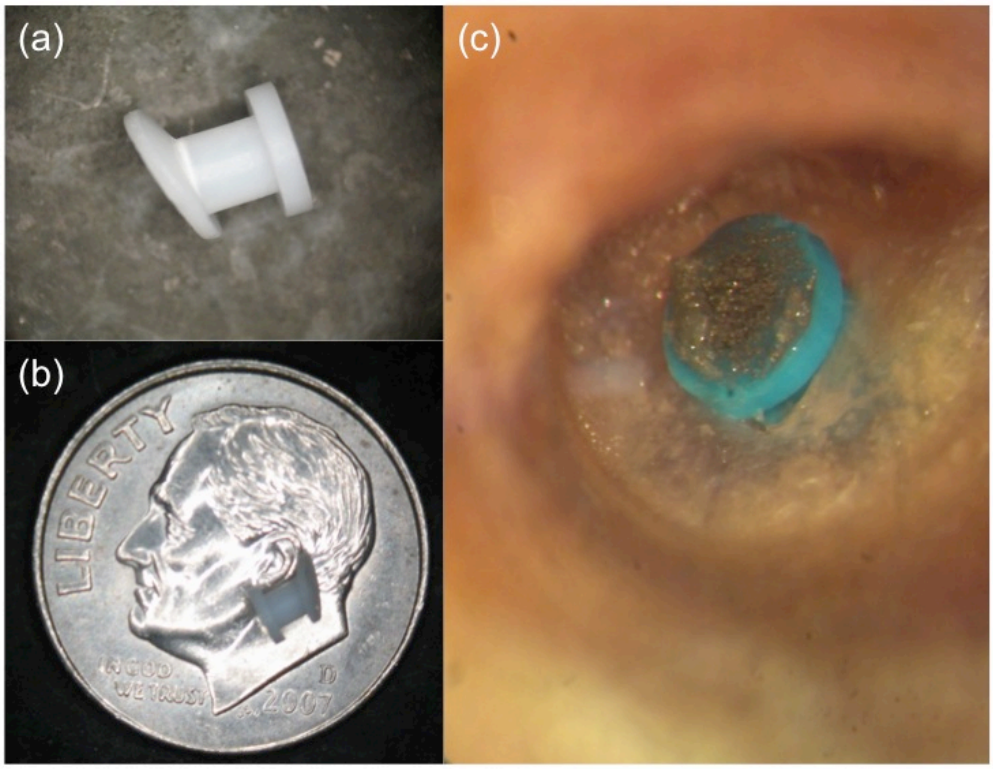

Fig. 61 Tympanostomy tube (a)(b) Armstrong V Grommet tympanostomy tube (white) used in the temporal bone study (b) tympanostomy tube with ferromagnetic cap after insertion into cadaveric TM. This tube is the identical tube as presented in (a)(b) but in turquoise.

Speaker baseline measurements were taken by placing an insert earphone into the ear canal of the cadaveric temporal bone and playing a frequency sweep of sound at varying input levels. These baseline measurements provide a control for comparison and a better understanding how natural sound will actuate the TM and attached ossicular chain. Next, the MDHDA was placed in the ear canal and coupled direct to the tympanostomy tube. The device was then held in place using bone wax with a small opening was made into the wax to allow for ear canal ventilation. The device was driven by various inputs between 100 and 400 mV at frequencies from 300 to 10,000 Hz and the stapes displacements were recorded. The range of displacements induced by the device was compared to those of natural sound. A cosine correction of 45 degrees

was applied to all measurements due to the angle between the measuring angle of LDV and the movement of the stapes.

The range of displacements induced by the device was compared to those of sound. A 200 mV input to the device produced a range of displacements equivalent to those of sound at 70 dB SPL (mean 0.44 nm; range 0.01-2.80). A 400 mV input produced range of displacements equivalent to those of sound at 80 dB SPL (mean 1.34 nm; range 0.02-8.87). The device was capable of actuating the eardrum through a ferromagnetic tympanostomy tube.

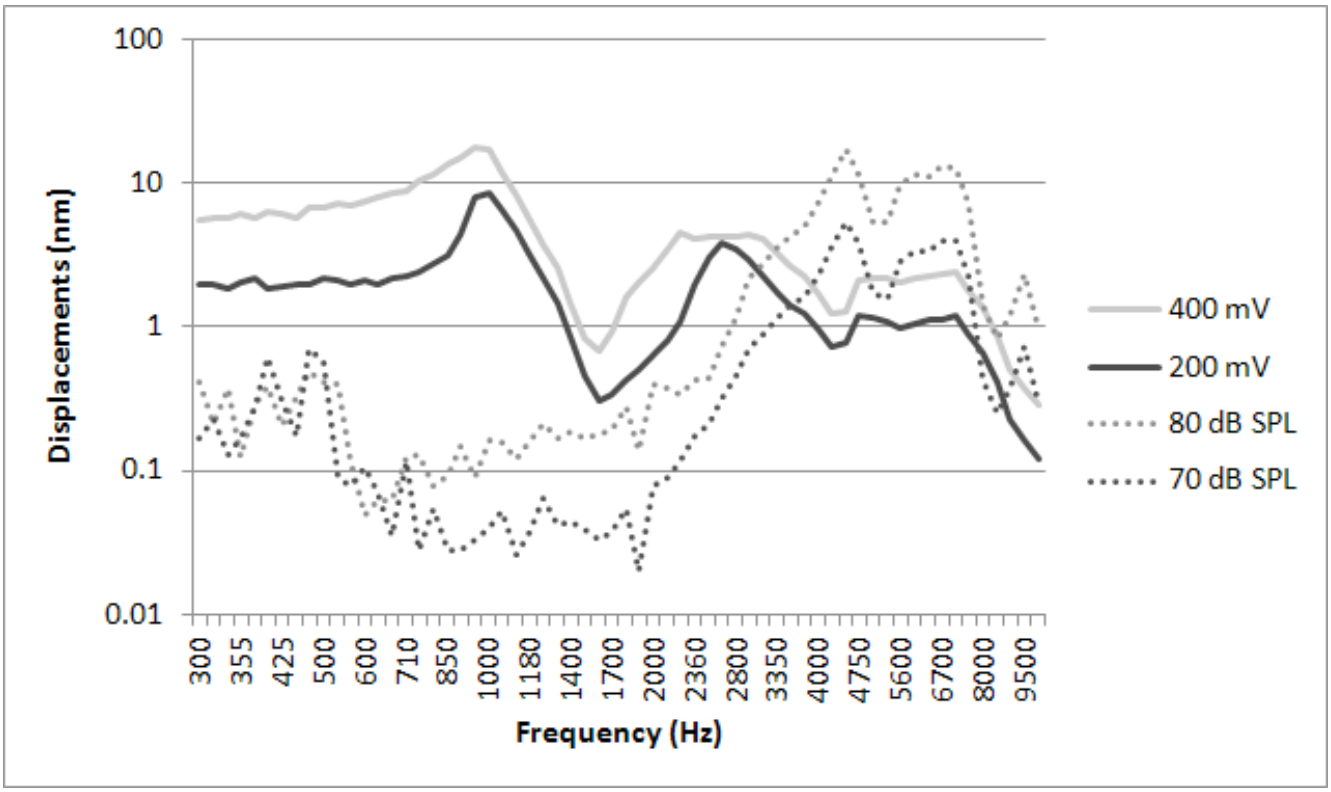

Fig. 62 Tympanostomy tube embodiment middle ear displacement. This figure demonstrates the speaker baseline displacements (dotted lines) of the posterior crus of the stapes of the temporal bone with a ferromagnetic tympanostomy tube placed in the TM. The solid lines are the displacements created when the MDHDA is coupled directly to the tube in the TM.

CHAPTER 4

Direct Hearing Device Clinical Performance

The success of the DHDA in bench and temporal bone testing led our research group to the preparation of a human clinical trial. Our group applied to the UC Irvine Medical Center Institution Review Board to test the DHDA in Dr. Hamid Djalilian's clinic. The request was approved and two short-term clinical performance tests have been conducted to evaluate the DHDA's ability to appropriately recreate sound in human subjects. The methods and results will be discussed in this chapter.

1. Institutional Review Board DHDA Human Clinical Performance Test

Our group submitted an application to the University of California Irvine Office of Research - Internal Review Board for a 60 subject human trial to test the effectiveness of the DHDA as a tympanic membrane and ossicular chain driver that could successfully transmit sound information.

The summary of the protocol narrative is included below and a full application is available through the UC Irvine Office of Research:

"Hearing loss is one of the most prevalent chronic conditions in the U.S., affecting over 10% of the population. Despite the disability that hearing loss causes, only 20% of patients with hearing loss use hearing aids. Patients cite cost, stigma, appearance and sound quality of conventional hearing aids as the main reasons for non-use. Implantable hearing devices have been developed to address the shortcomings of traditional hearing aids. However, they entail an invasive and expensive surgical approach.

In collaboration with the Department of Electrical Engineering and Computer Science, we have recently developed a new micro hearing aid, which is small, inexpensive, high quality, and invisible to the user. Like middle ear implants, this device will not produce acoustic feedback or occlusion effects, common to hearing aids. Furthermore, this approach offers several compelling advantages over middle ear implants, namely: no invasive surgery, greatly reduced cost, easy accessibility, and easy placement and removal.

The purpose of this project is to assess the efficacy of our new wearable direct drive micro hearing aid in individuals with mild to moderately severe sensorineural hearing impairment who had worn optimally fit hearing aids for at least 6 months and are dissatisfied with the sound quality. Outcome measures include: functional gain, speech recognition in quiet and noise, articulation index scores, perceived aided benefit, sound quality judgments, satisfaction, and presence of feedback and occlusion with the new direct drive hearing aid compared with those of the patients' optimally fit hearing aid."

UC IRVINE: OFFICE OF RESEARCH
INSTITUTIONAL REVIEW BOARD (IRB)

March 05, 2013

HAMID DJALILIAN
OTOLARYNGOLOGY – HEAD AND NECK SURGERY

RE: UCI IRB HS# 2011-8486 *Clinical Investigation of a New Direct Drive Micro Hearing Aid: A Clinical Trial*

The above-referenced human-subjects research project has been approved by the University of California, Irvine Institutional Review Board (UCI IRB). This approval is limited to the activities described in the approved Protocol Narrative, and extends to the performance of these activities at each respective site identified in the Application for IRB Review. In accordance with this approval, the specific conditions for the conduct of this research are listed below, and informed consent from subjects must be obtained as indicated. Additional conditions for the general conduct of human-subjects research are detailed on the attached sheet.

NOTE: Approval by the Institutional Review Board does not, in and of itself, constitute approval for the implementation of this research. Other institutional clearances and approvals may be required (e.g., EH&S, Radiation Safety, School Dean, other institutional IRBs). Research undertaken in conjunction with outside entities, such as drug or device companies, are typically contractual in nature and require an agreement between the University and the entity. Such agreements must be executed by an institutional official in Sponsored Projects, a division in the UCI Office of Research. The University is not obligated to legally defend or indemnify an employee who individually enters into these agreements and investigators are personally liable for contracts they sign. Accordingly, the project should not begin until all required approvals have been obtained.

Questions concerning the approval of this research project may be directed to the Office of Research, 5171 California Avenue, Suite 150, Irvine, CA 92697-7600; 949-824-6068 or 949-824-2125 (biomedical committee) or 949-824-6662 (social-behavioral committee).

Expedited Review: Category 9

Ruth A. Mulnard, DNSc, RN, CNRN, CIP, FAAN
Vice Chair, Institutional Review Board

Fig. 63 Confirmation letter from UC Irvine Office of Research regarding approval of DHDA human trial to be conducted at UC Irvine Medical Center.

2. Short Term Clinical Performance Test #1

The objective for this first short term study was to verify that the DHDA could successfully drive the TM and attached ossicular chain to transmit sound information in human subjects. Additionally, this trial would provide insight into the power requirements of the DHDA, TM interface mechanism, and ease of placement by otolaryngologist, comfort, and other operational insight that could not be determined through temporal bone studies. The subject used in this clinical performance test does not have hearing loss.

3. Short Term Clinical Performance Test #1 – Protocol

A. DHD Device in Clinical Performance Test #1

First, testing of the DHDA began with selecting the appropriate interface tip embodiment. While our research group had tested many different embodiments (custom mold, magnetic, tympanostomy tube), we opted for a simple flexible silicone polymer at a 30° angle. As presented in Chapter 3, the ear canal and TM do not meet perpendicularly, but instead at an angle that varies slightly from individual to individual. Therefore, a lightweight silicone tip (2 mg) 3 mm in diameter that creates a 30° to accommodated for ear canal and TM geometry was placed on the connection plate of the DHDA.

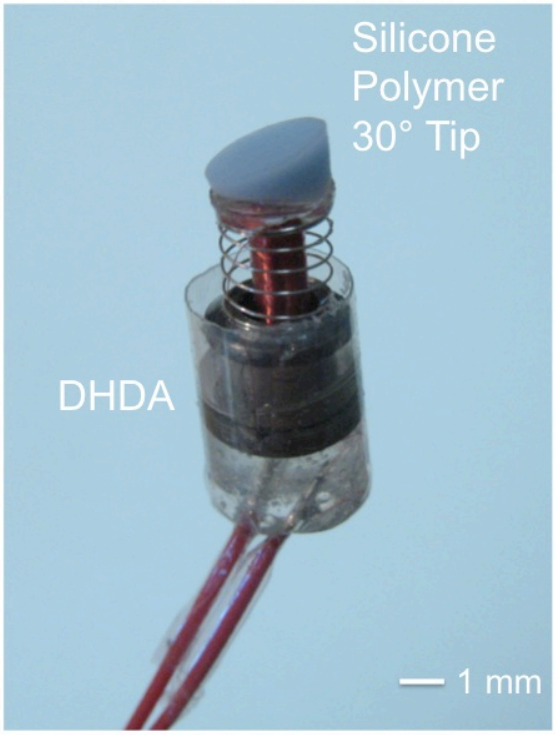

Fig. 64 DHDA used in short term clinical performance test #1. The design that was used was the DHDA with a flexible polymer tip formed at a 30°. This tip will accommodate the shape the ear canal forms with the TM. This tip will also not be custom fit to the umbo as in prior tests, and therefore will be tested on multiple locations of the TM to find the most appropriate driving location.

B. DHDA Clinical Testing Circuit

Next, a DHDA testing circuit was developed that would allow an easy interface to drive and monitor the DHDA activity simultaneously during the in clinic testing. As opposed to having a larger computer setup to drive the DHDA our research group opted for a small MP3 player (iPod Nano, Apple Inc. Cupertino CA) to drive the DHDA with the appropriate sound signals. Then, a small connector for the DHDA was attached to the circuit as well as a small resistor to monitor the current through the system. Lastly two oscilloscope connectors were added for monitoring the real time performance of the DHDA; Scope CH 1 to monitor the voltage drop across a small resistor (current in the system) and Scope CH 2 to monitor the voltage drop across the entire system. Not only is this system necessary for monitoring the signal and current delivered to the DHDA system, but also allows us to measure the power requirements of the DHDA when coupled to the TM.

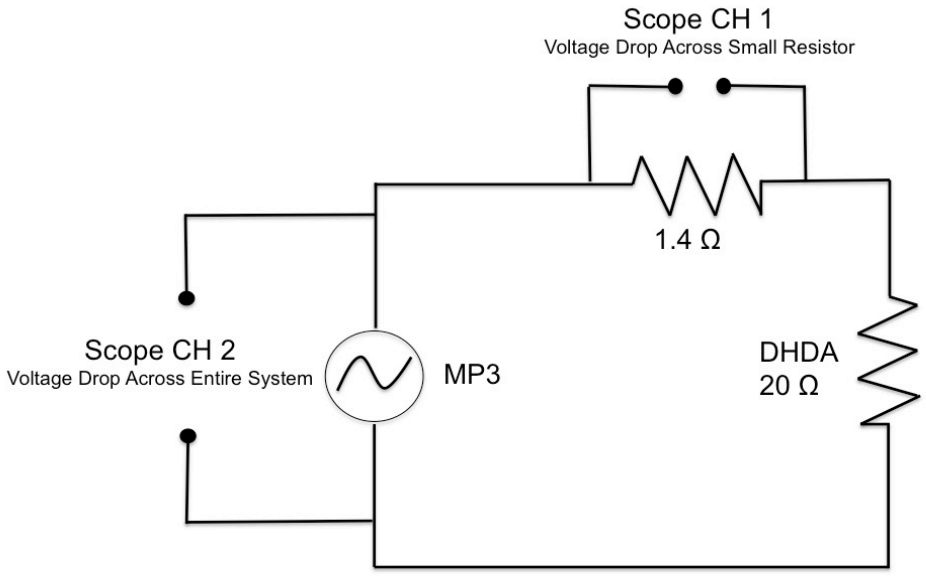

Fig. 65 DHDA clinical testing equivalent circuit. This circuit includes an MP3 player as the driver, a small resistor to monitory current in the system, the DHDA, and two oscilloscope connectors to monitor the device and system real time.

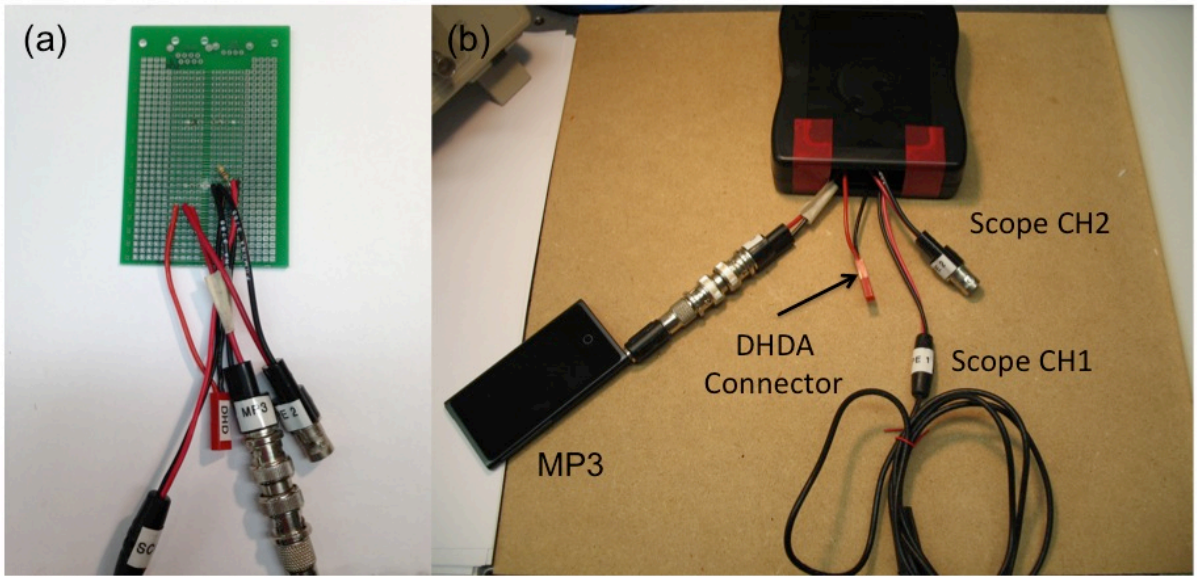

Fig. 66 DHDA clinical performance test driving circuit. This testing circuit consists of an MP3 player, a DHDA connector, and two oscilloscope connections. This circuit allows for real time monitoring of the current going through the device and system as well as an easy interface for DHDA and MP3 connections. While a more sophisticated testing setup will be used for long term trials, for a short in office testing, this setup met all needs of the system. A signal will be driven through the MP3 player and out through the DHDA while the voltage drop is recorded by the oscilloscope. (a) PCB DHDA testing circuit (b) enclosed DHDA test driving circuit.

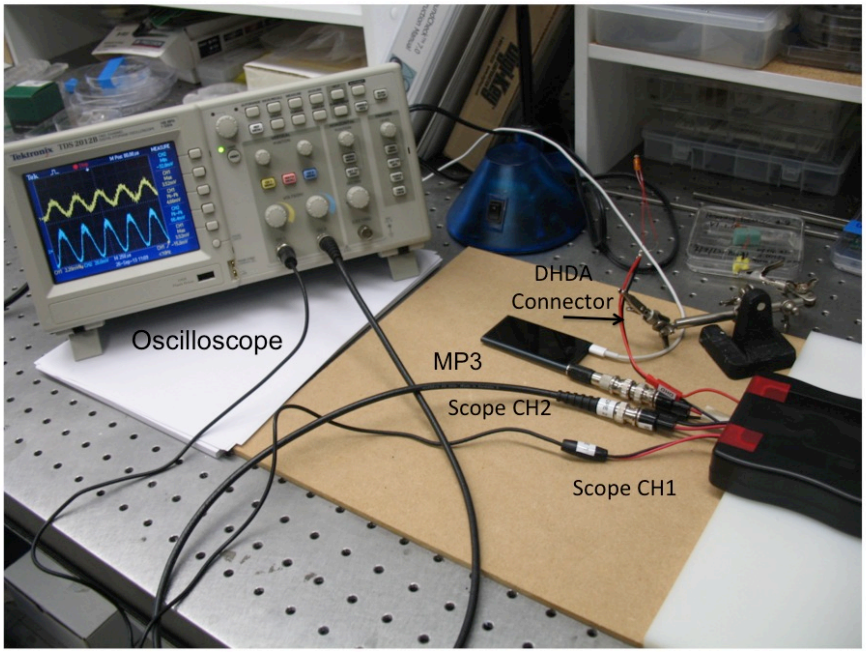

Fig. 67 DHDA clinical performance testing setup. This setup here includes the DHDA testing circuit, the oscilloscope, and a sample DHDA connected. It can be seen in the oscilloscope a pure tone being played through the DHDA and the voltage drop across both the entire system and the DHDA itself. This system is helpful for monitoring the real-time performance of the DHDA.

C. Tympanic Membrane Inspection and Cerumen Removal

Next, the subject would undergo an ear canal and tympanic membrane inspection. This included removal of wax from the canal to allow for appropriate placement of the DHDA as well as provide the most accurate results for the upcoming hearing test. Excessive cerumen (wax) buildup can lead to hearing loss because the wax prevents sound to be transmitted down the ear canal[14]. Therefore a clear ear canal is necessary to proceed with testing.

D. Subject Audiometry Testing and DHDA fitting

Upon completion of the TM inspection, an audiometry test was performed to determine the subjects hearing level at a variety of frequencies. This test will establish at what dB SPL level the subject's hearing threshold is at certain frequencies. Therefore when we begin testing the DHDA our group will know if there are certain frequencies that the subject will have more difficulty hearing compared to others. The hearing test was conducted in a double walled soundproof room using Ear Tone 3A insert earphones (Audiometrics, Oceanside, CA), and the audiometer used was a Grason-Stadler Audiometer, Model GSI 16 (Eden Prairie, MN).

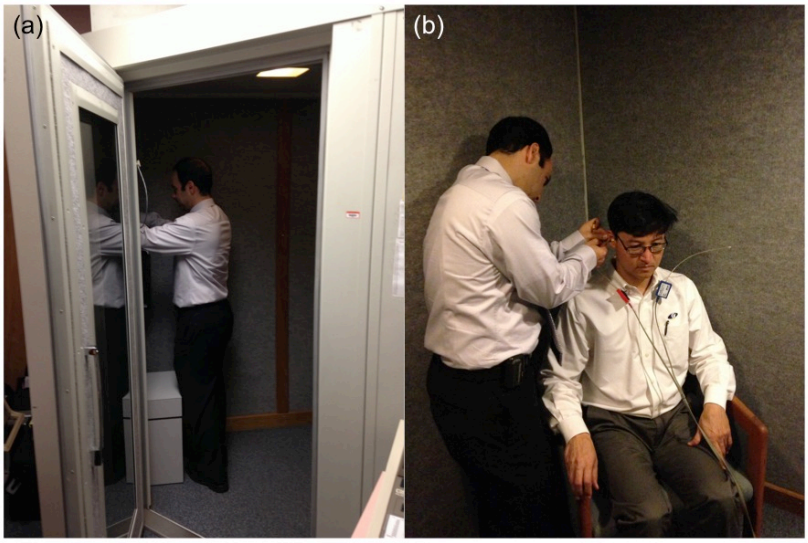

Fig. 68 Hearing test in sound booth at UCI Medical Center. (a) shows Dr. Hamid Djalilian preparing the sound booth for audiogram testing (b) Dr. Djalilian placing the insert earphones is Dr. Mark Bachman's right and left ear to evaluate his hearing level at a variety of frequencies.

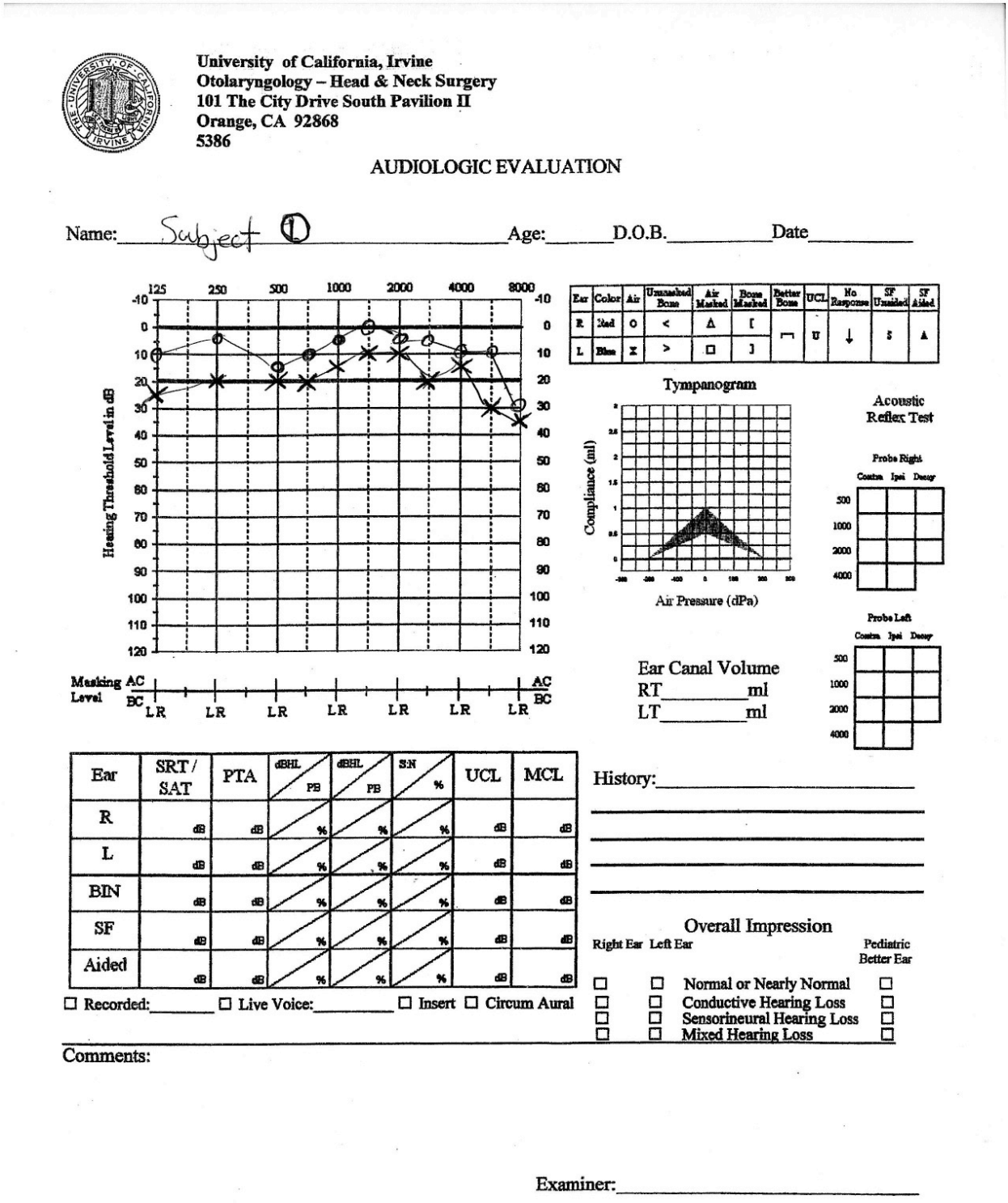

Fig. 69 Subjects hearing test (audiogram) results of both the left and right ear in response to pure tone frequencies. Anytime a subject has a hearing threshold above 20 dB SPL that is generally characterized as mild hearing loss. Therefore the subject has a little mild hearing loss, and it is most affected at the 8 kHz level, also known as a mild high frequency hearing loss.

Following the hearing test the subject was moved back to the clinic where the DHDA was fit in the ear canal to assure Dr. Djalilian could have appropriate visibility around the device in order to place in different locations of the TM. This trial did not include a fixture to permanently hold the DHDA in place. Instead Dr. Djalilian held the device in different locations during testing.

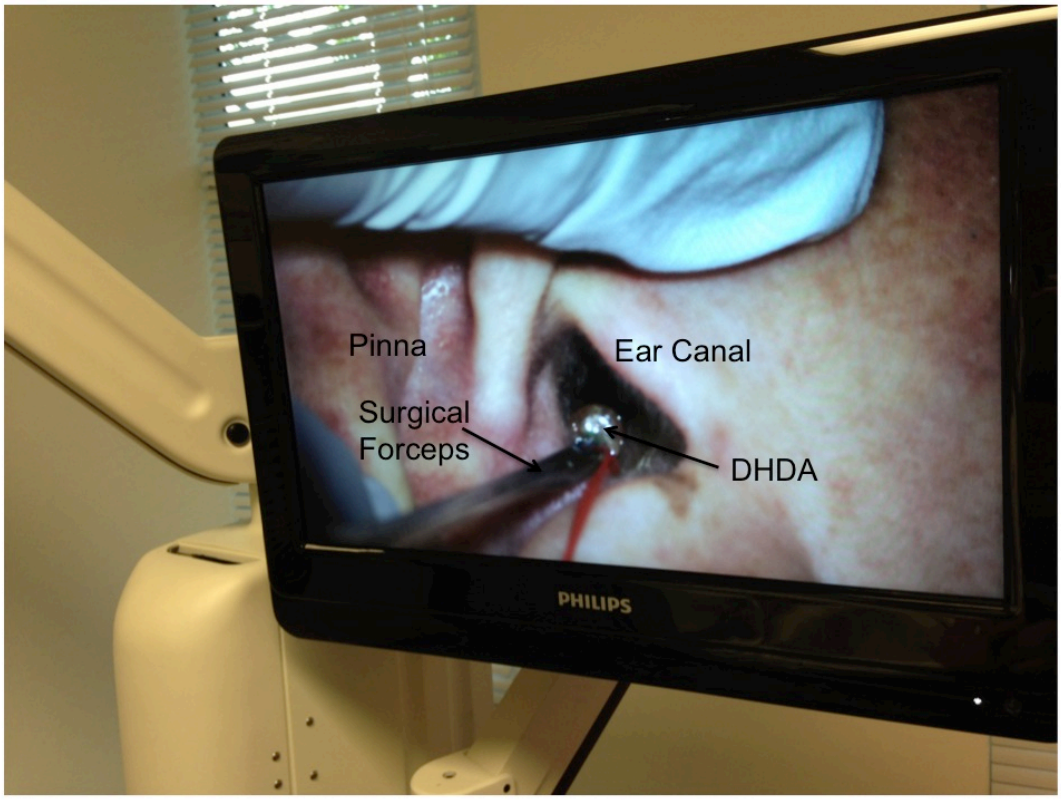

Fig. 70 DHDA ear canal fitting. Dr. Djalilian placed the device to assure appropriate fitting in the ear canal and to assure he had visibility around the device to place in contact with the TM during the short-term clinical performance test. This image was taken through the surgical microscope camera.

E. Short Term Clinical Performance Test

The short term clinical test had four main objectives for evaluting the DHDAs ability to succesfully recreate sound by mechaniclaly driving the TM and attached ossicular chain:

1. DHDA coupling location on TM
2. Sound matching experiments
3. Complex audiowaveform (music evaluation)
4. DHDA size and comfort of placements

Fig. 71 Short-term clinical performance test office setup. (a) Dr. Hamid Djaliian, Dr. Mark Bachman, Dr. Hossein Mahboubi and Dr. Amy Yao prepare and discuss the first DHDA clinical trial (b) Dr. Djalilian fits Dr. Bachman with an audiometry headset on his left ear. Pure tones will be played through the audiometry system to his left hear for sound matching experiments with the DHDA that is placed is his right ear.

Sound matching experiements were conducted by placing the DHDA in the subjects right ear, while the left ear was fited with an audiometry headset. The DHDA was held in place for the durantion of the test by Dr. Hamid Djaliain. The audiometer used was a Grason-Stadler Audiometer, Model GSI 16 (Eden Prairie, MN).

Pure tone sound files were preloaded onto the MP3 player: 250 Hz, 500 Hz, 1 kHz, 2 kHz, 4 kHz, and 8 kHz. Based on the results of the hearing test, we wanted to use frequencies where the hearing level of the right ear and left ear were most closely matched. These frequencies were 500 Hz, 1000 Hz, and 2000 Hz. While these results will be most accurate, for sound matching tests, all frequencies will be tested.

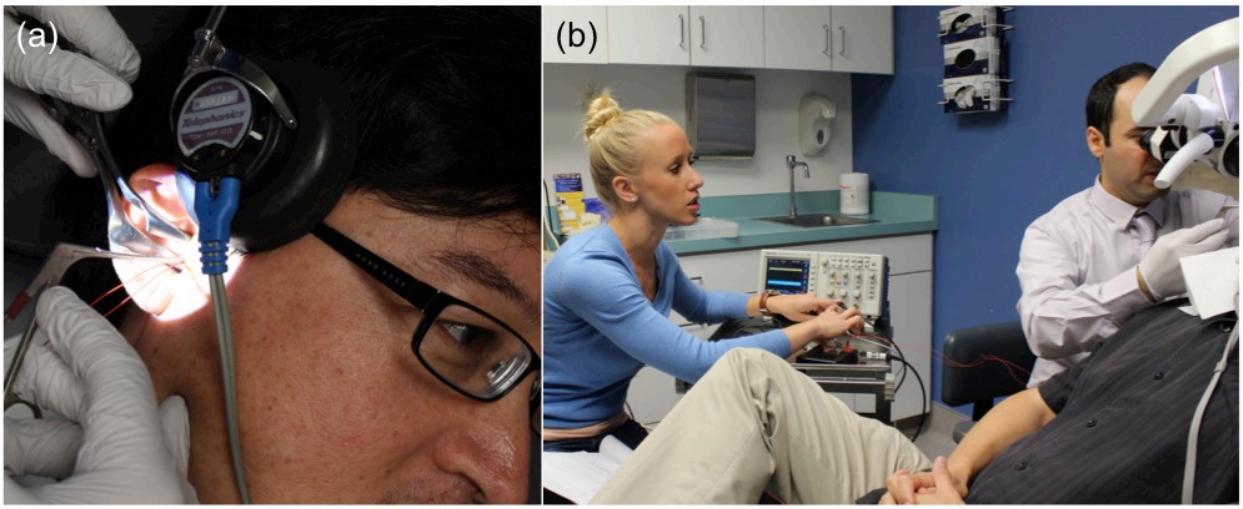

Fig. 72 Performance test #1 images (a) depicts the DHDA being placed in the ear canal (b) depicts the DHDA control system increasing the current being driven through the DHDA in attempt to match the dB SPL being produced by the audiometry earphone.

Before sound matching tests begin Dr. Djalilian placed the DHDA in a variety of locations on the TM to better understand the best place of mechanical coupling for driving the TM and attached ossicular chain. These locations will be evaluated for ease of placement as well as loudness of sound perceived by the subject while the DHDA driving current is held constant.

Sound matching testing began by playing a certain tone (frequency) through the audiometry headset and the exact same frequency through the DHDA. The DHDA delivers constant frequency sounds while the audiometer delivers pulsed sound. This will be something that will be changed in subsequent tests, where both audiometry headset and DHDA present pulsed sound delivered to both the right and left ear. The subject uses their right and left hands to indicate which side is perceived as louder, and then raises both hands when the sounds are perceived as equal. Once a an equal signal is received, the headset will deliver a 5 dB SPL sound

above or below that matched sound, and then back to the matched sound to confirm the subjects identification of matching sound level. Once that is confirmed, measurements of the DHDA testing circuit are taken for voltage drop across CH 1 and CH 2 to better understand what power requirements are needed to drive the DHDA a certain dB SPL. This procedure is then repeated for increasing dB levels and frequencies.

Fig. 73 DHDA short term performance test clinical setup. Two medical doctors were taking clinical observations, I was controlling the DHDA and its performance, Dr. Djalilian placed the DHDA in the right ear, and Dr. Mahboubi controlled the audiometry set for stimulating the left ear.

The DHDA will also be evaluated in its ability to transmit complex audio waveforms**.** This will be determined by playing music directly through the DHDA, and the song selected was 'Sparks' by Coldplay. Lastly, the DHDA will be evaluated for its fit and comfort when placed in

the subject's ear. Most importantly, is there visibly around the device to allow for the surgeon to accurately place the device and does it cause the patient any discomfort while operating.

4. Short Term Clinical Performance Test # 1 Results

A. Device modifications during short-term clinical performance test #1

At the onset of the trial, Dr. Djalilian was having trouble consistently reaching different locations on the TM with the original blue 30° lightweight silicone tip. Therefore we opted to remove the original interface tip and add a longer tip that better suited the needs of the trial. This was also made with the same flexible silicone polymer (only a different color – pink), and was molded and placed by Dr. Djalilian.

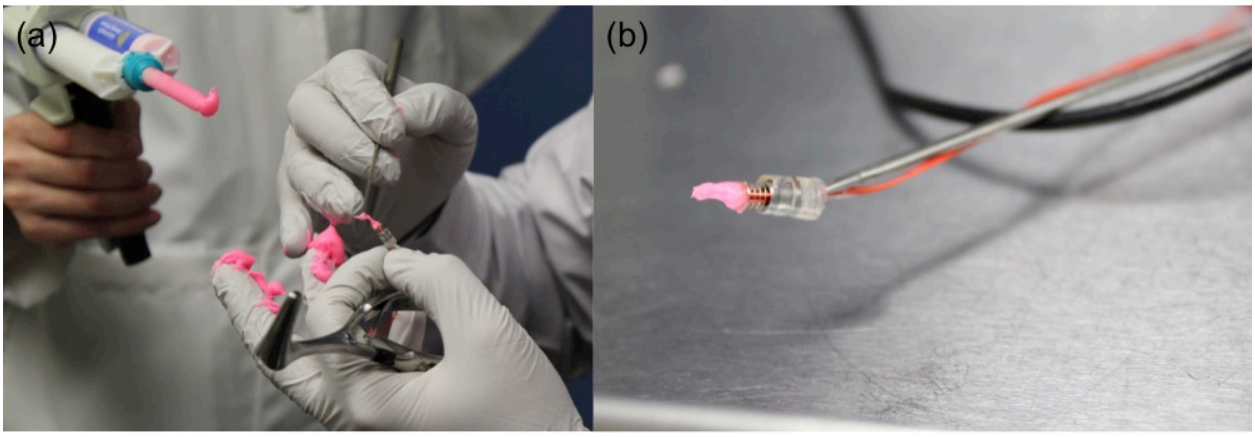

Fig. 74 DHDA contact tip modification. (a) During the clinical trial Dr. Djalilian wanted a longer contact tip extension to couple to DHDA to different areas of the TM and needed an extension to reach it more effectively. He used the flexible curable polymer and made a contact tip on the fly. (b) the final DHDA used for the short term performance test #1.

B. DHDA coupling location on TM

After the final device embodiment was prepared Dr. Djalilian began coupling the device to different locations on the TM while keeping the device stimulating frequency and voltage constant. Upon inception of the clinical trial, our group believed we would couple the DHD to

the umbo of the TM. When the DHDA was placed in the subject's ear canal and the device was tested at different contact points on the tympanic membrane, the lateral process of the malleus appears to be the most promising. The subject reported the sound to be louder when coupled to the lateral process as compared to other locations. This may be due to the anatomy of the lateral process of the malleus and how it protrudes slightly from the plane of the TM allowing for easier access as well as a more secure contact point[103].

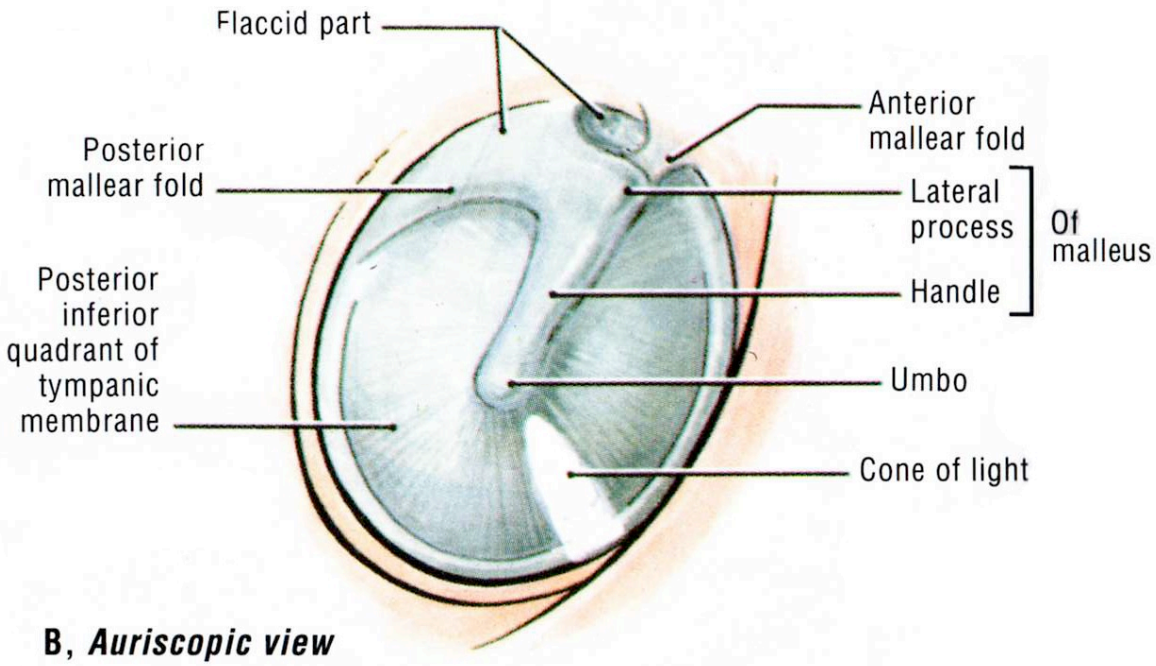

Fig. 75 Auriscopic view of the tympanic membrane (illustration by Dr. Emad Kayyam)[104]. Upon initiation of this trial the umbo was the perceived prime location from coupling the DHDA. However, it was discovered that the lateral process of the malleus proved more effective and appropriate.

C. DHDA sound matching results for clinical performance test #1

Sound matching testing went smoothly, with the subject easily able to match sound between the right and left ear using the hand raising signals. One improvement that will be made, based on

subject feedback, is to play pulsed sounds through the DHDA. This is because after an extended period of time the subject felt like they began getting accustomed to the pure tones (especially higher frequencies), and it would be more helpful and accurate to pulse the sound coming from both sources.

As expected the driving voltages required to achieve certain dB SPL levels in the human trials was substantially less than that of the cadaveric tests. For example to recreate a 2 kHz sound at 60 dB SPL in the human trial it took approximately a ~25 mV driving signal, and in the cadaver to achieve a 60 dB SPL it took a ~200 mV driving signal.

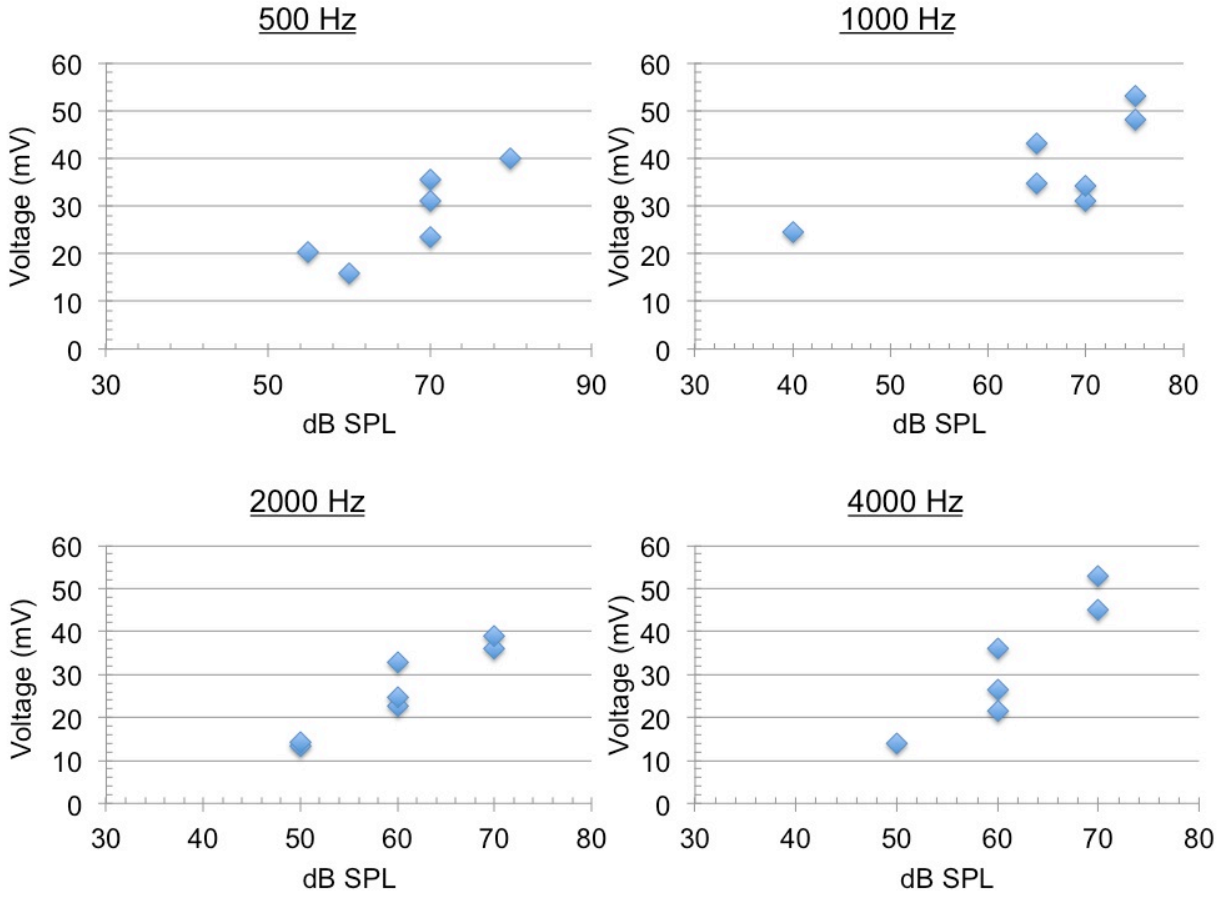

Fig. 76 DHDA Sound matching results for clinical performance test #1. This chart displays the results of the sound matching tests for frequencies: 500 Hz, 1000 Hz, 2000 Hz, and 4000Hz and the corresponding dB SPL that the subject reported the sound to match.

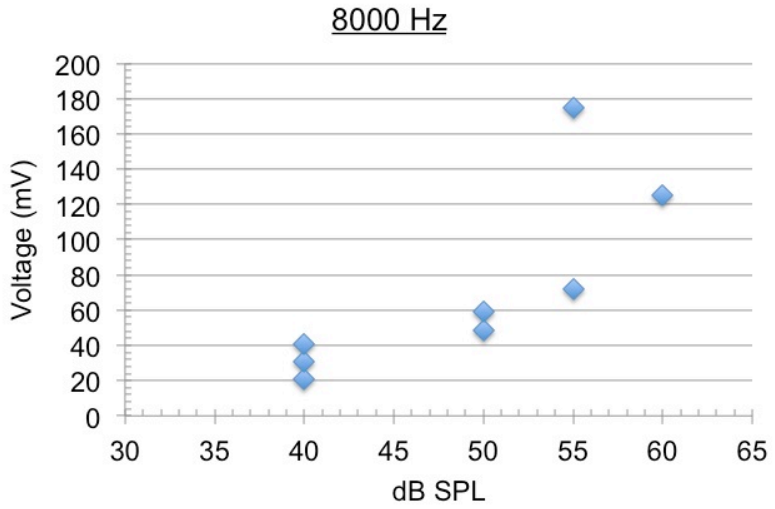

Fig. 77 DHDA Sound matching results for clinical performance test #1. This chart displays the results of the sound matching tests for 8000 Hz and the corresponding dB SPL that the subject reported the sound to match.

D. DHDA complex audio waveform evaluation

The subject described the sound quality as 'pure' and 'almost coming from inside my head'. The subject reported being able to hear the song completely, but the sound 'sometimes felt like it lost its richness on the lower end of the frequencies'. There was however, no scraping or muffled sound. The subject described the quality being best when to volume was high, and varied greatly depending on placement on the TM.

E. DHDA size, design, and comfort of placement

While the DHDA performed successfully during the clinical trial there are a few design changes that will be made for subsequent trials. First, for ease of placement by the otolaryngologist, a smaller device diameter is more desirable. This is because it is necessary to have plenty of visibility around the DHDA for appropriate coupling to the TM, and a 3 mm diameter would be more helpful to aid this process of placement. Secondly, the DHDA housing of the device used in the short-term clinical performance test caused a bit of irritation to the ear canal of the subject. Dr. Djalilian used an antibiotic spray to the entire ear canal and TM after

testing to avoid any possible infection due to the irritation of rubbing. This is because the housing of the DHDA was slightly longer than it should have been, and thus caused some uncomfortable rubbing along the ear canal of the subject anytime the device was being moved. In subsequent tests we will use a new softer polymer as well as design the housing gas such it will be flush with the outer flux guide and not create a potential edge that could cause irritation during rubbing or moving with the ear canal during placement.

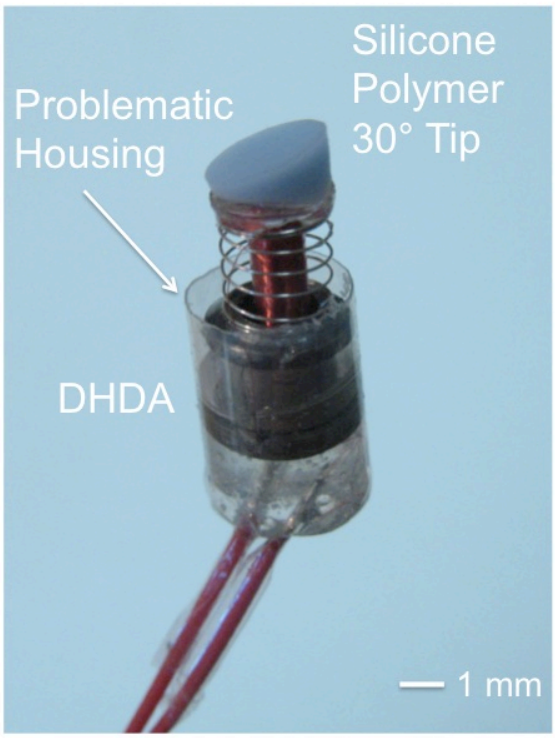

Fig. 78 Problematic housing of DHDA in short term clinical performance test #1. As seen in this figure the housing of the DHDA comes up slightly too far and presented a place that could run uncomfortably on the subjects ear canal. While this material was a flexible heat shrink polymer tubing, the osseous portion of the ear canal can be quite sensitive. In subsequent testing this housing will be sure to only cover the DHDA up to the top of the outer flux guide. Therefore the housing will be flush with the OFG and cannot cause additional irritation.

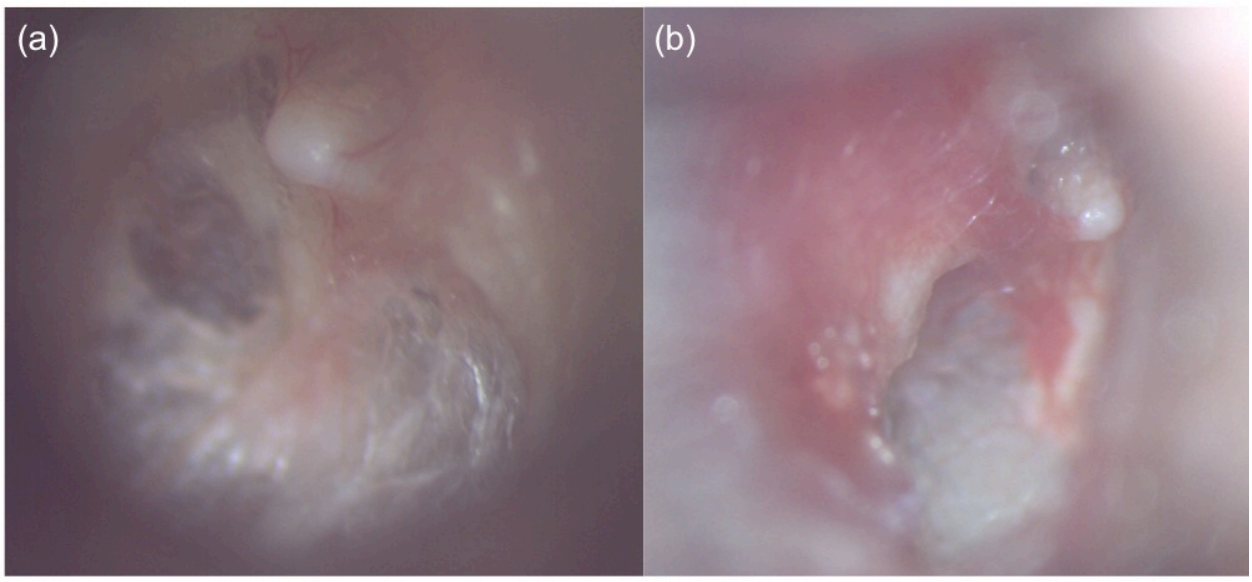

Fig. 79 Tympanic membrane irritation during short-term clinical performance test #1. (a) before DHDA performance test began (b) after performance test concluded. This irritation was due to the problematic housing of the device used. The subject reported slight irritation and sensitivity during the trial.

F. General short term clinical performance test #1 observations

Dr. Djalilian reported no sound generated from the device during clinical testing. The subject reported not being able to hear any sound unless the device was pressed to the TM. A local anesthetic was used on the TM prior to placement and a spray antibiotic was used after the clinical test was over. Additionally the wire used in this trial to connect the DHDA to the driving circuit had too much spring; and when dropped would bounce out of Dr. Djalilian grip. A more compliant and less bouncy wire will be used in subsequent tests.

5. Short Term Clinical Performance Test # 2

The first short term clinical trial provided much insight into the logistics of using the DHDA as a direct drive device in a clinical testing setting, providing ideas for design changes as well as additional performance tests to be evaluated. The design changes to be introduced in the second short-term clinical performance tests include: device diameter reduction, housing

modifications, interface tip modifications, and using of a new wire that connects the DHDA to the testing circuit. Additionally, sound matching testing using pulsed sound, speech discrimination tests performed, and comparison of sound quality produced by the DHDA and the MEDEL Vibrant Soundbridge Middle Ear Implant.

6. Short Term Clinical Performance Test # 2 - Protocol

A. DHDA design changes

The first changes that needed to be made for the next clinical trial were design changes. The first was creating a device that had a 3 mm diameter as compared to a 3.6 mm diameter. This was to increase the visibility for the surgeon placing the device to see around the device and be able to place the device in many precise locations on the TM. Fortunately, the only design modifications needed to be made were to the inner and outer flux guides to achieve this diameter. Therefore the IFG and OFG were reduced to 3 mm and assembled in the same fashion as the original device. Then, a new, more soft and compliant actuator housing was used and only covered the IFG, magnet, and OFG, as to assure no scraping could occur along the ear canal.

Next, an extension tip needed to be made to add to the connection plate of the DHDA. This extension tip will provide the additional length needed to reach different locations of the TM. The extension tip was made of malleable wire (Belden copper wire 30 AWG model 8041; Chicago IL), a flexible silicone tip, and an adhesive to attach the tip to the connection plate of the DHDA. Thirteen different tips were made of varying length; this would allow for Dr. Djalilian to determine in the clinic which extension tip would be most appropriate based on the ear canal/TM

geometry of the subject. Lastly a more compliant wire was used to attach the DHDA to the clinical test driving circuit (Category 2671/32; Daburn Electornics & Cable; Dover NJ).

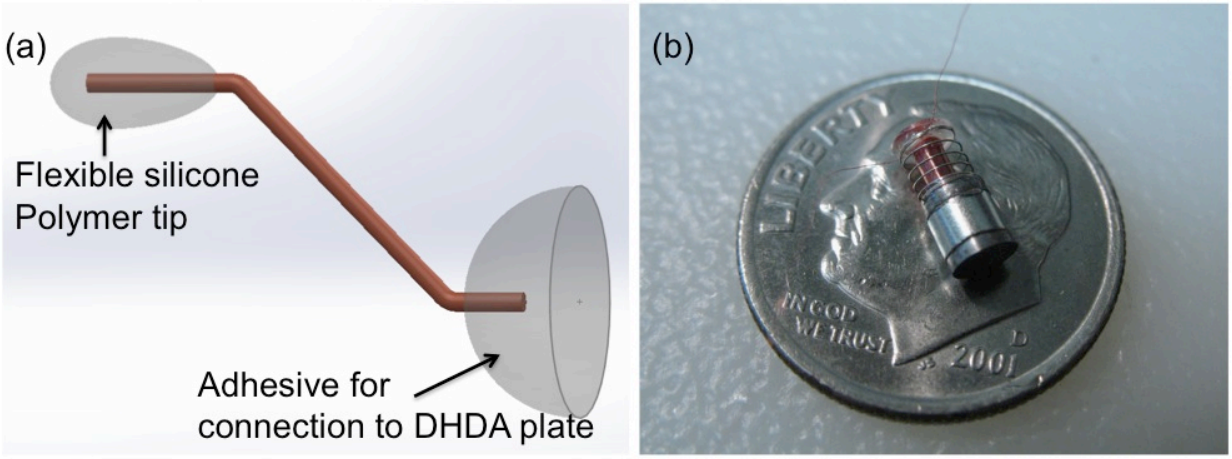

Fig. 80 DHDA design changes for short term clinical performance test #2 (a) the extension tip used for the DHDA. This tip will be attached to the DHDA connection plate. It consists of a flexible polymer contact tip, flexible wire extension, and adhesive for attachment to the connection plate of the DHDA. (b) 3mm diameter DHDA design. Dr. Djalilian desired a smaller diameter to allow for more visibility during placement, and thus the 3 mm design was used.

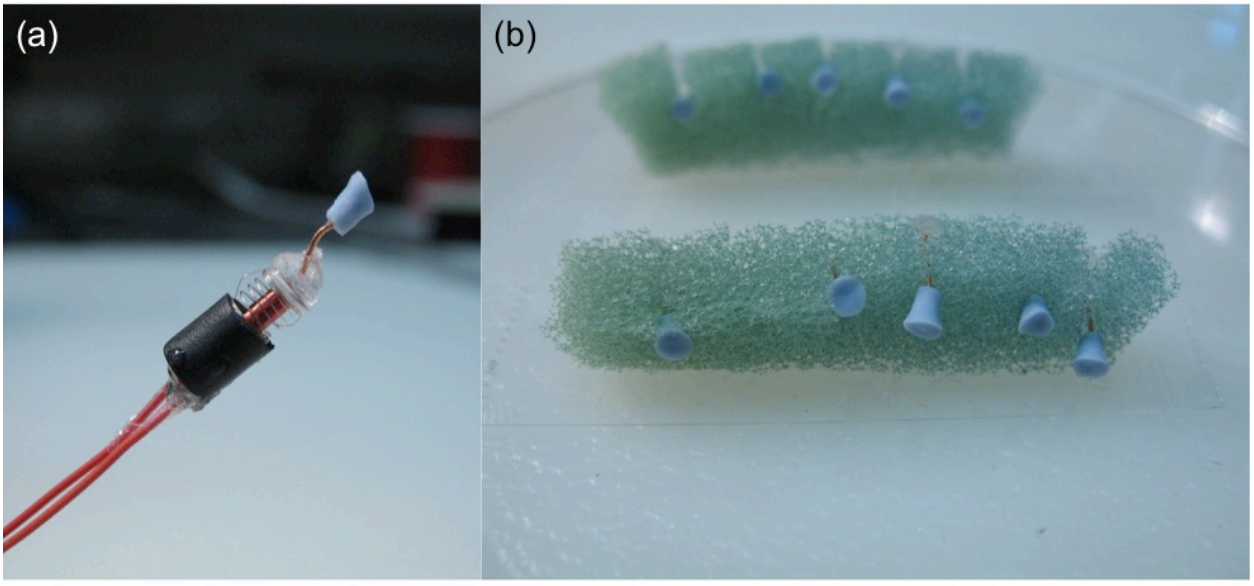

Fig. 81 DHDA used short term clinical performance test # 2 (a) DHDA with new extension tip, 3 mm design, and smaller housing (b) different sizes of the extension tips so Dr. Djalilian can select the appropriate fit for the subjects ear canal and TM.

B. DHDA sound matching testing

Sound matching experiments will be conducted in the same fashion as clinical performance test #2, however, this time sounds delivered through the DHDA will be pulsed as opposed to continuous. This is because, first, the audiometry system delivers pulsed sound, and second, it was observed by the subject that hearing a constant pure tone can lend it self to accommodation. Therefore a pulsed signal is most appropriate and will allow the subject to more accurately identify when the sounds produced by the DHDA and audiometry set are matched.

C. DHDA speech discrimination testing

Our group was interested in confirming the DHDA's ability to successfully transmit speech information. While our preliminary studies showed success in recreating complex audio waveforms (music), we were very interested to know how well the device could transmit speech. A commonly used speech discrimination test was used, Northwestern University Auditory Test No. 6[105,106]. This speech discrimination test is composed of four lists of 50 consonant-nucleus-consonant (CNC) monosyllabic words each. Two lists of this test were used, 2A and 3A. The first, list 2A was delivered at a higher volume that the subject could definitely hear. The second list was delivered just at hearing threshold. The two lists were recorded and loaded onto the MP3 player for testing. A 1-second pause was given between each word, creating a total test time of approximately 3 minutes and 30 seconds.

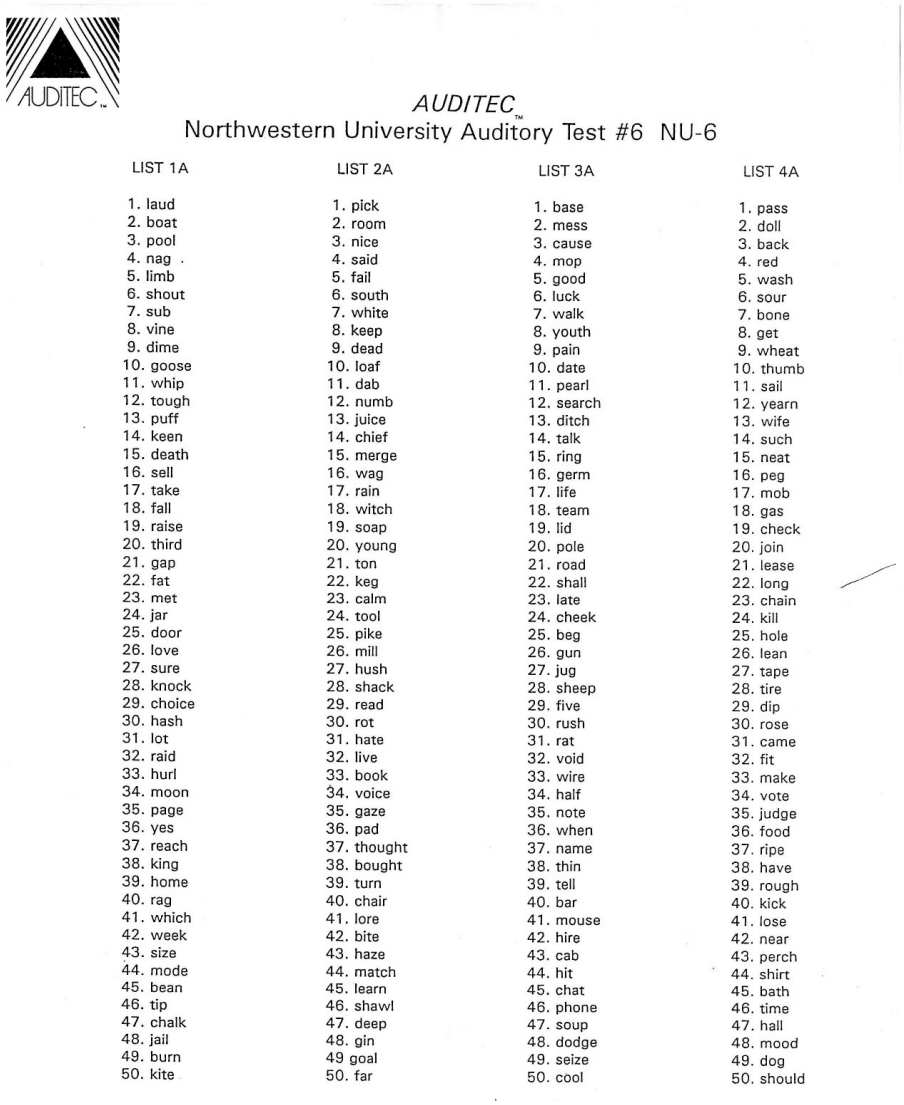

AUDITEC™

Northwestern University Auditory Test #6 NU-6

LIST 1A	LIST 2A	LIST 3A	LIST 4A
1. laud	1. pick	1. base	1. pass
2. boat	2. room	2. mess	2. doll
3. pool	3. nice	3. cause	3. back
4. nag	4. said	4. mop	4. red
5. limb	5. fail	5. good	5. wash
6. shout	6. south	6. luck	6. sour
7. sub	7. white	7. walk	7. bone
8. vine	8. keep	8. youth	8. get
9. dime	9. dead	9. pain	9. wheat
10. goose	10. loaf	10. date	10. thumb
11. whip	11. dab	11. pearl	11. sail
12. tough	12. numb	12. search	12. yearn
13. puff	13. juice	13. ditch	13. wife
14. keen	14. chief	14. talk	14. such
15. death	15. merge	15. ring	15. neat
16. sell	16. wag	16. germ	16. peg
17. take	17. rain	17. life	17. mob
18. fall	18. witch	18. team	18. gas
19. raise	19. soap	19. lid	19. check
20. third	20. young	20. pole	20. join
21. gap	21. ton	21. road	21. lease
22. fat	22. keg	22. shall	22. long
23. met	23. calm	23. late	23. chain
24. jar	24. tool	24. cheek	24. kill
25. door	25. pike	25. beg	25. hole
26. love	26. mill	26. gun	26. lean
27. sure	27. hush	27. jug	27. tape
28. knock	28. shack	28. sheep	28. tire
29. choice	29. read	29. five	29. dip
30. hash	30. rot	30. rush	30. rose
31. lot	31. hate	31. rat	31. came
32. raid	32. live	32. void	32. fit
33. hurl	33. book	33. wire	33. make
34. moon	34. voice	34. half	34. vote
35. page	35. gaze	35. note	35. judge
36. yes	36. pad	36. when	36. food
37. reach	37. thought	37. name	37. ripe
38. king	38. bought	38. thin	38. have
39. home	39. turn	39. tell	39. rough
40. rag	40. chair	40. bar	40. kick
41. which	41. lore	41. mouse	41. lose
42. week	42. bite	42. hire	42. near
43. size	43. haze	43. cab	43. perch
44. mode	44. match	44. hit	44. shirt
45. bean	45. learn	45. chat	45. bath
46. tip	46. shawl	46. phone	46. time
47. chalk	47. deep	47. soup	47. hall
48. jail	48. gin	48. dodge	48. mood
49. burn	49 goal	49. seize	49. dog
50. kite	50. far	50. cool	50. should

Fig. 82 Speech discrimination test used in short-term clinical performance test # 2. Specifically list 2A and 3A were delivered to the subject and speech discrimination percentages were evaluated.

D. Sound quality comparison between DHDA and MEDEL Vibrant SoundBridge.

This experiment would be a strictly qualitative evaluation of the sound quality of music transmitted by the DHDA as compared to the MEDEL Vibrant SoundBridge. The music would be delivered through the MP3 player used in all other clinical experiments. While the Vibrant SoundBridge is an implantable device the manufacturer offers a testing kit to Otolaryngologists who implant their devices as a way for the patient to test the sound quality prior to implantation.

The small floating mas transducer that is normally implanted onto the incus, is in packaged in a small polymer housing and has a flat silicone disc at the end to couple directly to the TM of the subject. The device has a standard audio connector and can be plugged directly into the MP3 player. Therefore the DHDA will be coupled to the TM, the song played, and a quality evaluation taken. Next, the Vibrant Soundbridge will be placed, the song played, and a qualitative evaluation taken.

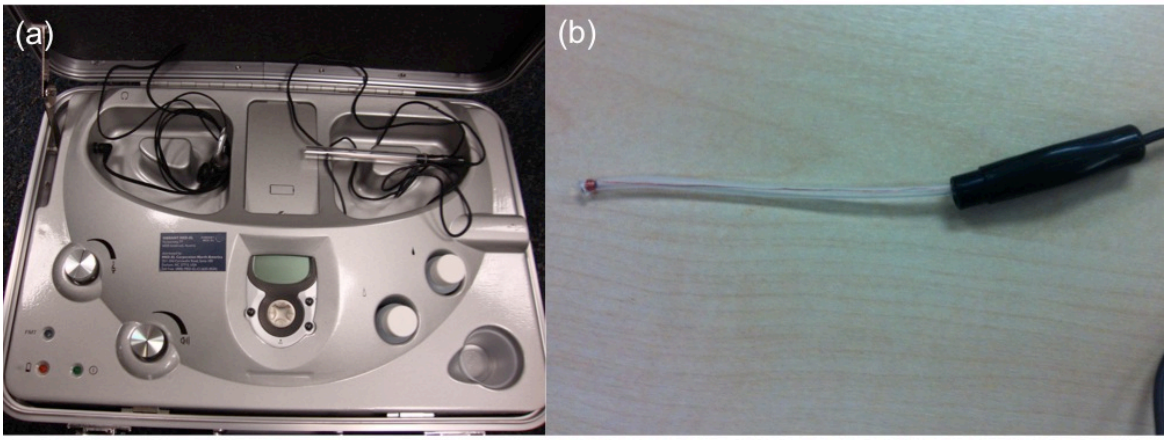

Fig. 83 MEDEL Vibrant Soundbridge Middle Ear Implant (MEI) testing system (a) the testing case with sound controls. The MEI is an implantable device, yet they provide otolaryngologists with a testing system that allows patients to hear the quality of sound the device produces by touching the floating mass transducer (that is normally attached to the incus) to the TM. (b) floating mass transducer middle ear implant within a long plastic protective sheath.

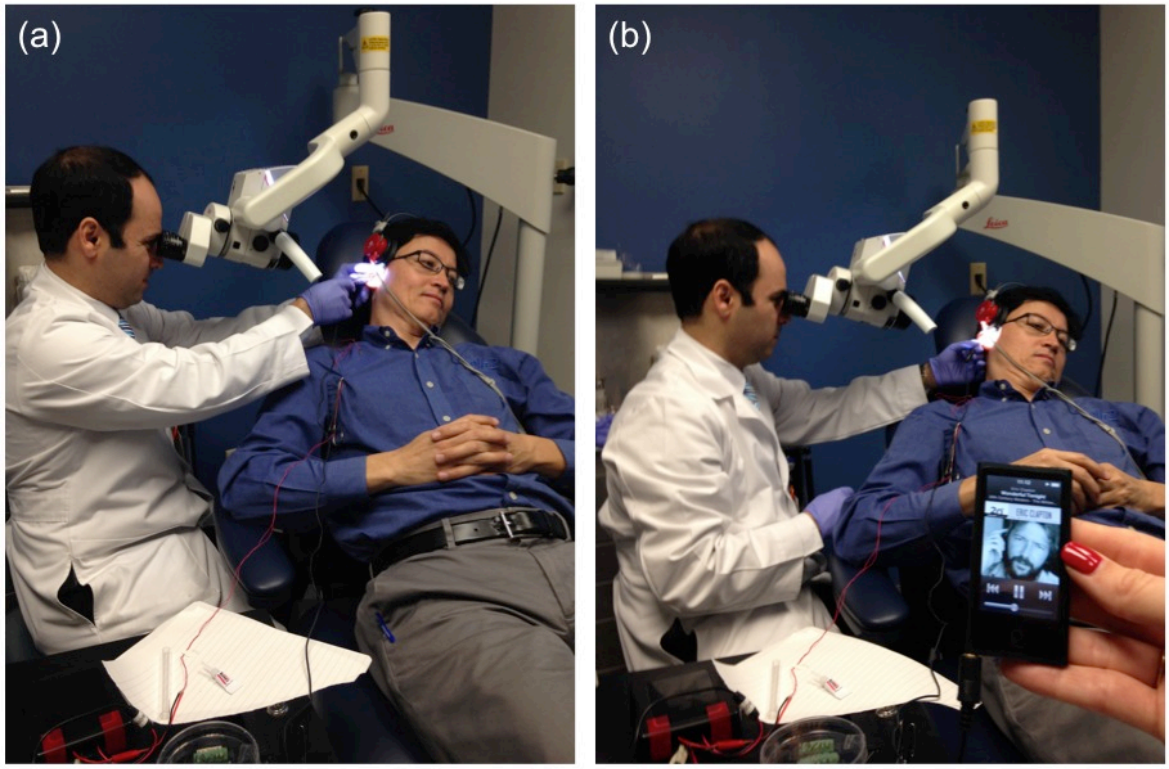

Fig. 84 Short term clinical performance test #2 (a) Dr. Djalilian placing the DHDA within the ear canal (b) music being played through the Vibrant Soundbridge middle ear implant.

7. Short Term Clinical Performance Test # 2 Results

A. DHDA design changes

The new smaller design provided increased visibility and ease of manipulation as reported by Dr, Djalilian. The extension tip proved useful and easier to reach different locations of the TM. The design had the silicone polymer contact tip to be 2 mm in diameter, and after initial trials, it was concluded that even that smaller diameter was too large. Dr. Djalilian reduced the size of the tip to 1 mm in diameter and proceeded with testing. The trial provided insight as to the fact the DHDA requires a very small contact point with the TM in order to transmit sound information. The softer housing made a marked improvement in comfort for the subjects' ear canal. During

this experiment the subject reported not being able to feel the device whatsoever and felt no occlusion and that air was freely flowing through the ear canal.

B. *DHDA sound matching results for clinical performance test #2*

Sound matching testing went smoothly, and the use of pulsed pure tones in both the left and the right ear proved beneficial for the subject and their ability to continually differentiate sound as apposed to becoming accustomed to the continuous pure tone delivery.

Additionally the driving voltages needed to achieve a certain dB SPL level at a certain frequency were quite similar from the first clinical performance test to the second. For example, the 2000 Hz pure tone at 60 dB SPL required ~24 mV in trial #1 and ~36 mV in trial #2. There is a small amount of instruct fluctuation in the system when making voltage measurements on the oscilloscope, and with this taken into account the data from the two trials appears to be consistent.

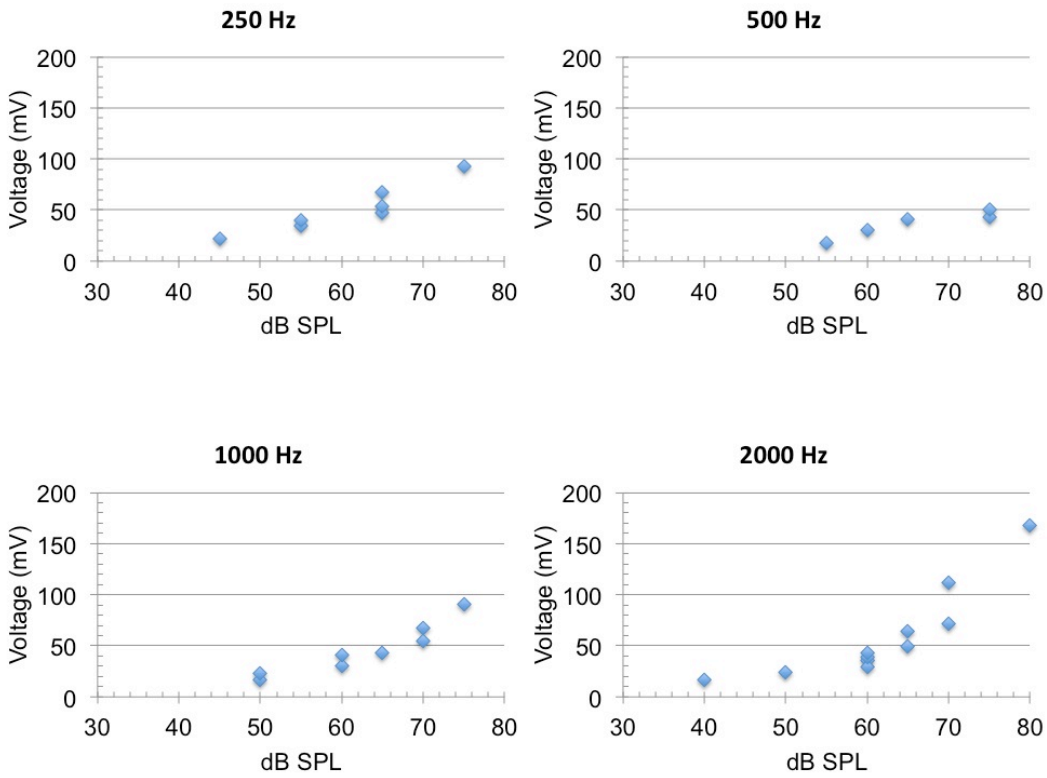

Fig. 85 DHDA Sound matching results for clinical performance test #2. This chart displays the results of the sound matching tests for 250 Hz, 500 Hz, 1000 Hz, and 2000 Hz and the corresponding dB SPL that the subject reported the sound to match. This sound was delivered as pulsed pure tones in contrast to clinical performance test #1 that delivered continuous pure tones.

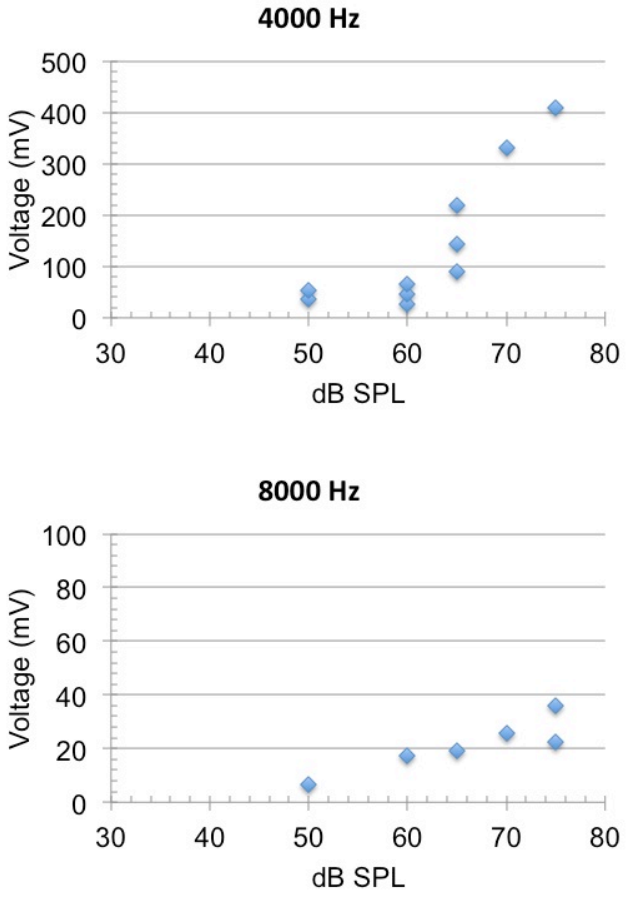

Fig. 86 DHDA Sound matching results for clinical performance test #2. This chart displays the results of the sound matching tests for 4000 Hz and 8000 Hz and the corresponding dB SPL that the subject reported the sound to match. This sound was delivered as pulsed pure tones in contrast to clinical performance test #1 that delivered continuous pure tones.

C. DHDA speech discrimination testing

Speech discrimination tests were delivered through the DHDA and percentage word discrimination recorded. List 2A and 3A were recorded and loaded onto the MP3 player to be delivered through the DHDA. List 2A was delivered at maximum MP3 volume as a validation test to see if speech can be well understood. The subject scored 47/50, receiving a 94% speech discrimination percentage (SDP). The second list, 3A, was delivered through the subject just at hearing threshold. On test 3A the subject received a 44/50 score, resulting in 88% SDP. The

subject reported that any missed words were a result of distraction and not that the words could not be understood.

D. Sound quality comparison between DHDA and MEDEL Vibrant SoundBridge

The subject rated the DHDA with a score of 7/10. It was reported that the subject could hear all background noise in the room in addition to perfectly hearing the song being delivered to the DHDA (papers shuffling, whispering, etc.). The subject reported that all ambient noise was perfectly heard; there was no occlusion, and no sound distortion. Moreover, the subject described the sound as very good, but it wasn't the typical music experience because all ambient noise was still being heard.

The Vibrant SoundBridge received a 6/10 score, with the largest shortcoming being a smaller dynamic range, and thus could not hear certain elements of the song as could be heard with the DHDA. The subject reported increased occlusion with the MEDEL device. This is most likely due to the larger plastic housing and larger diameter contact plate that couples to the TM.

8. Direct Hearing Device Discussion and Conclusions

The DHD represents a new hearing prosthesis approach with the ability to overcome the shortcomings of current hearing prosthesis technologies by addressing the need for an invisible device for moderate to severe hearing loss that does not require invasive surgery. A key technology needed for this is a micro actuator small enough to fit in the bony portion of the ear canal. In bench testing, our DHDA demonstrated a linear frequency response, low THD, and small acoustic noise production. The smoothly varying frequency response is acceptable for a

feed-forward actuator and reduces the computation requirements of the digital signal processor in the prosthesis. When the complex dynamics of human hearing are considered, the smooth response also simplifies the combined dynamic system between the DHDA and human hearing anatomy (e.g., tympanic membrane, ossicles) making the implementation of a clinical device more practical.

The THD was measured to be 0.2% on average, putting it below the 0.5% level that is considered to be adequate for an implantable hearing aid [107].

Research that utilizes human cadaver temporal bones, generally uses specimens obtained within 48 hours after death and frozen, and are thus considered 'fresh'. These fresh temporal bones most closely mimic the mechanical properties of live human middle ears [108], [86,90]. The temporal bone used in this experiment had been refrigerated and preserved in formalin solution for 8 years. Formalin fixation changes the mechanical properties of human tissue, generally resulting in human tissue becoming stiffer [108]. Therefore the magnitude of displacement obtained with the formalin fixed cadaver should be reduced compared to a 'fresh' cadaver due to the increase in stiffness of the TM and ossicular chain.

The temporal bone experiments demonstrated that the DHDA when coupled to the tympanic membrane could recreate the appropriate displacements of the ossicular chain when compared to the acoustic baseline frequency responses.

The frequency response of the stapes displacement when driven by the DHDA did not match the baseline stapes response when driven by sound. Since the DHDA by itself demonstrated a non-flat response, it is likely the coupling of the two systems (DHDA and the ossicles) resulted in this complex frequency response that is different than normal hearing. Contributing factors could include point actuation forces compared to distributive forces, preload

forces on the ossicular chain, and coupling dynamics between the DHDA and tympanic membrane. Further experiments are needed to determine the main factors contributing to the coupled frequency response.

Overall, the bench testing demonstrated the DHDA's ability to produce low distortion movements at the displacements and frequencies typically found during normal hearing. The cadaveric testing demonstrated that DHDA could effectively couple to tympanic membrane and drive the ossicular chain at similar displacements as those found with acoustic stimulation.

The preliminary clinical trial confirmed that the DHDA is able to successfully transmit sound information by mechanically driving the tympanic membrane. This trial also provided insight into the possible locations where a direct drive device can couple to the TM. The device was coupled to a variety of locations on the TM to determine the best location for driving, and the lateral process of the malleus appears to be most promising. Moreover, the subject's positive assessment of the sound quality the DHD produces compared to traditional headphones is encouraging and supportive of the direct drive mechanism. Power consumption for the live human subject was markedly lower than that for the cadaver.

Future work will focus on improving the interface between the DHDA and the tympanic membrane, securing the device in place, and optimizing the actuator design. We have presented a DHDA that enables a semi-implantable hearing prosthesis similar in principle to a middle ear implant but does not require surgery. The DHDA is located deep in the ear canal and couples directly to the bony portion of the tympanic membrane. This device recreates sounds through mechanical movements of the tympanic membrane and attached ossicular chain. It was demonstrated that the DHDA could move the ossicular chain at frequencies and magnitudes appropriate for normal hearing, with little distortion, and with minimal noise generation. The

DHDA has demonstrated in preliminary cadaveric testing to be an appropriate driver capable of achieving the proper range of displacements that occur during natural hearing. A short-term clinical performance test was conducted and concluded that the DHDA can successfully transmit high quality sound through mechanical coupling. This work lays the foundation for continued cadaveric and human testing as well as development of the DHDA as a clinical device.

CHAPTER 5

Chromatic Pupillometry Diagnostic System

1. Pupillometry Introduction

The pupillary light reflex (PLR) is the constriction and dilation of the pupil in response to light that thus modifies the amount of light that reaches the retina[109]. Light that reaches the retina in one eye causes a signal to pass through the optic nerve, onto the thalamus, then to the midbrain, where efferent neurons induce a consensual response and pupillary constriction of both eyes. The PLR is an important diagnostic tool to evaluate the integrity of the visual sensory system, motor output to the pupillary muscles, and central pathways that control the PLR[110–115]. Pupillometry, or the measure of the pupil diameter, has been used as an indicator in a variety of pathologies such as heart failure[116], head injury[110], autonomic neuropathy[117], etc. More recently, it has been suggested that the PLR can be used as an indicator and useful diagnostic tool in the detection of cognitive disorders such as Parkinson's and Alzheimer's disease[118,119].

There are three groups of photoreceptors that control the human PLR: rods, cones, and the newly discovered intrinsically photosensitive retinal ganglion cells (ipRGCs)[120–122]. This group of ipRGCs communicates directly with the brain and are found to be involved in both image forming and non-imaging forming processes. They contribute to the pupillary light reflex, sleep, regulation of the circadian rhythm, and other behavioral and physiological responses to environmental illumination[123–127]. This subset of retinal ganglion cells produce the photopigment melanopsin[123] and show a delayed latency and prolonged response after light stimulus offset[128].

This finding has lead researchers to support the belief that ipRGCs play a significant role in the sustained PLR.

2. Chromatic Pupillometry

Chromatic pupillometry has emerged as a more specialized type of testing, compared to basic white light exposure, and allows for contributions of photoreceptor groups of the PLR to be examined[129–131]. Through the work of Dacey et al.[121,128], Kardon et al.[112,129], and Park et al.[131] the relative contributions and health of rod, cone, and melanopsin producing ipRGCs of the human PLR can be determined with a brief clinical protocol. If we make the assumption that the function of the ipRGCs is a good indicator to the integrity of the rest of the RGC population[131], then this assay may provide insight into previously observed differentiation in PLR response in disease state compared to healthy. It has been shown the ipRGCs contribute to behavioral functions such as circadian photoentrainment, PLR, migraine, sleep/alertness, and mood[123]. These cells are known to have a complex role in regulation of many systems, therefore if we can obtain better insight into their integrity and function, then potentially the health of the ipRGC can be directly compared to certain disease states.

3. Chromatic Pupillometry Goggles

The work presented here is a pilot study using the findings from Park et al.[131] to investigate the response of the ipRGCs of the PLR in 35 healthy subjects. To carry out the testing our group developed a novel chromatic pupillometry goggle device that consists of both stimulating and recording hardware in a single portable device. Moreover, this work sought to

establish a protocol for breakdown and analysis of components of the PLR when dominated by each of the different photoreceptor groups.

4. Methods

The study utilized our custom pupillometry system to measure the pupil light reflect in response to specific stimuli to evaluate the three major cell populations that control the PLR as discovered by Park et al.[131]

A. Apparatus

The chromatic pupillometer used in the experiment is a custom device consisting of both stimulating and recording hardware in one apparatus. Both components are integrated into a pair of goggles that a user can easily put on and remove without assistance. The chromatic pupillometry goggles (CPG) contain the light stimulating sphere on the left eye and eye recording system on the right eye, thus recording the consensual pupil response.

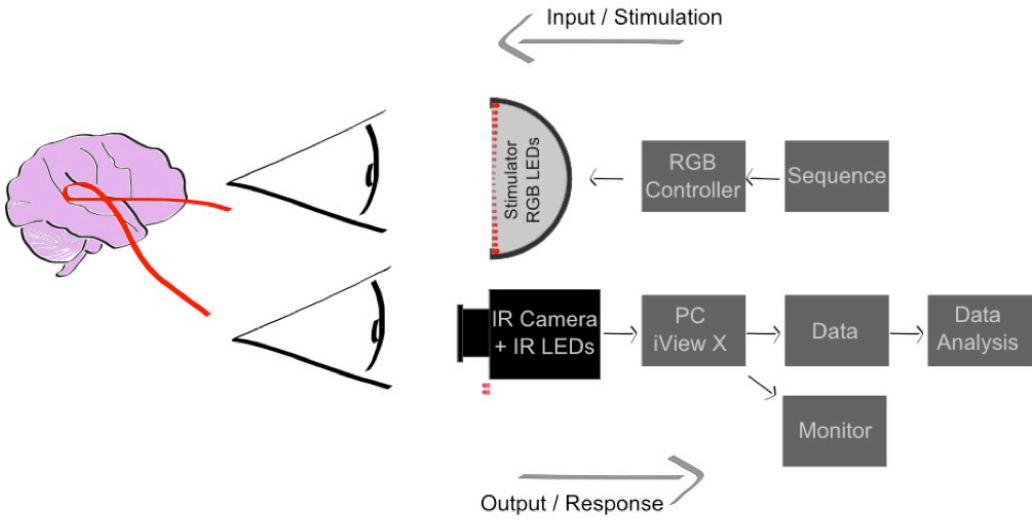

Fig. 87 Chromatic pupillometry testing setup for stimulating and recording of the consensual pupil response.

B. Light Stimulation

The left side of the CPG contains the light stimulation hardware. This is composed of a hollow plastic sphere coated with titanium dioxide for increased reflectance. Six RGB (Red, Green, Blue) LEDs (12V 5050 RGB-SMD-LED, LED Shop; Leipzig Germany) are mounted on a polystyrene ring at a 45° angle and sealed within the hemisphere with corresponding wavelengths; red 630nm, green 530nm, blue 470nm. This configuration creates uniform light dispersion within the hemisphere. The light-stimulating sphere is controlled by a 8-bit RGB microcontroller (MS-35 CONRAD GmbH; Munich, Germany). The stimulator is calibrated by a spectroradiometer (JETITechnische Instrumente GmbH; Jena, Germany) to verify the desired light characteristics of the device (luminance, radiance, dominant wavelength, color purity).

C. Pupil recording

The right side of the CPG contains the eye-tracking unit for pupil recording measurements. The unit consists of a camera (CMOS C-Cam-2A CONRAD GmbH; Munich, Germany) and four infrared LEDs (GaAIAs Infrared Emitter IRL81A Siemens GmbH; Munich, Germany). All components are mounted on a vertical and horizontal sliding stage to allow adjustment of viewing field for different facial geometries.

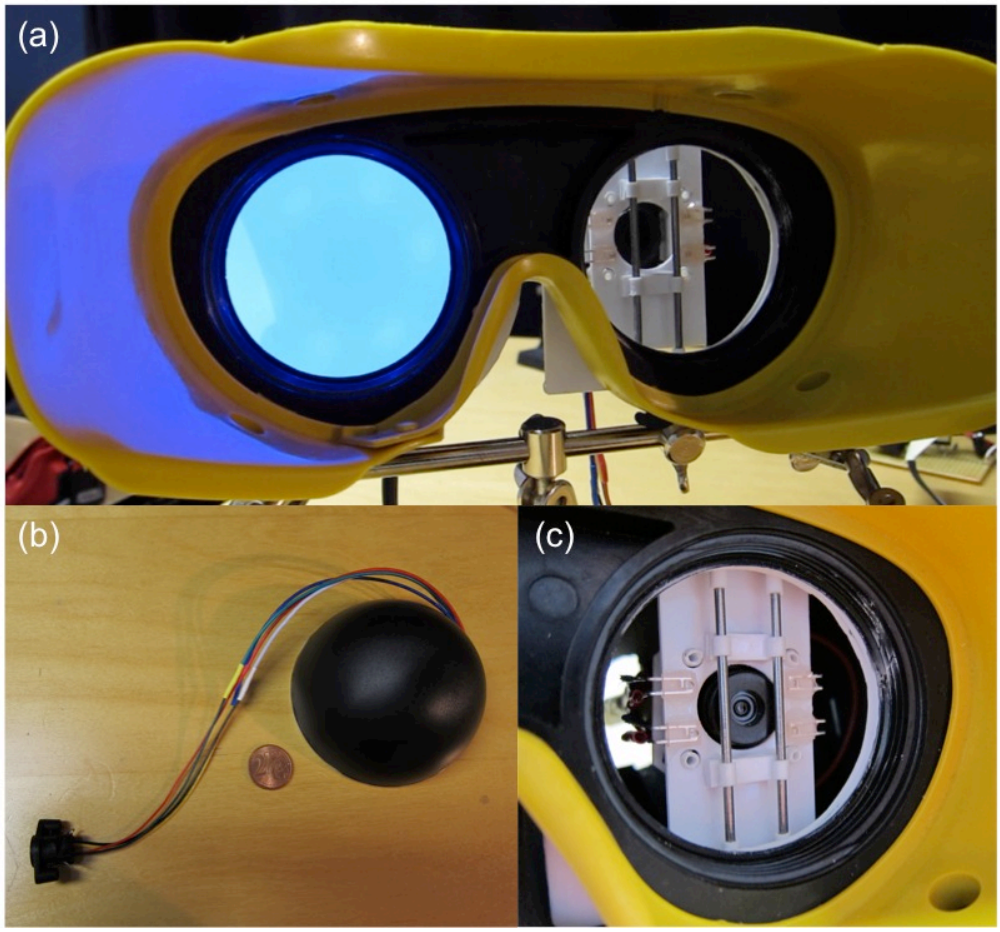

Fig. 88 Chromatic pupillometry goggles a) view of entire goggle system with the light stimulating sphere on the left eye and the eye tracking system on the right eye b) light stimulating sphere when removed from the goggle base c) close up view of the eye tracking system composed of a camera and IR LEDs mounted on a horizontal and vertical slide to accommodate for different facial geometry of subjects.

D. Subjects

32 healthy subjects ages 21-70 years with no known visual abnormalities participated in the experiment. Subjects who displayed excessive eye blinking or off-center gaze during the study were not included, due to inability to accurately measure the pupil. Informed consent was acquired from every subject prior to participation in the study. This research study adhered to the tenets of the Declaration of Helsinki and was approved by the internal review board at the Hochschüle München Faculty of Applied Sciences and Mechatronics and the Ludwig Maximilians Universität Generation Research Program.

E. Stimulation protocol

Based on the discoveries by Park et al[131], there are optimal lighting conditions (specific wavelength and intensity) to selectively activate each of the receptor systems. Lorenz et al[132] modified the established protocol of Park to reduce discomfort and excessive blinking from healthy patients, and modification we also used in our study. Light stimulation for the study was controlled by the LED driven CPG. Subjects were subjected to 3-5 minutes of low light dark adaptation while being informed and consented about the study. Subjects then put on the CPG and the lighting protocol began. The stimulation protocol (Fig. 89) consists of 30-second dark adaptation while a baseline pupil diameter measurement is taken. Next, a red stimulus (620nm ± 10nm) with a luminance of 120 cd/m^2 for 1-second duration is repeated three times with a 10-second dark period in between. This is followed by a blue stimulus (473nm ± 10nm) with a luminance of 120 cd/m^2. The pupil diameter is then recorded for 30 seconds after the last stimuli.

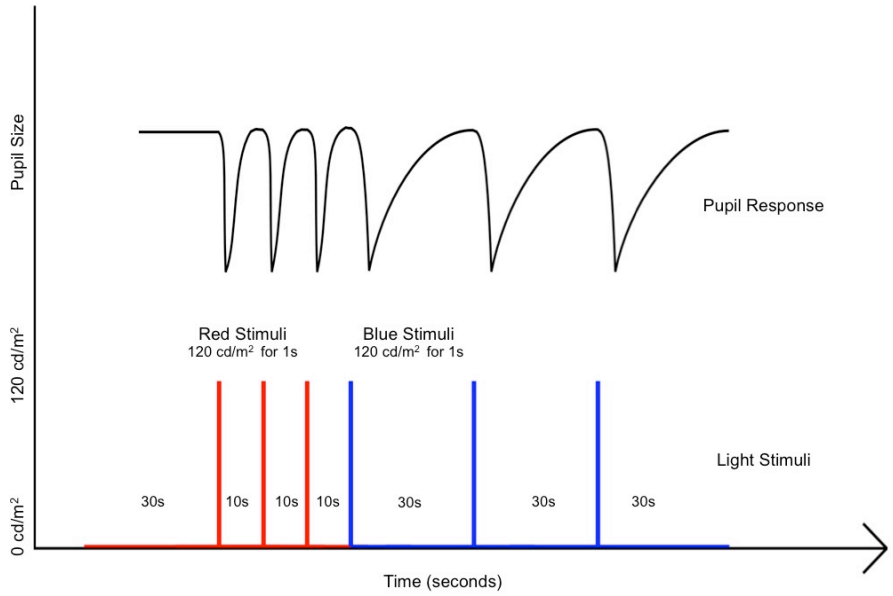

Fig. 89 Light stimulation protocol and corresponding pupil response. This stimulation sequence begins with a 30 second baseline measurement in complete darkness. Next, three 1s red flashes with 10s between are applied to asses the function of the cones. After the cone assessment three 1s blue flashes (photopically matched) with 30s between are supplied to the subject to evaluate the ipRGC function. Lastly, a 30s baseline measurement is taken after all light pulses have been delivered.

F. Data Analysis – SMI Eye Tracking System

The eye tracking system that would be used to process the video coming in from the CPG at the onset of the experiment was iView X (SMI SensoMotoric Instruments; Teltow, Germany). After 10 subjects completed testing, it was apparent that this system continually was less that effective at border detection of the pupil and thus was not properly obtaining pupil diameter information throughout the experiment. Attempting to filter through the artifacts when the pupil size was lost through the image capture system proved less accurate. To assure correctness of the results we simultaneously recorded video files of all subjects and designed a custom eye tracking software to analyze the pupil response post testing.

G. Custom Pupil Tracking Software

The pupil response video signal is recorded by a USB video capture device at 25 frames per second creating a 352x288 pixels image. The video files were subsequently processed by specifically designed LabVIEW (National Instruments, Austin Texas) software. The routine includes sequenced steps to obtain raw pupil size data. The original grey value image is converted to a binary image for pupil background separation. Oval shape detection determines the location and diameter of the pupil, by which a region of interest (ROI) is defined (Figure 90a). The ROI is annulus formed and fitted around the pupil diameter. At a step size of 10° radial lines (blue) determine edge strength profiles (Figure 90b) between the inner and outer circle of the ROI. Thereby the pupil-iris transition edges (yellow dots) are accurately detected by the maximum edge strength (Figure 90c) and pupil non-circularities are resolved due to the 36 edge detection points. The resulting pupil diameter is represented by a fitted circle (red) (Figure 90d).

Furthermore, median filtering is applied on the pupil diameter-time signal, to reduce impact and occurrences of artifacts by eye-blinks.

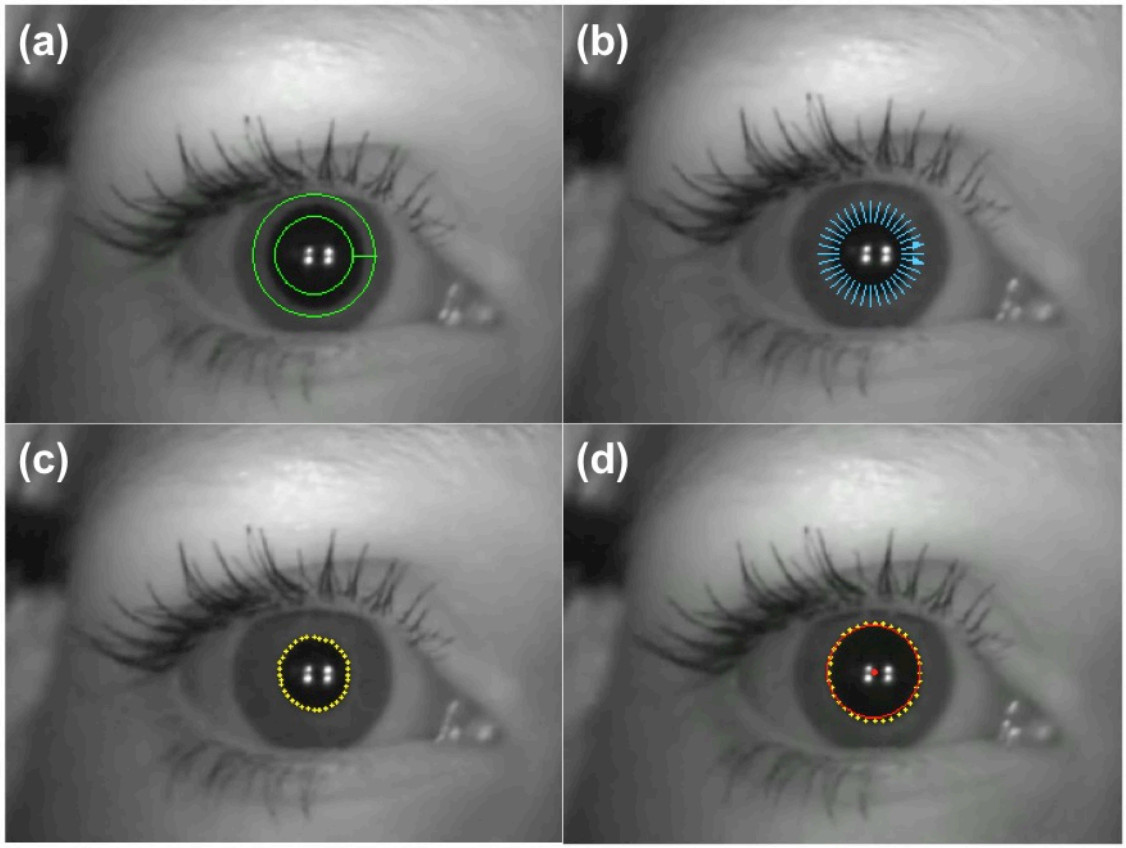

Fig. 90 Custom pupil detection software a) region of interest definition with inner and outer pupil boundaries c) radial cuts for individual edge detection measurements c) found pupil edges and d) resulting circle interpolation.

5. Clinical Test Results

With the emergence of the PLR as a diagnostic tool many groups are presenting different characteristics of the PLR to be most helpful in diagnosis. Some groups focus on percent pupil contraction[129,132], maximum contraction acceleration[119], or contraction velocity[110], etc. Our group sought to combine parameters of the PLR as reported from colleagues into a single analysis protocol. In addition to previously explored PLR characteristics our group suggests two new parameters that we believe are most insightful when looking at the post illumination pupil

response to red and blue light, the T_{75} and dilation response curve separation (DRCS). We believe with the new discoveries of Park[131] in a protocol that isolates the function of the three photoreceptive elements (rods, cones, melanopsin) our analysis of the PLR can be more targeted and effective in evaluation the origin of a potential disorder or disease.

The protocol presented here evaluates the integrity of the cones and the ipRGCs of the PLR.

1. Baseline pupil diameter (mm): obtained from a 30 second baseline measurement
2. Average contraction velocity (ACV) (mm/s): measured from onset of contraction to first occurrence of the minimum diameter
3. Minimum contraction diameter (mm): minimum contraction observed from a 1 second light stimulus
4. Delta Δ (mm): baseline minus minimum diameter
5. Average dilation velocity (ADV) (mm/s): measured from minimum contraction for 1-second duration
6. T_{75} (seconds): time from minimum contraction until 75% pupil recovery relative to the baseline diameter
7. Dilation response curve separation (DRCS): area between curves measurement of the PLR dilation when driven by cones as compared to the PLR when driven by ipRGCs

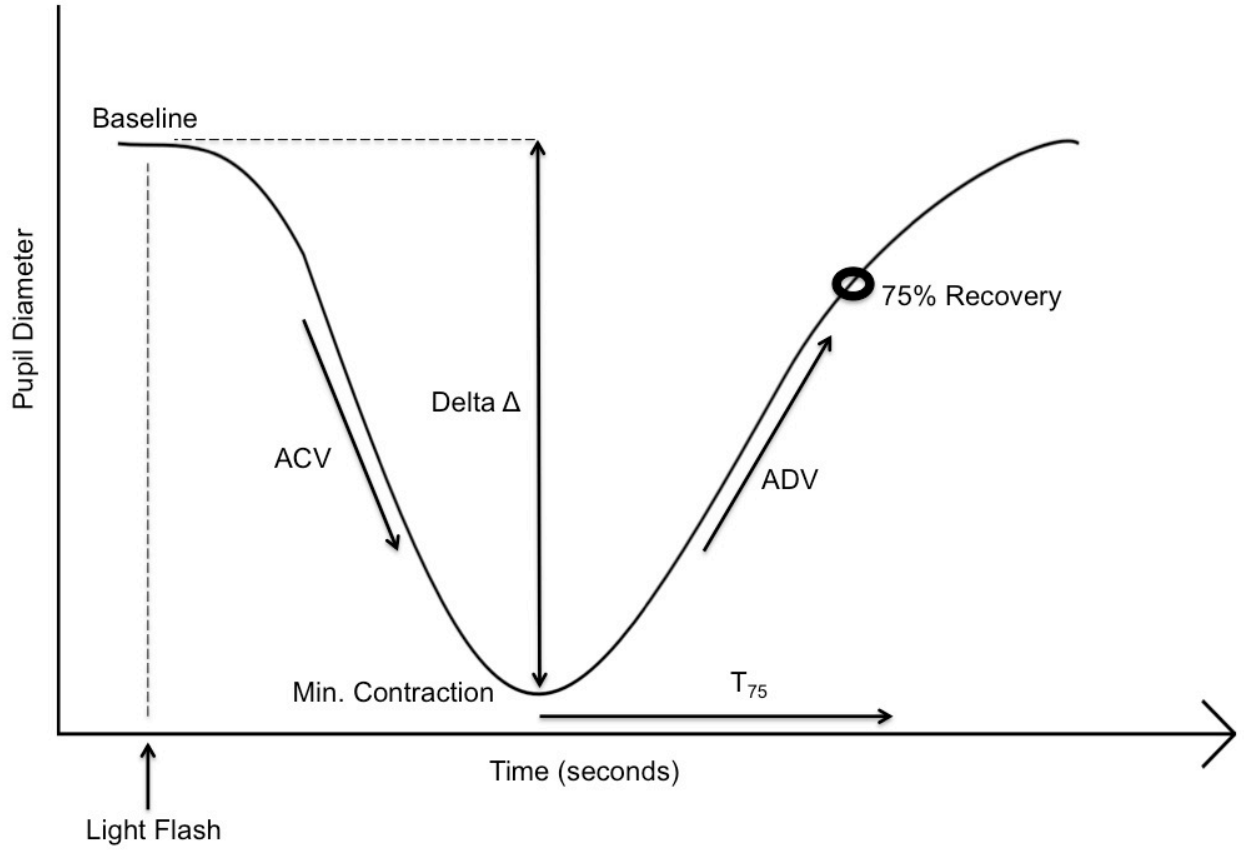

Fig. 91 Pupillogram adapted from Pawari et al [133] that exhibits the pupil response for a single light stimuli and corresponding measurements taken. Measurements include: baseline pupil diameter, ACV (average contraction velocity), minimum contraction diameter, delta (baseline diameter minus min. contraction diameter), average dilation velocity (ADV), and T_{75} (time required for pupil to return to 75% baseline).

Subject	Age	Baseline (mm)	ACV Red (mm/s)	ACV Blue (mm/s)	ADV Red (mm/s)	ADV Blue (mm/s)	Min. Blue (mm)	Δ Blue (mm)	Min. Red (mm)	Δ Red (mm)	T_{75} Red (s)	T_{75} Blue (s)
14	23	6.18	2.38	2.57	1.51	1.74	3.40	2.77	4.02	2.16	3.70	5.97
15	24	4.85	1.94	1.92	1.18	0.82	2.58	2.27	2.97	1.88	2.33	6.00
18	25	7.11	2.13	2.74	1.28	0.97	3.74	3.37	4.49	2.63	3.24	8.96
20	24	6.93	2.36	1.50	1.10	0.94	4.04	2.89	4.86	2.07	2.64	8.76
27	25	7.50	2.15	2.69	1.24	1.09	4.05	3.45	5.08	2.43	3.04	6.44
28	39	6.59	2.44	2.42	1.25	1.11	2.97	3.62	3.66	2.93	4.32	12.36
30	34	7.33	1.64	1.96	0.98	0.88	3.72	3.61	4.70	2.63	4.32	9.00
31	26	6.97	2.36	2.85	1.15	0.68	3.49	3.48	4.28	2.69	4.28	9.00
32	33	6.90	1.96	2.48	1.10	0.88	3.59	3.32	4.40	2.50	4.32	9.20
33	32	6.47	2.63	2.30	1.53	1.56	3.88	2.59	4.31	2.16	2.12	2.96
Avg. ± St.Dev		6.68 ±0.75	2.20 ±0.29	2.34 ±0.43	1.23 ±0.17	1.07 ±0.33	3.55 ±0.47	3.14 ±0.47	4.28 ±0.61	2.41 ±0.33	3.43 ±0.88	7.86 ±2.58

Fig. 92 Resulting pupillometry measurements for healthy subjects. This table displays subjects' age (years), baseline pupil diameter, average contraction velocity (ACV), average dilation velocity (ADV), minimum pupil diameter, delta (baseline - minimum), and T_{75} (seconds) for both the red and blue light stimuli. The presented values are calculated by taking the average of the three trials of red and blue light.

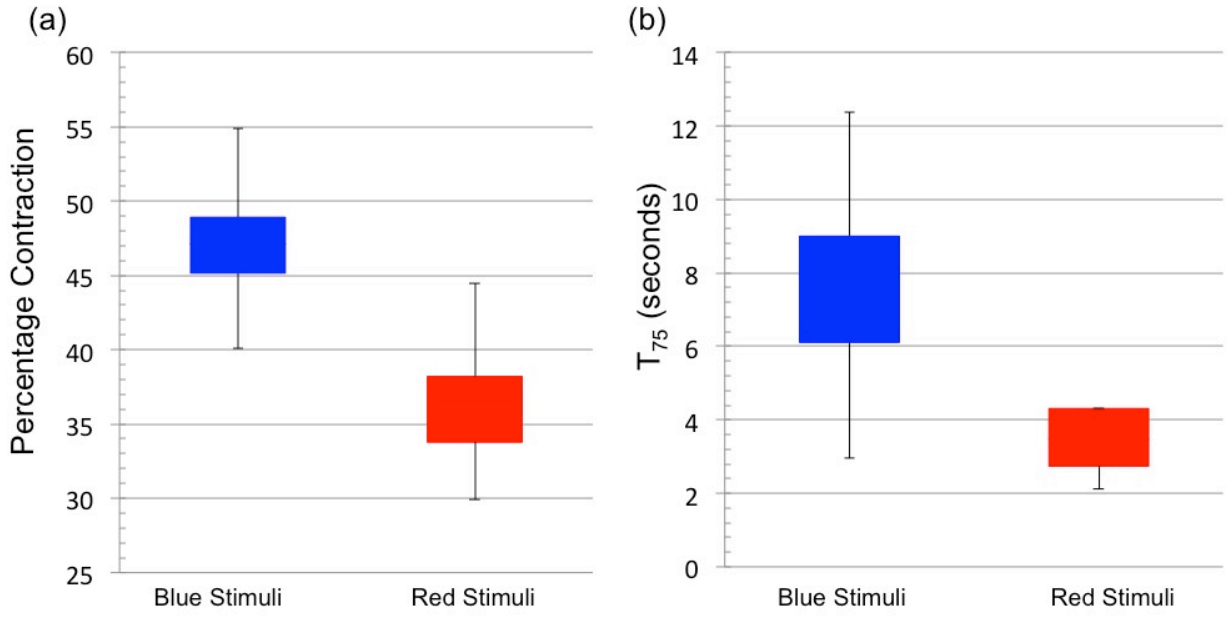

Fig. 93 Box plot representing a) maximum pupil contraction in response to blue and red stimuli b) T_{75} (time required for pupil to return to 75% baseline diameter) for blue and red stimuli. Both measurements confirm the intrinsic slow response of the ipRGCs as well as provide measures to quantify it.

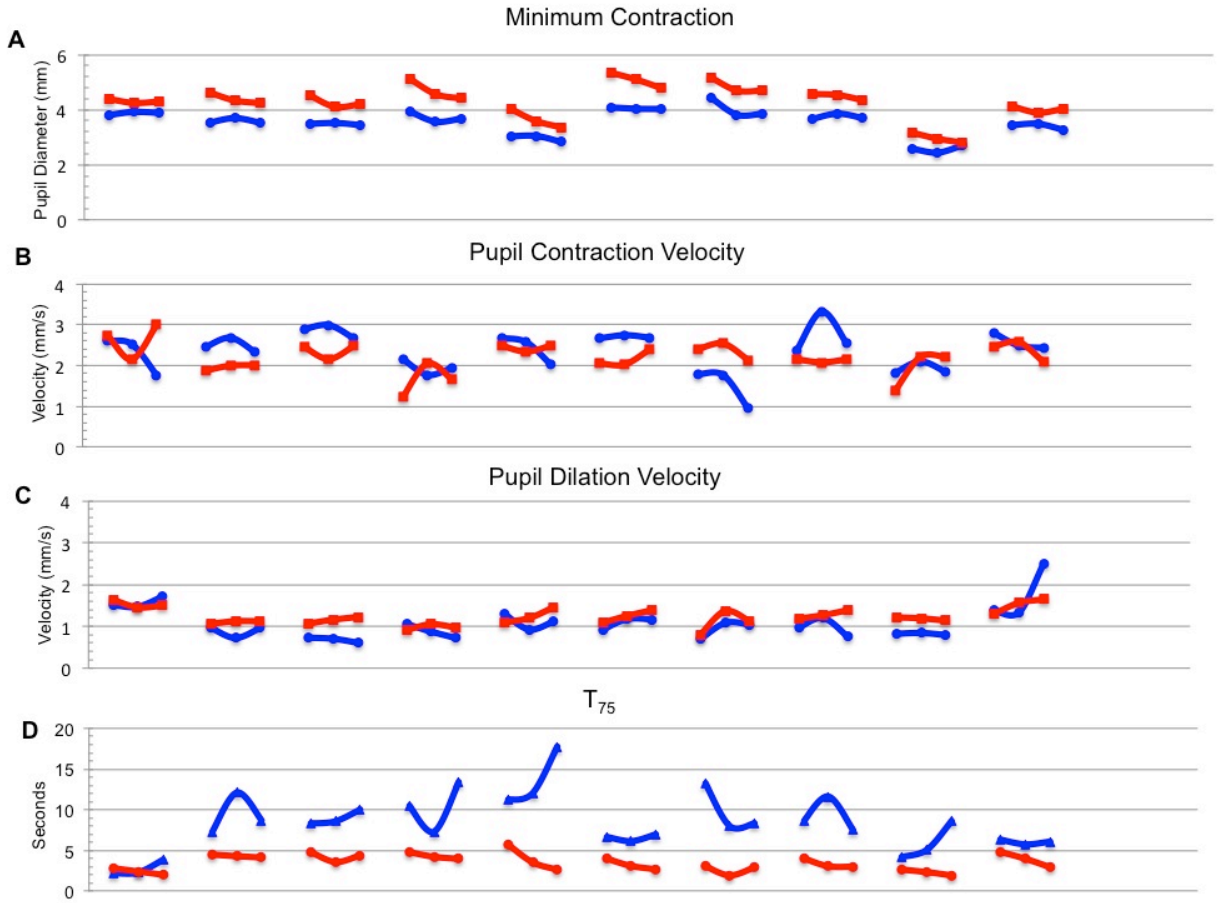

Fig. 94 Trend graphs for each individual subject. Each line with three data points represents a subject and the data for each of the three trials of both red and blue light stimuli a) minimum pupil diameter in response to red and blue stimuli. It is evident that the blue light stimulus causes a larger contraction as compared to the red stimuli b) ACV measurements indicate that the contraction of the pupil in response to different lighting stimuli seem closely matched c) ADV trends towards the blue dilating slower than the red stimulus d) The time to reach 75% of the starting diameter, T_{75}, is a measure of the late dilation pupil response and is an indicator of the sympathetic nervous system drive[133]. This figure represents the values of the T_{75} for all trials of the red and blue stimuli.

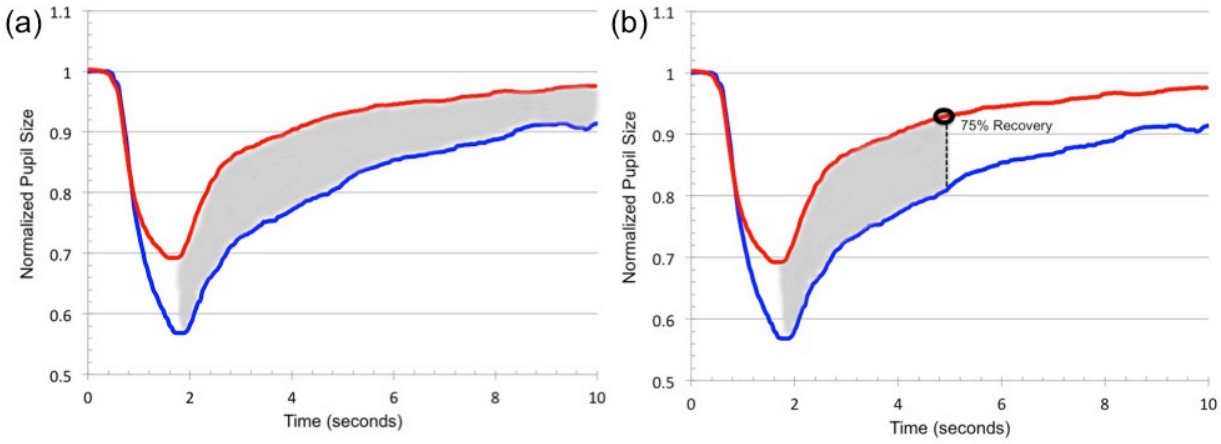

(c)

1. $F = \int_0^T (y - \bar{y})\, dt$

2. $F = \int_0^{T_{75}} (y - \bar{y})\, dt$

3. $F = \sum_0^N (y_i - \bar{y}_i) \cdot (\Delta T)$

Fig. 95 Dilation response curve separation a) the dilation response of the PLR when dominated by cones (red stimulus) versus melanopsin (blue stimulus) has markedly different morphology. The melanopsin derived PLR is characterized by a slow sustained miosis[121,128,131,134–136]. Intrasubject comparison of these two normalized responses provides an additional measure of the viability of the ipRGCs. The two averaged responses were overlaid and the area between curves measured (gray area). Measurements were taken from the occurrence of the minimum in the PLR to 10 seconds after light stimuli b) Additional measure calculated the DRCS from the minimum to the T_{75} of the cone response, providing an intrinsic boundary of this measurement based on the subjects own PLR c) Set of equations used for calculating the dilation response curve separation. 1) *y* is defined as the cone driven response $\bar{y}$ is defined as the melanopsin driven response. 2) The dilation response curve separation was evaluated from the occurrence of the minimum to the T_{75} of the cone response.

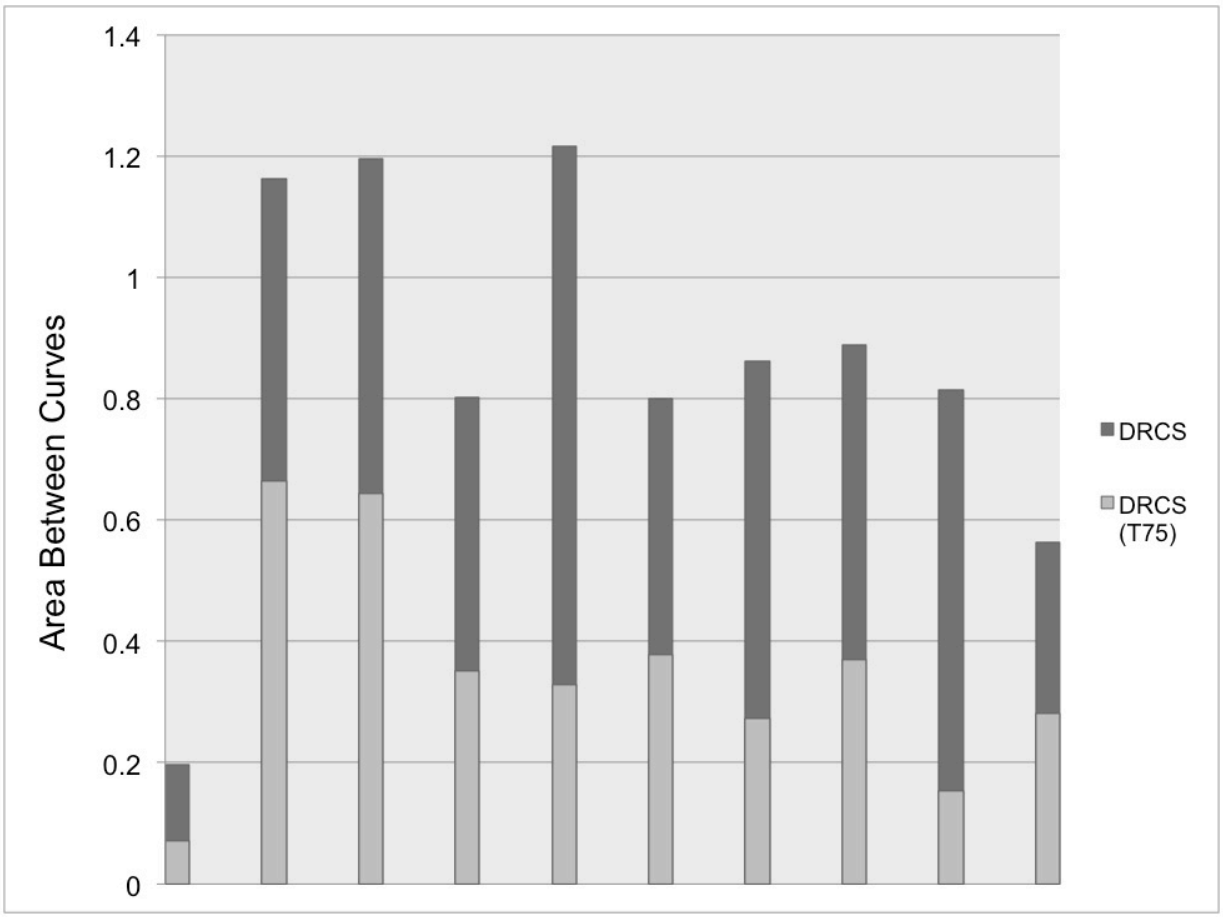

Fig. 96 Dilation response curve separation for 10 healthy subjects. DRCS is the measurement of the area between curves of the normalized pupil response when stimulated with red light (cone activation) and blue light (ipRGC activation). DRCS (dark gray) and DRCS T_{75} are displayed in the figure.

6. Conclusion and Discussion

The goal of this study was to explore the feasibility of a simple, inexpensive, portable system for probing the response of ipRGCs using pupillary light reflex, with a simple protocol and a well-defined analysis. This work was guided by the findings of Park et al[131] which shed light on the conditions for evaluating the contribution of each of the respective photoreceptive elements. Our protocol and analysis specifically targets the ipRGCs, using only red and blue light in the evaluation. The physical device incorporates both a pupillometry camera and a light dome into a head worn system, eliminating the need for a specialized or dedicated room, thus allowing tests to be performed at points of interest such as at a school, senior center, small clinic,

or in domestic residences. Our device used only consumer-grade electronics, suggesting that the units can be manufactured with good quality at affordable cost.

Our data from the unit follows that of other published works, with characteristic pupil response curves for both red and blue light, with the blue light dilation velocity being consistently slower than for red. Errors in pupil diameter from the camera system were small, and the system could track pupil response at 30 measures per second. Two pupil recognition algorithms (commercial software and custom software) were explored and both agreed within 10%; in addition, both agreed with analysis by researchers who performed some image analysis by hand. Despite its low cost, the system can be used with commercial pupil imaging software or custom algorithms.

The protocol utilized three separate measurements of pupil response to impulses of red light and blue light. The short duration of one second provided enough stimulus to trigger a strong pupil response, while minimizing discomfort to the subject. The use of three measures in succession provided enough data to improve the statistical quality of the data, while limiting eye fatigue. The entire procedure took less than two and one half minutes to perform.

Analysis of the pupil response curves is somewhat complex, owing to the goal of isolating the ipRGC response as well as expected differences in pupil size, and differences in overall pupil response among populations. Following the findings of Park, we believe the relevant information for ipRGCs is to be found in comparisons of the dilation velocities of red and blue stimuli.

Our analysis first calibrates all data against nominal pupil size (after adjustment to dark conditions) to take normal pupil size into account. Following this, our focus is on comparing red and blue dilation responses. Unfortunately, conventional dilation indicators such as ADV[133] and

time to recovery[137] are relatively poor at shedding light on the differences between responses, since the dilation response curves are very structured and since baseline shifts in pupil size may appear over time. We attempted to identify a simple moment that describes the differences in the curves with minimal assumptions about the underlying mechanism. To this end, we have proposed the use of a time integrated difference between the red dilation response and the blue dilation response. This has the benefit of including all parts of the curve and does not assume linear dilation (or "velocity"). We calculated two version of this, one with an integration to baseline, and one with the integration to an agreed upon endpoint, namely 75% of maximum for the red curve. We believe this to be the most neutral comparison we could make between the two curves. A true understanding of the underlying mechanism and a model for the pupil response could suggest more specific analysis, including model dependent approaches. However, in the absence of a good underlying model, we suggest that the time integrated dilation differences is an appropriate measure.

Future studies should be conducted to explore the suitability of this measure to correlate ipRGC activity with other physiological conditions, such as age, activity level, emotional state, sleep quality, and disease states. The protocol would benefit by increasing the time between light stimuli to give the pupils more time to recover.

We believe the system, protocol, and analysis presented here demonstrates the feasibility of bringing ipRGC assessment into widespread adoption through a low cost, portable system. Moreover, our proposed the analysis provides a method for neutral analysis of pupil response when comparing red and blue stimulation, as is required for ipRGC assessment.

CHAPTER 6

Balance and Gait Monitoring Insole

Introduction to Gait and Balance Monitoring

The complex human balance system is primarily based on three components: the vestibular system located in the inner ear, visual feedback, and proprioception. Any impairment in these three categories can significantly affect an individual's sense of balance. The importance of balance and gait monitoring is applicable to a variety of fields such as: evaluation of neurological disorders, early disease detection in children[138], new medication monitoring, post surgery monitoring, elderly fall risk, and post sports injury analysis, all of which can cause impairments to balance and postural control.

Specifically, elderly fall risk is of major concern to society due to its high occurrence, detrimental effects on the quality of life of elders, and financial cost. Falls cause not only physical but also psychological trauma, reduced activity, loss of independence, and even death[139]. Additionally, the direct medical costs for elderly fall risk totaled $19 billion USD in 2000 for non-fatal fall injures[139]. Thus, elderly fall risk is not only a social problem but a financial problem as well.

When a patient has a prospective balance impairment physicians recommend a balance assessment using a posturography machine. Traditional posturography machines, which quantify a patient's postural control, are extremely costly and require operation by a technician and physical therapist for balance evaluation. Although this technology provides complex and useful information for balance evaluation, it requires a visit to the physician, multiple technicians for operations and is extremely costly.

With the technology boom sensors and micro processing chips are becoming smaller and cheaper and thus can be integrated into "smart clothes" and smaller more feasible technology for daily use. Therefore since the technology is becoming more cost effective the possibility of integrating these sensors into technologies for home use is becoming more feasible. Using the technology used in the posturography and integrating it into an in-home system would be extremely useful for those patients who have difficulty leaving the home on a regular basis.

Researchers at the University of Pittsburgh found that abnormal gait in high functioning older adults can be an indicator for subtle brain abnormalities. Different spatial and temporal parameters of gait such as speed, stride length and double support time can be associated with subclinical infarcts or brain atrophy[140]. This group found that high functioning older adults that have poorer gait speed, shorter stride, and longer double support time are associated with high white matter disease and subclinical strokes[140]. A group in Boston, found that velocity, cadence (number of steps per minute), step length, stride length appear to be effective tools for evaluation of physical therapy outcomes[138]. Specifically, for the evaluation of patients suffering from Multiple Sclerosis and hemiparesis[138]. Researchers at the Albert Einstein College of Medicine found that neurological gait abnormities in elderly subjects are a significant predictor of the risk of development of dementia[141].

With additional research those with balance impairments can use these technologies to ameliorate some of the disadvantages that come with a balance and gait disorders and improve daily life. Through the use of inertial sensors and pressure sensors, information about postural control and balance ability can be attained.

Existing Technology

The concept of monitoring gait and balance through an insole type device has been around since the 1970's with many research groups looking at different aspects of gait to determine disease state. Many gait and balance systems are commercially available today, this includes insole type devices as well as pressure mats. Some examples of commercially available insole systems are: The Novel "Pedoport" System, TECHNO Concepts "Dynafoot", The iShoe, Moticon "Sensor Insole", and Medilogic's "Medilogic Insole". Some examples of commercially available pressure mats include: The GaitRite System, Teckscn Walkway, Footmaxx Metascan Pressure Mat, and RSscan Footscan Gait System.

Applications

While many of these existing technologies for monitoring balance and gait have worked effectively, they are primarily deployed in high-tech gait laboratories and rehabilitation clinics. These devices have complex, costly, and proprietary data analysis packages that limit certain applications of gait analysis. More specifically, these devices are less tailored for home use and everyday living. This research project was motivated to develop a platform technology that could be used in many environments from the grocery store, to the home, and to regular checkups at the clinic. This would provide not only the individual but care providers insight into the patients well being outside of the clinic that can better guide treatment and future therapy.

StabilitySole

The StabilitySole has been through a series of design iterations starting with the use of an actual shoe insole to house the electronics to the now current method of a thin laminate sensing layer[142]. The data acquisition has developed from a real time wireless system to a data logging

system. The motivation for migrating to a logging system was the power efficiency and size of the electronics, as well as the lack of need to see the data real time. The laminate insole consists of four piezoresistive pressure sensors, one three-axis accelerometer, and a data-logging unit that is embedded in an ankle strap.

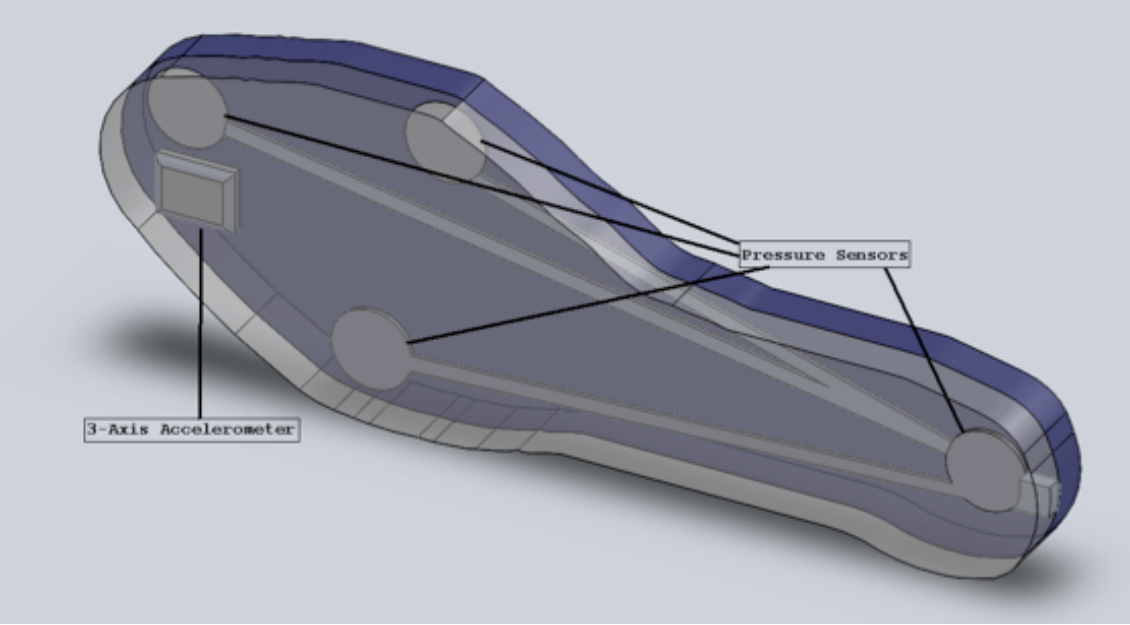

Fig. 97 StabilitySole concept design. This design contains four pressure sensors and one three-axis accelerometer for monitoring gait and balance.

Fig. 98 StabilitySole Insole placed in a shoe. This first prototype used a wireless data transfer system. Later models utilized a data logging system that was more power efficient and size appropriate.

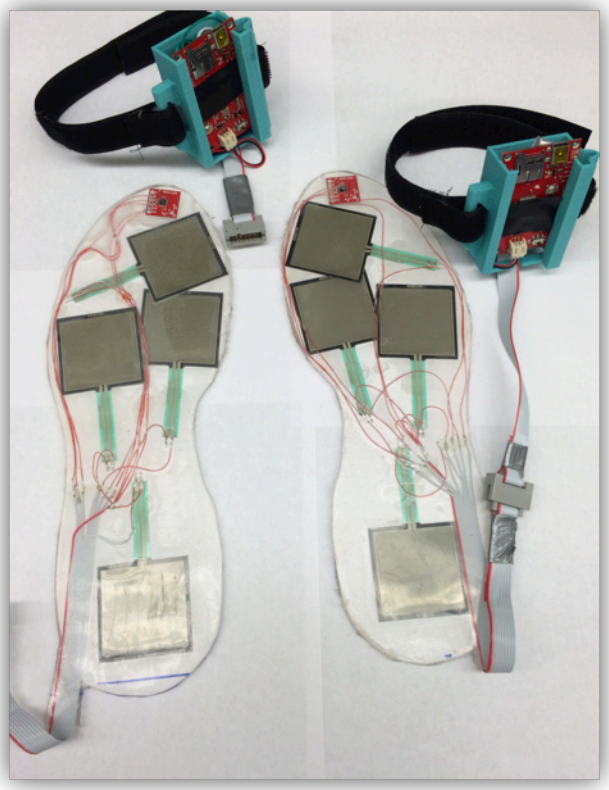

Fig. 99 StabilityStole film prototype deployed in the hip and knee replacement study. This design uses a thin laminate sensing layer and a data-logging unit.

The StabilitySole has been used in a variety of testing situations from balance training to dance injury analysis, and is currently undergoing a study in the UCI Department of Orthopedic Surgery. As discussed in the introduction of this dissertation osteoarthritis is a large health care issues facing older adults, with pain of the joints being incredibly debilitating. A common treatment for failing joints is joint replacement. An orthopedic surgeon at the UCI Medical Center, Dr. Ran Schwartzkopf, performs many of these replacements each year but is interested in a technology that can provide him a quantitative indicator as to how the surgery has affected the patient. Therefore our device is being used to look at a subjects gait before surgery and after. The device will be used in the clinic as well as the home setting to get long term feedback as to

how the patient is recovering after this surgery to better adjust future treatment and rehabilitation.

Conclusions

The StabilitySole represents the direction of at home monitoring systems that can allow patients to take a more participatory role in their health care, and specifically mobility. Individuals can self evaluate their progress day to day and use these guidelines to make informed decisions about their abilities. This tool has a large spectrum of applications from gait and balance to rehabilitation to weight management that would give patients a quantitative insight into their daily activity and how that relates to their well-being.

CHAPTER 7

Summary and Conclusions

The aging population is growing and producing unprecedented demands on the health care system, with health care costs in 2012 totaling over $12 trillion[143]. The current healthcare paradigm is focused on a provider model of healthcare. The changing demographics will not allow our system to support this model. A new health model where patients and other stakeholders (e.g. family, community) actively participate in healthcare may be sustainable.

The old paradigm was[144]:

1. Reactive: where interventions are made after health has deteriorated
2. Generic: individuals are treated the same regardless of personal needs
3. One sided: where "doctors know best" and patients are relatively uneducated
4. Uneven: Quality of health care varies by region and economic status

The new paradigm is[144]:

1. Preventative: the focus on interventions that prevent disease
2. Personalized: interventions are tailored to individuals
3. Participatory: where patients, providers, and caregivers all play a role
4. Parity: allows for level access to health interventions and information

However, these people need to be empowered, and technology may be able to play a large role here. The way that technology can play a role is still unclear and research will be needed to explore this. The older adult population, which is so important as both a burden and as an emerging market for healthcare, has unique needs, requirements, limitations, and preferences

that must be considered. This impacts not only what kinds of devices are developed and how they are designed, but also how disease is going to be managed. Technology in this field will have many common requirements: portability, small size, integratable, ease of use, low cost, good aesthetics, high functions/effectiveness, and a natural feel.

The work contained in this doctoral dissertation is driven by the needs of older adults, and represents examples of the types of technologies and design methods that will be needed to keeping older adults healthy.

The DHD demonstrates an approach to solve many of the problems associated with current hearing technology that cause older adults to not want to use them. This device is invisible, eliminating any social stigma or aesthetic concerns; it is held constantly in place, eliminating the need for battery replacement, adjustment, or misplacing the device; it reduces occlusion and feedback and improves sound quality, to allow older adults to better understand the world around them and reduce feelings of isolation due to sensory impairment.

The chromatic pupillometer investigates the implementation of a non-invasive diagnostic device to evaluate potential neurological disorder. With a device like this, there is the opportunity for early screening of neurological disorders in a short and convenient test, which would better serve heath care providers to detect a potential problem before the onset of detrimental side effects.

The StabilitySole represents the direction of at home monitoring systems that can allow patients to take a more participatory role in their health care, and specifically mobility. Individuals can self evaluate their progress day to day and use these guidelines to make informed decisions about their capabilities and limitations. This tool has a large spectrum of applications

from gait and balance to rehabilitation to weight management that would give patients a quantitative insight into their daily activity and how that relates to their well-being.

REFERENCES

1. Vincent GK, Velkoff V. The Next Four Decades The Older Population in the United States : 2010 to 2050. *US Dep Commer Econ Stat Adm US Census Bur*. 2010;(May).

2. Older Americans 2012: Key Indicators of Well-Being. *Fed Interag Forum Aging Relat Stat*. 2012.

3. National Center for Health Statistics. *Health, United States, 2012: With Special Feature of Prescription Drugs*. Hyattsville, MD.; 2014.

4. Helal A, Mokhtari M, Abdulrazak B. *The Engineering Handbook of Smart Technology for Aging, Disability, and Independence*. A John Wiley & Sons, Inc. Publication; 2008.

5. Cheek P, Nikpour L, Nowlin HD. Aging well with smart technology. *Nurs Adm Q*. 2005;29(4):329–38. Available at: http://www.ncbi.nlm.nih.gov/pubmed/16260997.

6. Park S, Jayarman S. Enhancing the Quality of Life Through Wearable Technology. *IEEE Eng Med Biol Mag*. 2003;(June):41–48.

7. Covinsky KE, Palmer RM, Fortinsky RH, et al. Loss of independence in activities of daily living in older adults hospitalized with medical illnesses: increased vulnerability with age. *J Am Geriatr Soc*. 2003;51(4):451–8. Available at: http://www.ncbi.nlm.nih.gov/pubmed/12657063.

8. Pirkl JJ. The Demographics of Aging. *Transgenerational Des Matters*. 2009. Available at: http://transgenerational.org/aging/demographics.htm.

9. Czaja SJ, Charness N, Fisk AD, et al. Factors predicting the use of technology: findings from the Center for Research and Education on Aging and Technology Enhancement (CREATE). *Psychol Aging*. 2006;21(2):333–52. doi:10.1037/0882-7974.21.2.333.

10. Charness N, Boot WR. Aging and Information Technology Use: Potential and Barriers. *Curr Dir Psychol Sci*. 2009;18(5):253–258. doi:10.1111/j.1467-8721.2009.01647.x.

11. Fisk A., Rogers WA, Charness N, Czaja SJ, Sharit J. *Designing for older adults: Principles and creative human factors approaches (2nd ed.)*. Boca Raton, FL: CRC Press; 2009.

12. Czaja SJ. *The Impact of Aging on Access to Technology*.; 2003.

13. National Library of Medicine and the National Institutes of Arthritis and Musculoskeletal and Skin Diseases. Osteoarthritis. *MedlinePlus*. Available at: http://www.nlm.nih.gov/medlineplus/osteoarthritis.html.

14. Wallhagen MI, Pettengill E, Whiteside M. SENSORY IMPAIRMENT IN OLDER ADULTS. *Am J Nurs*. 2006;106(10).

15. Association A. 2012 Alzheimer's Disease Facts and Figures. *Alzheimer's Dement*. 2012;8(2).

16. Cavalieri TA. Management of Pain in Older Adults. *J Am Osteopath Assoc*. 2005;105(3):12–17.

17. Thomas E, Peat G, Harris L, Wilkie R, Croft PR. The prevalence of pain and pain interference in a general population of older adults: cross-sectional findings from the North Staffordshire Osteoarthritis Project (NorStOP). *Pain*. 2004;110(1-2):361–8. doi:10.1016/j.pain.2004.04.017.

18. Kochkin S. MarkeTrak VIII : 25-Year Trends in the Hearing Health Market. *Arch Intern Med*. 2009;(October).

19. *Deafness and Hearing Loss*.; 2014:Media Center Fact Sheet #300. Available at: http://www.who.int/mediacentre/factsheets/fs300/en/.

20. Agrawal Y, Platz EA, Niparko JK. Prevalence of Hearing Loss and Differences by Demographic Characteristics Among US Adults. *Arch Intern Med*. 2008;168(14):1522–1530.

21. Bagai A, Thavendiranathan P, Detsky A. Does This Patient Have Hearing Impairment. *JAMA J Am Med Assoc*. 2006;295(4).

22. BioGraphix Media. Human Ear Anatomy. Available at: http://www.biographixmedia.com/human/ear-anatomy.jpg.

23. Kochkin S. MarkeTrak VII: Obstacles to adult non-user adoption of hearing aids. *Hear J*. 2007;60(4):24.

24. Chung K. Challenges and Recent Developments in Hearing Aids: Part II. Feedback and Occlusion Effect Reduction Strategies, Laser Shell Manufacturing Processes, and Other Signal Processing Technologies. *Trends Amplif*. 2004;8(4):125–164. doi:10.1177/108471380400800402.

25. Counter P. Implantable hearing aids. *Proc Inst Mech Eng H*. 2008;222(6):837–52.

26. Shinners MJ, Hilton CW, Levine SC. Implantable hearing devices. *Curr Opin Otolaryngol Head Neck Surg*. 2008;16(5):416–9. doi:10.1097/MOO.0b013e32830a49f0.

27. Uziel A, Mondain M, Hagen P, Dejean F, Doucet G. Rehabilitation for high-frequency sensorineural hearing impairment in adults with the symphonix vibrant soundbridge: a comparative study. *Otol Neurotol*. 2003;24(5):775–83.

28. Hough JVD, Matthews P, Wood MW, Dyer RK. Middle ear electromagnetic semi-implantable hearing device: results of the phase II SOUNDTEC direct system clinical trial. *Otol Neurotol*. 2002;23(6):895–903.

29. Palmer C V. A contemporary review of hearing aids. *Laryngoscope*. 2009;119(11):2195–204. doi:10.1002/lary.20690.

30. *NIDCD Fact Sheet: Hearing Aids*. Bethesda, MD Available at: www.nidcd.nih.gov.

31. *NIDCD Fact Sheet- Hearing and Balance - Hearing Loss and Older Adults*. Bethesda, MD; 2013. doi:10.1037/e302862003-001.

32. *Fact Sheet: Buying a Hearing Aid*.; 2011. Available at: https://www.entnet.org/HealthInformation/buyingHearingAid.cfm.

33. Phonak - Hearing Aids Overview - Milo/Milo Plus. Available at: http://www.phonak.com/com/b2c/en/products/hearing_instruments/milo/overview.html.

34. M S, D S, N D, S S, S W, T A. Real-world safety experience with a 24/7 hearing device. *Hear Rev*. 2011;18(1):18–23.

35. Tenholder J. Lyric and safety. 2011;(May):2–3.

36. Phonak Inc. Lyric Hearing Aids. Available at: http://www.lyrichearing.com/.

37. Beutner D, Hüttenbrink KB. [Passive and active middle ear implants]. *Laryngorhinootologie*. 2009;88 Suppl 1:S32–47. doi:10.1055/s-0028-1119493.

38. University of California Irvine School of Medicine Department of Otolaryngology - Head and Neck Surgery. Bone Anchored Hearing Aid. Available at: http://www.ent.uci.edu/clinical-specialties/ear-surgery/bone-anchored-hearing-aid. Accessed May 20, 2014.

39. Banga R, Lawrence R, Reid A, McDermott A-L. Bone-anchored hearing aids versus conventional hearing aids. *Adv Otorhinolaryngol*. 2011;71:132–9. doi:10.1159/000323711.

40. Baguley DM, Bird J, Humphriss RL, Prevost a T. The evidence base for the application of contralateral bone anchored hearing aids in acquired unilateral sensorineural hearing loss in adults. *Clin Otolaryngol*. 2006;31(1):6–14. doi:10.1111/j.1749-4486.2006.01137.x.

41. Cochlear Baha 4 Systems.

42. Janssen RM, Hong P, Chadha NK. Bilateral bone-anchored hearing aids for bilateral permanent conductive hearing loss: a systematic review. *Otolaryngol Head Neck Surg*. 2012;147(3):412–22. doi:10.1177/0194599812451569.

43. Lustig LR, Arts H a, Brackmann DE, et al. Hearing rehabilitation using the BAHA bone-anchored hearing aid: results in 40 patients. *Otol Neurotol*. 2001;22(3):328–34. Available at: http://www.ncbi.nlm.nih.gov/pubmed/11347635.

44. McDermott A-L, Williams J, Kuo M, Reid A, Proops D. The birmingham pediatric bone-anchored hearing aid program: a 15-year experience. *Otol Neurotol*. 2009;30(2):178–83. doi:10.1097/MAO.0b013e31818b6271.

45. Mylanus E, Snik FM, Cremers RJ. Patients' Opinions of Bone-Anchored vs Conventional Hearing Aids. *Arch Otolaryngol Head Neck Surg*. 1995;121(4):421–425. doi:10.1001/archotol.1995.01890040045007.

46. Zeng F-G. Trends in cochlear implants. *Trends Amplif*. 2004;8(1):1–34. Available at: http://www.ncbi.nlm.nih.gov/pubmed/15247993.

47. Wilson BS. Cochlear implants: Current designs and future possibilities. *J Rehabil Res Dev*. 2008;45(5):695–730. doi:10.1682/JRRD.2007.10.0173.

48. Dorman M, Wilson B. The Design and Function of Cochlear Implants. *Am Sci*. 2004;92(5):436. doi:10.1511/2004.5.436.

49. Gray H. *Anatomy of the Human Body*. Twentieth . (Lewis WH, ed.). Philadelphia: Lea & Febiger 1918; 1918.

50. Ropshkow O. Cochlea Cross Section. *Wikipedia Free Encycl*. Available at: http://en.wikipedia.org/wiki/File:Cochlea-crosssection.svg. Accessed May 14, 2014.

51. Oticon Medical. Acquisition of Neurelec brings new capabilities in cochlear implants. Available at: http://www.oticonmedical.com/Medical/About Oticon Medical/News/neurelec-acquisition-april-2013.aspx#.U35EwFhdUlU. Accessed May 24, 2014.

52. National Institute on Deafness and Other Communication Disorders. Cochlear Implants. *NIH Publ No 11-4798*. 2013.

53. Ear with Cochlear Implant. *NIH Med Arts*. Available at: https://www.nidcd.nih.gov/staticresources/health/images/ear_coch.jpg. Accessed May 21, 2014.

54. NIH NIDCD. *FACT SHEET - Cochlear Implants*.; :1–2. Available at: http://report.nih.gov/NIHfactsheets/Pdfs/CochlearImplants(NIDCD).pdf.

55. American Speech-Language-Hearing Association. Cochlear Implant Frequently Asked Questions. Available at: http://www.asha.org/public/hearing/Cochlear-Implant-Frequently-Asked-Questions/.

56. MED-El Corporation. MED-EL Electrodes. Available at: http://www.medel.com/us/electrodes/. Accessed May 14, 2014.

57. Cochlear. Cochlear Hybrid Implant. Available at: http://www.cochlear.com/wps/wcm/connect/sea/home/discover/electro-acoustic-implants/hybrid-system/implant/hybrid-implant. Accessed May 20, 2014.

58. Wilska A. Eine Methode zur Bestimmung der Hörschwellenamplituden des Trommelfells bei verschiedenen Frequenzen. *Scand Arch Physiol*. 1935;72(161-165).

59. Haynes DSMF. *Middle Ear Implantable Hearing Devices*.

60. Truy E, Philibert B, Vesson J-F, Labassi S, Collet L. Vibrant soundbridge versus conventional hearing aid in sensorineural high-frequency hearing loss: a prospective study. *Otol Neurotol*. 2008;29(5):684–7. doi:10.1097/MAO.0b013e31817156df.

61. Yanagihara N, Honda N, Sato H, Hinohira Y. Piezoelectric semi-implantable middle-ear hearing device: Rion device E-type, long-term results. *Cochlear Implants Int*. 2004;5 Suppl 1:186–8. doi:10.1002/cii.224.

62. Komori M, Yanagihara N, Hinohira Y, Hato N, Gyo K. Re-implant of the Rion Semi-Implantable Hearing Aid E-type. *Otolaryngol - Head Neck Surg*. 2010;143(2):P103–P103. doi:10.1016/j.otohns.2010.06.180.

63. Tysome JR, Moorthy R, Lee A, Jiang D, O'Connor AF. Systematic review of middle ear implants: do they improve hearing as much as conventional hearing AIDS? *Otol Neurotol*. 2010;31(9):1369–75. doi:10.1097/MAO.0b013e3181db716c.

64. Backous DD, Duke W. Implantable middle ear hearing devices: current state of technology and market challenges. *Curr Opin Otolaryngol Head Neck Surg*. 2006;14(5):314–8. doi:10.1097/01.moo.0000244187.66807.30.

65. Luetje C. Phase III clinical trial results with the Vibrant Soundbridge implantable middle ear hearing device: A prospective controlled multicenter study. *Otolaryngol - Head Neck Surg*. 2002;126(2):97–107. doi:10.1067/mhn.2002.122182.

66. MED-EL Vibrant SoundBridge Middle Ear Implant. Available at: http://www.medel.com/us/vibrant-soundbridge. Accessed May 14, 2014.

67. Mosnier I, Sterkers O, Bouccara D, et al. Benefit of the Vibrant Soundbridge device in patients implanted for 5 to 8 years. *Ear Hear*. 2008;29(2):281–4. Available at: http://www.ncbi.nlm.nih.gov/pubmed/18595192.

68. Labassi S, Beliaeff M. Retrospective of 1000 patients implanted with a vibrant Soundbridge middle-ear implant. *Cochlear Implants Int*. 2005;6 Suppl 1(September 1996):74–7. doi:10.1179/cim.2005.6.Supplement-1.74.

69. Colletti V, Soli SD, Carner M, Colletti L. Treatment of mixed hearing losses via implantation of a vibratory transducer on the round window. *Int J Audiol*. 2006;45(10):600–8. doi:10.1080/14992020600840903.

70. Roland PS, Shoup a G, Shea MC, Richey HS, Jones DB. Verification of improved patient outcomes with a partially implantable hearing aid, The SOUNDTEC direct hearing system. *Laryngoscope*. 2001;111(10):1682–6. doi:10.1097/00005537-200110000-00002.

71. Silverstein H, Atkins J, Thompson JH, Gilman N. Experience with the SOUNDTEC implantable hearing aid. *Otol Neurotol*. 2005;26(2):211–7. Available at: http://www.ncbi.nlm.nih.gov/pubmed/15793407.

72. Ototronix. Maxum Hearing Implant. Available at: http://www.mymaxum.com/. Accessed May 14, 2014.

73. Bruschini L, Forli F, Santoro A, Bruschini P, Berrettini S, Division CI. Fully implantable Otologics MET Carina TM device for the treatment of sensorineural hearing loss . La protesi totalmente impiantabile Otologics MET Carina TM per il trattamento. 2009:79–85.

74. Jenkins H a., Niparko JK, Slattery WH, Gail Neely J, Fredrickson JM. Otologics middle ear transducer^{TM} ossicular stimulator: Performance results with varying degrees of sensorineural hearing loss. *Acta Otolaryngol*. 2004;124(4):391–394. doi:10.1080/00016480410016298.

75. Miller P. Otologics files for bankruptcy. *St. Louis Business Journal*. http://www.bizjournals.com/stlouis/blog/BizNext/2012/07/otologics-files-for-bankruptcy.html.

76. Otologics LLC. Fully Implantable Carina Hearing Device. *Natl Libr Med*. Available at: http://openi.nlm.nih.gov/detailedresult.php?img=3199819_CTO-08-09-g-008&req=4 .

77. Kroll K, Grant IL, Javel E. The Envoy(R) Totally Implantable Hearing System, St. Croix Medical. *Trends Amplif*. 2002;6(2):73–80. doi:10.1177/108471380200600208.

78. Envoy Medical. Esteem The Hearing Implant. Available at: http://envoymedical.com/the-esteem-implant/.

79. Chen D a, Backous DD, Arriaga M a, et al. Phase 1 clinical trial results of the Envoy System: a totally implantable middle ear device for sensorineural hearing loss. *Otolaryngol Head Neck Surg*. 2004;131(6):904–16. doi:10.1016/j.otohns.2004.05.027.

80. Barbara M, Manni V, Monini S. Totally implantable middle ear device for rehabilitation of sensorineural hearing loss: preliminary experience with the Esteem, Envoy. *Acta Otolaryngol*. 2009;129(4):429–32. doi:10.1080/00016480802593505.

81. Perkins R. Earlens tympanic contact transducer: a new method of sound transduction to the human ear. *Otolaryngol Head Neck Surg*. 1996;114(6):720–8. Available at: http://www.ncbi.nlm.nih.gov/pubmed/8643293.

82. Perkins R, Fay JP, Rucker P, Rosen M, Olson L, Puria S. The EarLens system: new sound transduction methods. *Hear Res*. 2010;263(1-2):104–13. doi:10.1016/j.heares.2010.01.012.

83. Perkins RC, Fay J, Nilsson MJ, Puria S, Levy SPC. The EarLens Photonic Transducer: Extended Bandwidth. *Otolaryngol -- Head Neck Surg*. 2011;145(2 Suppl):P102–P102. doi:10.1177/0194599811416318a193.

84. EarLens Corporation. Clinical and Scientific Information. Available at: http://www.earlenscorp.com/technology/studies/.

85. Chittka L, Brockmann A. Perception space--the final frontier. *PLoS Biol*. 2005;3(4):e137. doi:10.1371/journal.pbio.0030137.

86. Goode RL, Killion M, Nakamura K, Nishihara S. New knowledge about the function of the human middle ear: development of an improved analog model. *Otol Neurotol*. 1994;15(2):145.

87. Chien W, Ravicz ME, Rosowski JJ, Merchant SN. Measurements of human middle- and inner-ear mechanics with dehiscence of the superior semicircular canal. *Otol Neurotol*. 2007;28(2):250–7. doi:10.1097/01.mao.0000244370.47320.9a.

88. Decraemer WF. Area change and volume displacement of the human tympanic membrane under static pressure. *ReVision*. 1992;di:99–104.

89. Decraemer WF, Dirckx JJ, Funnell WR. Shape and derived geometrical parameters of the adult, human tympanic membrane measured with a phase-shift moiré interferometer. *Hear Res*. 1991;51(1):107–21. Available at: http://www.ncbi.nlm.nih.gov/pubmed/2013538.

90. Kurokawa H, Goode RL. Sound pressure gain produced by the human middle ear. *Otolaryngol Head Neck Surg*. 1995;113(4):349–55. Available at: http://www.ncbi.nlm.nih.gov/pubmed/7567003.

91. Djalilian H, Mahboubi H. A Novel Method to Determine Standardized Anatomic Dimensions and Variation of the Osseous External Auditory Canal. *Otol Neurotol*.13–18.

92. Paulsen RR. *Statistical Shape Analysis of the Human Ear Canal with Application to In-the-Ear Hearing Aid Design*.; 2004.

93. Leysieffer H, Baumann JW, Müller G, Zenner HP. An implantable piezoelectric hearing aid transducer for inner ear deafness. II: Clinical implant. *HNO*. 1997;45(10):801–15.

94. Vecchia P, Hietanen M, Ahlborn A. International Commission on Non-Ioninzing Radiation Protection: Guidelines on Limits of Exposure to Static Magnetic Fields. *Health Phys*. 2009;96(4):504–514.

95. Mannan MS. *Lees' Loss Prevention in the Process Industries: Hazard Identification Assessment and Control*. 4th ed. Butterworth-Heinemann; 2012.

96. Chien W, Ravicz ME, Merchant SN, Rosowski JJ. The effect of methodological differences in the measurement of stapes motion in live and cadaver ears. *Audiol Neurootol*. 2006;11(3):183–97. doi:10.1159/000091815.

97. Mahboubi H, Paulick P, Kiumehr S, Merlo M, Bachman M, Djalilian HR. Investigation of a Novel Completely-in-the-Canal Direct-Drive Hearing Device : A Temporal Bone Study. 2012.

98. Homma K, Du Y, Shimizu Y, Puria S. Ossicular resonance modes of the human middle ear for bone and air conduction. *J Acoust Soc Am*. 2009;125(2):968–79. doi:10.1121/1.3056564.

99. Mahboubi H, Malley MJD, Paulick P, Merlo MW, Bachman M, Djalilian HR. Completely-in-the-Canal Magnet-Drive Hearing Device: A Temporal Bone Study. *Otolaryngol -- Head Neck Surg*. 2012;(December 21). doi:10.1177/0194599812471608.

100. Vaile L, Williamson T, Waddell A, Gj T. Interventions for ear discharge associated with grommets (ventilation tubes) (Review). *Cochrane Rev*. 2006;The Cochra(2).

101. Schmitt BD. Ventilation Tube Surgery. *"My Child is Sick Am Acad Pediatr Books Publ by RelayHealth*. 2012. Available at: http://www.summitmedicalgroup.com/library/pediatric_health/hhg_ventilation_tubes_surgery/.

102. Yau YY a., Mahboubi H, Malley MJD, et al. Direct-Drive Acoustic Amplification Using a Tympanostomy Tube. *Otolaryngol -- Head Neck Surg*. 2013;149(2 Suppl):P96–P96. doi:10.1177/0194599813495815a187.

103. Gulya AJ. *Glasscock-Shambaugh Surgery of the Ear*. (Gulya AJ, Minor LB, Poe D, eds.). PMPH-USA; 2010:29–43.

104. Agur AM, Dalley AF. *Grants Atlas of Anatomy*. Tympanic M. Lippincott Williams & Wilkins; 13th edition; 2012:886.

105. Tillman TW, Carhart R. An Expanded Test for Speech Discrimination Utilizing CNC Monosyllabic Words - Northwester University Auditory Test No.6. *USAF Sch Aerosp Med*. 1966;Aerospace (6).

106. Kerr a G, Smyth GD. Routine speech discrimination tests. *J Laryngol Otol*. 1972;86(1):33–41. Available at: http://www.ncbi.nlm.nih.gov/pubmed/5007952.

107. Hong E-P, Park I-Y, Seong K-W, Cho J-H. Evaluation of an implantable piezoelectric floating mass transducer for sensorineural hearing loss. *Mechatronics*. 2009;19(6):965–971. doi:10.1016/j.mechatronics.2009.07.001.

108. Stieger C, Candreia C, Kompis M, et al. Laser Doppler vibrometric assessment of middle ear motion in thiel-embalmed heads. *Otol Neurotol*. 2012;33(3):311–8. doi:10.1097/MAO.0b013e3182487de0.

109. Silverthorn DU. *Human Physiology: An Integrated Approach*. 4th Editio. Pearson Education Inc.; 2007. doi:0805368515.

110. Diego S, Hospital LE. Quantitative pupillometry, a new technology: normative data and preliminary observations in patients with acute head injury. Technical note. *J Neurosurg*. 2003;98(1):205–13. doi:10.3171/jns.2003.98.1.0205.

111. Kawasaki A, Munier FL, Leon L, Kardon RH. Pupillometric quantification of residual rod and cone activity in leber congenital amaurosis. *Arch Ophthalmol*. 2012;130(6):798–800. doi:10.1001/archophthalmol.2011.1756.

112. Kardon R, Anderson SC, Damarjian TG, Grace EM, Stone E, Kawasaki A. Chromatic pupillometry in patients with retinitis pigmentosa. *Ophthalmology*. 2011;118(2):376–81. doi:10.1016/j.ophtha.2010.06.033.

113. Bergamin O. Latency of the Pupil Light Reflex: Sample Rate, Stimulus Intensity, and Variation in Normal Subjects. *Invest Ophthalmol Vis Sci*. 2003;44(4):1546–1554. doi:10.1167/iovs.02-0468.

114. Bergamin O, Zimmerman MB, Kardon RH. Pupil light reflex in normal and diseased eyes. *Ophthalmology*. 2003;110(1):106–114. doi:10.1016/S0161-6420(02)01445-8.

115. Purves D, Augustine G, Fitzpatrick D. *Neuroscience*. Fourth Edi. Sinauer Associates, Inc.; 2008.

116. Keivanidou A, Fotiou D, Arnaoutoglou C, Arnaoutoglou M, Fotiou F, Karlovasitou A. Evaluation of autonomic imbalance in patients with heart failure : A preliminary study of pupillomotor function. 2010;17(1):65–72.

117. Dütsch M, Marthol H, Michelson G, Neundörfer B, Hilz MJ. Pupillography refines the diagnosis of diabetic autonomic neuropathy. *J Neurol Sci*. 2004;222(1-2):75–81. doi:10.1016/j.jns.2004.04.008.

118. Stergiou V, Fotiou D, Tsiptsios D, et al. Pupillometric findings in patients with Parkinson ' s disease and cognitive disorder. *Int J Psychophysiol*. 2009;72:97–101. doi:10.1016/j.ijpsycho.2008.10.010.

119. Fotiou DF, Stergiou V, Tsiptsios D, Lithari C, Nakou M, Karlovasitou a. Cholinergic deficiency in Alzheimer's and Parkinson's disease: evaluation with pupillometry. *Int J Psychophysiol*. 2009;73(2):143–9. doi:10.1016/j.ijpsycho.2009.01.011.

120. Foster RG, Provencio I, Hudson D, Fiske S, De Grip W, Menaker M. Circadian photoreception in the retinally degenerate mouse (rd/rd). *J Comp Physiol A*. 1991;169(1):39–50. Available at: http://www.ncbi.nlm.nih.gov/pubmed/1941717.

121. Gamlin PDR, McDougal DH, Pokorny J, Smith VC, Yau K-W, Dacey DM. Human and macaque pupil responses driven by melanopsin-containing retinal ganglion cells. *Vision Res*. 2007;47(7):946–54. doi:10.1016/j.visres.2006.12.015.

122. Kawasaki A, Kardon RH. Intrinsically photosensitive retinal ganglion cells. *J Neuroophthalmol*. 2007;27(3):195–204. doi:10.1097/WNO.0b013e31814b1df9.

123. Schmidt TM, Chen S-K, Hattar S. Intrinsically photosensitive retinal ganglion cells: many subtypes, diverse functions. *Trends Neurosci*. 2011;34(11):572–80. doi:10.1016/j.tins.2011.07.001.

124. Mure LS, Rieux C, Hattar S, Cooper HM. Melanopsin-dependent nonvisual responses: evidence for photopigment bistability in vivo. *J Biol Rhythms*. 2007;22(5):411–24. doi:10.1177/0748730407306043.

125. Chen S-K, Badea TC, Hattar S. Photoentrainment and pupillary light reflex are mediated by distinct populations of ipRGCs. *Nature*. 2011;476(7358):92–5. doi:10.1038/nature10206.

126. Berson DM. Strange vision: ganglion cells as circadian photoreceptors. *Trends Neurosci*. 2003;26(6):314–20. doi:10.1016/S0166-2236(03)00130-9.

127. Hanifin JP, Brainard GC. Photoreception for Circadian, Neuroendocrine, and Neurobehavioral Regulation. *J Physiol Anthropol*. 2007;26(2):87–94. doi:10.2114/jpa2.26.87.

128. Dacey DM, Liao H-W, Peterson BB, et al. Melanopsin-expressing ganglion cells in primate retina signal colous and irradiance and project to the LGN. *Nature*. 2005;433(7027):741–5. doi:10.1038/nature03344.

129. Kardon R, Anderson SC, Damarjian TG, Grace EM, Stone E, Kawasaki A. Chromatic pupil responses: preferential activation of the melanopsin-mediated versus outer photoreceptor-mediated pupil light reflex. *Ophthalmology*. 2009;116(8):1564–73. doi:10.1016/j.ophtha.2009.02.007.

130. Gooley JJ, Ho Mien I, St. Hilaire M a., et al. Melanopsin and Rod-Cone Photoreceptors Play Different Roles in Mediating Pupillary Light Responses during Exposure to Continuous Light in Humans. *J Neurosci*. 2012;32(41):14242–14253. doi:10.1523/JNEUROSCI.1321-12.2012.

131. Park JC, Moura AL, Raza AS, Rhee DW, Kardon RH. Toward a Clinical Protocol for Assessing Rod , Cone , and Melanopsin Contributions to the Human Pupil Response. 2011:6624–6635. doi:10.1167/iovs.11-7586.

132. Lorenz B, Strohmayr E, Zahn S, et al. Chromatic Pupillometry Dissects Function of the Three Different Light-Sensitive Retinal Cell Populations in RPE65 Deficiency. 2012;53(9). doi:10.1167/iovs.12-9974.

133. Patwari PP, Stewart TM, Rand CM, et al. Pupillometry in congenital central hypoventilation syndrome (CCHS): quantitative evidence of autonomic nervous system dysregulation. *Pediatr Res*. 2012;71(3):280–5. doi:10.1038/pr.2011.38.

134. Young RS, Kennish J. Transient and sustained components of the pupil response evoked by achromatic spatial patterns. *Vision Res*. 1993;33(16):2239–52. Available at: http://www.ncbi.nlm.nih.gov/pubmed/8273290.

135. Lucas RJ, Hattar S, Takao M, Berson DM, Foster RG, Yau K-W. Diminished pupillary light reflex at high irradiances in melanopsin-knockout mice. *Science*. 2003;299(5604):245–7. doi:10.1126/science.1077293.

136. Güler AD, Ecker JL, Lall GS, et al. Melanopsin cells are the principal conduits for rod-cone input to non-image-forming vision. *Nature*. 2008;453(7191):102–5. doi:10.1038/nature06829.

137. Léon L, Crippa S V, Borruat F-X, Kawasaki A. Differential effect of long versus short wavelength light exposure on pupillary re-dilation in patients with outer retinal disease. *Clin Experiment Ophthalmol*. 2012;40(1):e16–24. doi:10.1111/j.1442-9071.2011.02665.x.

138. Holden MK, Gill KM, Magliozzi MR, Nathan J, Piehl-Baker L. Clinical gait assessment in the neurologically impaired. Reliability and meaningfulness. *Phys Ther*. 1984;64(1):35–40. Available at: http://www.ncbi.nlm.nih.gov/pubmed/6691052.

139. Stevens JA, Corso PS, Finkelstein EA, Miller T. The costs of fatal and nonfatal falls among older adults. *Inj Prev*. 2006;12(290-295).

140. Rosano C, Brach J, Longstreth Jr WT, Newman AB. Quantitative measures of gait characteristics indicate prevalence of underlying subclinical structural brain abnormalities in high-functioning older adults. *Neuroepidemiology*. 2006;26(1):52–60. doi:10.1159/000089240.

141. Verghese J. Abnormality of Gait as a Predictor of Non-Alzheimer's Dementia. *N Engl J Med*. 2002;347(22).

142. Paulick P, Djalilian H, Bachman M. StabilitySole: Embedded Sensor Insole for Balance and Gait Monitoring. In: Duffy V, ed. *Digital Human Modeling SE - 19*.Vol 6777. Lecture Notes in Computer Science. Springer Berlin Heidelberg; 2011:171–177. doi:10.1007/978-3-642-21799-9_19.

143. The World Bank. Health Expenditure Total % of GDP.

144. Bachman M. Technology for Living and Caring (The Internet of Health Things). In: *Presentation to Toshiba America Electronic Components, Inc.*